NKS-296
ISBN 978-87-7893-372-0

Consequences of severe radioactive releases to Nordic Marine environment

Mikhail Iosjpe [1]
Mats Isaksson [2]
Hans Pauli Joensen[3]
Juhani Lahtinen[4]
Kai Logemann[5]
Sigurður Emil Pálsson [6]
Per Roos[7]
Vesa Suolanen[8]
Vesa-Pekka Vartti[4]

[1] Norwegian Radiation Protection Authority, Norway
[2] University of Gothenburg, Sweden
[3] Fróðskaparsetur Føroya, Faroe Islands
[4] Radiation and Nuclear Safety Authority, Finland
[5] University of Iceland, Iceland
[6] Geislavarnir Rikisins, Iceland
[7] Technical University of Denmark, Denmark
[8] Technical Research Centre of Finland, Finland

January 2014

Abstract

Consequences of hypothetical severe radioactive releases to Nordic marine environment – the Baltic Sea and the North Atlantic - has been considered.

As a reference, releases from a 3000 MW_{th} nuclear power plant reactor size was used for the Baltic Sea area accidents. Individual dose to human could be ten to some hundreds of millisieverts in local sea area. In the Baltic Sea area, individual dose was 0.01 mSv after one year and 0.1 mSv after five years from the release event. The collective dose estimate was 880 manSv.

In case of hypothetical submarine accidents at the North Atlantic, the marine fluxes are important factors. According to simulation results, e.g. maximum concentration near the source region at the Icelandic coast sinks below 1% only after 300 days.

Consequences of an accident of a modern submarine for e.g. to Kattegat region was calculated. The arising doses can be equal or higher than from natural sources. The models predictions seem to reach nice consistence with measured values in qualitative and quantitative considerations.

Key words

severe radioactive releases, accidents, marine environment, nuclear power plants, submarines, doses, validation

NKS-296
ISBN 978-87-7893-372-0

Electronic report, January 2014
NKS Secretariat
P.O. Box 49
DK - 4000 Roskilde, Denmark
Phone +45 4677 4041
www.nks.org
e-mail nks@nks.org

Consequences of severe radioactive releases to Nordic marine environment

Final report for the NKS-B COSEMA activity 2013
Contract AFT/B(13)3

Contributors:

Mikhail Iosjpe, Norwegian Radiation Protection Authority, Norway
Mats Isaksson, University of Gothenburg, Sweden
Hans Pauli Joensen, Fróðskaparsetur Føroya, Faroe Islands
Juhani Lahtinen, Radiation and Nuclear Safety Authority, Finland
Kai Logemann, University of Iceland, Iceland
Sigurður Emil Pálsson, Geislavarnir Rikisins, Iceland
Per Roos, Technical University of Denmark, Denmark
Vesa Suolanen, Technical Research Centre of Finland, Finland
Vesa-Pekka Vartti, Radiation and Nuclear Safety Authority, Finland

January 2014

page

CONTENTS

1 INTRODUCTION

The report considers consequences of hypothetical severe nuclear accident releases into Nordic marine environment. The considered marine area comprises the Baltic Sea (Sweden, Denmark, Finland) and the North Atlantic (Iceland, Faroe Islands, Norway) areas. As hypothetical severe accident scenarios are considered nuclear power plant accidents at the Baltic Sea area and submarine accidents at the North Atlantic and also at Kattegat shallow waters.

Research on radioactive source terms of extremely severe nuclear power plant and submarine accidents has been done. This enables to estimate possible radioactive releases and further consequences of various elements and nuclides to marine environment. One recent reference is of course the Fukushima accident and estimated releases there.

The marine fluxes and flow circumstances in general are studied since they are important factors especially for the North Atlantic release and dispersion analyses. Untypical release events at the North Atlantic need comprehensive knowledge of marine flows to be used in safety analyses.

Based on hypothetical severe accidents scenarios, consequence calculations have been done. It should be emphasised that the considered severe accident cases, considered in this study, do not directly attach any existing Nordic nuclear power plant. The considered radioactive releases will, however, provide specified references for consideration of environmental consequences of severe - or minor – radioactive releases to Nordic marine environment.

A review on measured data of the Baltic Sea marine environment will be presented. This enables to make also some model validation considerations in the study.

This report is the final report of the planned two years COSEMA research activity in the NKS-B research programme.

2 HYPOTHETICAL SEVERE NUCLEAR ACCIDENT IN NORDIC ENVIRONMENT

Around the Baltic Sea there are several nuclear power plant units also in Sweden and in Finland. In Forsmark there are three BWR's (2x2928 MW_{th} and one 3300 MW_{th}). In Ringhals there are four reactors: one BWR (2540 MW_{th}) and three PWR's (2652, 3135 and 2775 MW_{th}). In Oskarshamn there are three BWR's: 1375 MW_{th}, 1800 MW_{th} and 3300 MW_{th}. In Olkiluoto there are two BWR's (2500 MW_{th}) and in Loviisa two PWR's (2x1500 MW_{th}) (Lahtinen, J., 2012). A summary of nuclear facilities around the Baltic Sea is presented e.g. in an earlier study (Nielsen, S.P., et al., 2010).

In can be concluded that the greatest thermal reactor power of 3300 MW (corresponds to about 1000 MW_e) represent the highest level of radionuclide inventories which could partially be released from the core in a hypothetical severe accident. This kind of reference accident case, so called worst case accident scenario, does not refer to any specific reactor in Nordic countries, but provides a picture of highest environmental consequences which could appear with very low probability. Consequences of smaller radioactive releases to Nordic marine environment can then quite easily be estimated based on the worst case accident results. Severe nuclear power plant accidents releases and consequences are considered from locations of current nuclear power plants in Finland and Sweden.

A severe nuclear power plant or submarine accident could result e.g. from operational reasons, coolant leakages (LOCA-accidents) or external treats. The radioactive source term from a severe damaged reactor core is in the study mainly assumed to be consisted of soluble substances like caesium and iodine radionuclides. The source term evaluation will be based on an assumption that functioning of all cooling safety systems of the considered reactor has been lost. In this case the reactor core is expected to melt finally significantly, causing possibly large releases of volatile nuclides to the marine environment. The effect of duration of the source term will also be considered, because it is expected that a shorter release will produce elevated seawater and sediment concentrations at the local sea area, near the considered nuclear power plant or a submarine vessel. The released radionuclides will further disperse via marine flows to the whole Baltic Sea area or to the North Atlantic. Despite large dilution, the released radionuclides will cause some collective exposure also in the whole Baltic and North Sea areas.

Nuclear-powered submarine accidents near Iceland, the Faroese or Norway coasts might create special threats for the local marine ecology. These untypical radioactive release events in the North Atlantic are considered in consequence assessments of the COSEMA activity as well.

References

Lahtinen, J., COSEMA activity working report, 2012.

Nielsen, Sven P., Lüning, M., Ilus, E., Outola, I., Ikäheimonen, T., Mattila, J., Herrman, J., Kanisch, G., Osvath, I., 2010, Baltic Sea, Radionuclides in the Environment, ISBN 978-0-470-71434-8.

3 MARINE FLOWS

3.1 Baltic Sea area

Water exchange of the Baltic Sea

Per Roos, Technical University of Denmark - DTU

The Baltic Sea is a 413 000 km^2 mediterranean sea with a volume of 22 000 km^3 which may be viewed as a large estuary with brackish water and a surface salinity gradient that goes from 3‰ in the northern Bothnian Bay to 15 ‰ close to the Danish Straits. The water exchange is characterized by a large annual fresh water inflow due both to precipitation (225 km^3) and river inflow (440 km^3) from the 1.6 million km^2 drainage area. This input of fresh water is balanced by an outflow through the Danish Straits and to minor extent by evaporation. To maintain the salinity, inflows of salty Atlantic water must occur. While high-frequency inflows and outflows happen continuously in the Danish Straits mainly the same water is moved back and forth and the net inflow of salty water is negligible.

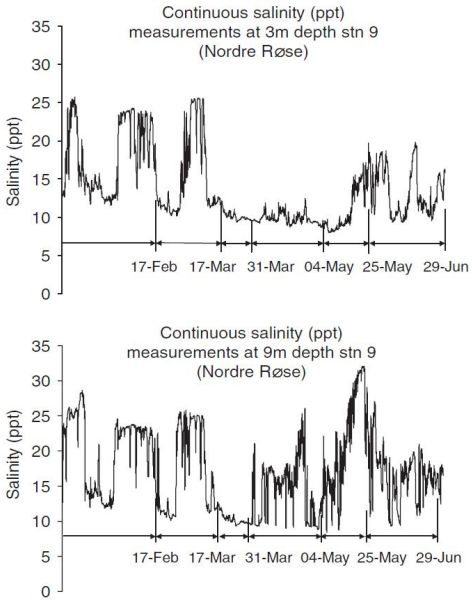

Fig. 1. Continous salinity measurements in the Öresund at 3 and 9m depth during 6 months showing high-frequency salinity changes. (Roos and Valeur, 2006).

The stratification of the water column in this transition area between the Baltic Sea and the North Sea is characterized by a sharp halocline located at 5-15m depth which separates low salinity outflowing surface water from slowly inflowing high salinity North Sea water. High-frequency mixing of the water column due to changing atmospheric conditions (wind strength, wind direction and atmospheric pressure)

results in rapid changes of the surface salinity especially during winter time when the temperature gradient of the water column is small (Figure 1).

Large net inflows are rare and sporadic and occurs only in connection with exceptional climate situations with extended high-pressure periods (lowered sea level of the Baltic Sea) followed by an extended period of low pressure over the Kattegat and the Baltic (resulting in high water level) combined with strong south-westerly winds. For the inflowing saltwater to be able to reach the deeper parts of the Baltic Sea and renew the older bottom water the inflowing water must be of low temperature and have a salinity exceeding 17 ‰.

The main restrictions for water exchange between the Baltic Sea and the Atlantic Ocean are the Danish straits and further into the Baltic Sea the Drogden sill (southern Öresund, max depth 8m) and the Darss sill (southeastern Belt Sea, max depth 15m). The outflowing surface water is characterized by low salinity water which is maintained up to the northern Kattegat where the low salinity surface water forms a front towards the saline Skagerrak water. The Baltic outflow generally follows the Swedish and Norwegian coast and can be traced, for instance, by its lower salinity up to the Arctic Ocean.

	Average Depth (m)	Maximum Depth (m)	Surface Area (10^3 km^2)	Volume (km^3)
Arkona Basin	36.4	50	8.53	310.5
Öresund	11.7	34	0.929	10.8
Fehmarn Belt	16.3	37	9.7	158.1
Samsø Belt	13.2	60	8.14	107.6
Southern Kattegat	23.8	60	9.10	216.6
Central Kattegat	20.0	115	8.12	162.1
Northern Kattegat	30.5	105	5.07	154.4

Table 1 Main characteristics of the basins in the transition area between the Baltic Sea and the Atlantic Ocean (Gustafsson, 2000).

Due to the frequent strong stratification of the water column in the transition area net movement of a released contaminant in this region is very much dependent on water depth of the release but also on the time of the year. Major inflows to the Baltic Sea is much more likely to occur during autumn to spring than during summer time for instance. A release of a contaminant summertime at depth in Kattegat would thus probably with small probability be transferred to the Baltic Sea.

References

Roos,P., Valeur, J. *Cont. Shelf Res.*, 26, 474-487 (2006)

Gustafsson B.G., *Estuaries,* 23(2), 231-252 (2000)

Marine flows around the Forsmark and Ringhals nuclear power plants

Mats Isaksson, University of Gothenburg - GU

Modelling of the water movements and ecological impact has been performed for the estuarine area outside the Forsmark power plant. Model estimations by Engqvist & Andrejev (1999) of the water exchange of the area adjacent to the plant as well as for the whole Baltic showed good resemblance with observed circulation.

Kumblad et al. (2006) was able to estimate the concentration of radionuclides in a modelled ecosystem with bioconcentration factors for plants and adsorption coefficients (K_d) as input parameters. The model was based on site-specific carbon dynamics and three radionuclide specific mechanisms: plant uptake, excretion by animals, and adsorption organic surfaces. The model suggest that the water exchange rate in the area is important considering radionuclide exposure to organisms, due to dilution of the water as well as by replacing the plankton with organisms that are not contaminated.

Concerning the vicinity of the Ringhals nuclear power plant, Holtegaard Nielsen (2005) presents data for the circulation in the Kattegat. In contrast to the common description that a large part of the area is governed by a basic estuarine circulation, Nielsen found anti-cyclonic circulation in a large part of the upper layer. This circulation was driven by a density gradient at the border between Kattegat and Skagerrak.

Spokes et al. (2006) found that the coastline and the islands within the Kattegat influence the entire Kattegat Sea region. The influence of the land masses gives rise to horizontal gradients in a large number of parameters. Atmospheric transport and deposition must therefore, according to Spokes et al., be modelled using the individual atmospheric conditions.

References

Andrejev, O., Myrberg, K., Alenius, P., Lundberg, P. A., 2004. Mean circulation and water exchange in the Gulf of Finland – a study based on three-dimensional modelling, Boreal Environmental Research, 9:1-16.

Engqvist, A., Andrejev, O., 1999. Water Exchange of Öregrundsgrepen - A Baroclinic 3D-model Study. Swedish Nuclear Fuel and Waste Management Co., Stockholm, Sweden. SKB TR 99-11.

Holtegaard Nielsen, M., 2005. The baroclinic surface currents in the Kattegat. Journal of Marine Systems 55, 97-121.

Kumblad, L., Kautsky, U. & Næslund, B., 2006. Transport and fate of radionuclides in aquatic environments - the use of ecosystem modelling for exposure assessments of nuclear facilities. Journal of Environmental Radioactivity 87, 107-129.

Spokes, L., Jickells, T., Weston, K., Gustafsson, B.G., Johnsson, M., Liljebladh, B., Conley, D., Ambelas-Skjødth, C., Brandt, J., Carstensen, J., Christiansen, T., Frohn, L., Geernaert, G., Hertel, O., Jensen, B., Lundsgaard, C., Markager, S., Martinsen, W., Møller, B., Pedersen, B., Sauerberg, K., Sørensen, L.L., Hasager, C.C., Sempreviva, A.M., Pryor, S.C., Lund, S.W.,

Larsen, S., Tjernström, M., Svensson, G. & Zagar, M., 2006. MEAD: An interdisciplinary study of the marine effects of atmospheric deposition in the Kattegat. Environmental Pollution 140, 453-462.

Marine flows around the Loviisa nuclear power plant

Vesa Suolanen, Technical Research Centre of Finland - VTT

Generally, in the Gulf of Finland there is a circulation flow counter-clockwise, following the coasts of Estonia, Russia and Finland (Adrejev, et al., 2004). Thus the salinity of the water is slightly lower at the coastal area of Finland than in the coast of Estonia.

The islands restrict to some extent sea water flow from the Loviisa nuclear power plant local sea area Hästholmsfjärden to elsewhere of the Gulf of Finland. About distance of five kilometres from the plant, the areal density of islands decreases and the average depth of the sea is about 30 - 40 meters.

The water exchange rate of the local sea area beside the plant is 57 m^3/s in normal operational use mode. Without cooling flow rate of the plant, natural water exchange rate in local sea area is about 28 m^3/s. The corresponding water turnover of the local sea is about eight times per year. So the cooling flow rate determines the water exchange rate in normal operational use of the plant.

In this study it is however conservatively assumed that the cooling system is damaged during the release and dispersion phases of radionuclides in a severe nuclear power plant accident event. The effective dilution in local sea area is smaller in the case of natural flow circumstances in the local sea area.

3.2 Faroe Islands

Hans Pauli Joensen, Fróðskaparsetur Føroya, Faroe Islands

A brief overview of ocean currents and radioactivity around the Faroe Islands is given in this section.

Main currents

Figure 2 gives an overview of the main surface current systems in the North Atlantic and the Nordic Seas (AMAP, 2010; Aure, J. *et. al*., 1998).

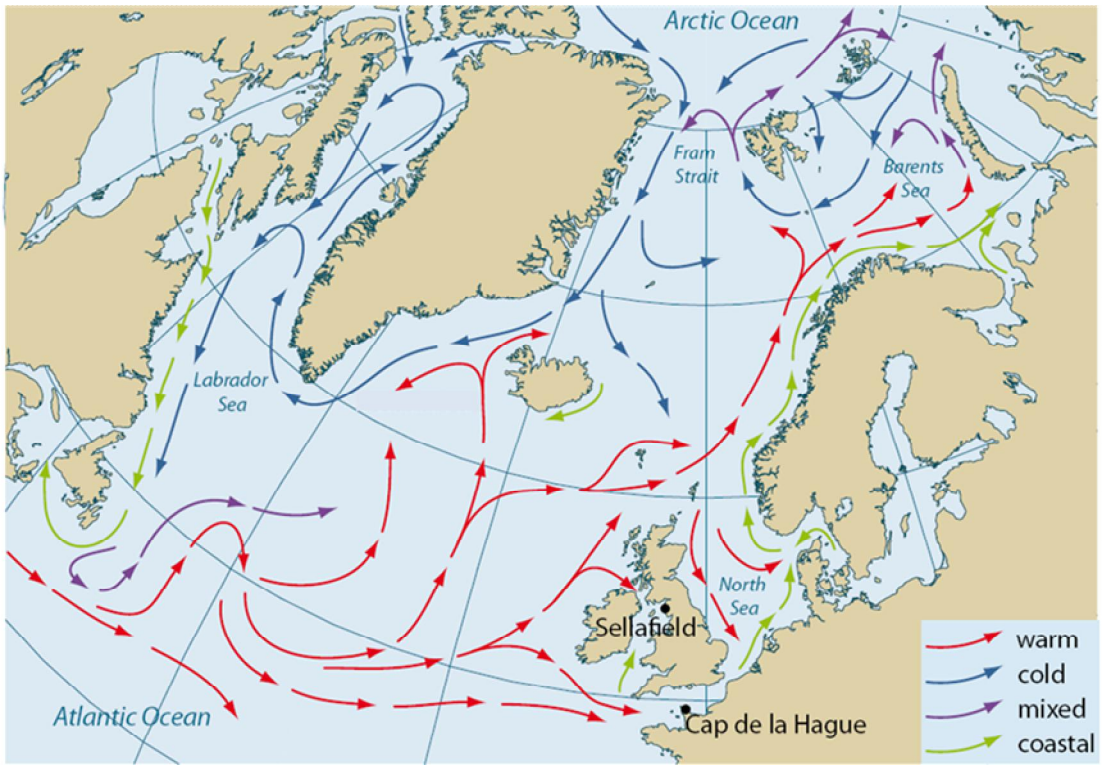

Fig. 2. Overview of main currents in the North Atlantic area (AMAP, 2010; Aure *et. al*., 1998)

The main currents in the upper layer closer to the Faroe Islands and Iceland are illustrated in Figure 3 (Hansen, 2000). Warm North Atlantic Water (NAS, IS) is flowing northward with branches around the Faroe Islands and Iceland into the Norwegian Sea in the north, where it is cooled down and partly sinks to deeper layers. The main water flux into the Norwegian Sea is between Iceland and Scotland. A slope current is northward along the Scottish and the Norwegian shelf. Cold water (the East Greenland Current, EGS) flows from north southward along East Greenland through the Denmark Strait in the south, and continues westward south of Greenland. A northern branch flows eastward north of Iceland and towards the Faroe Islands (the East Icelandic Current, EIS), where it meets warm Atlantic Water. The Icelandic Front (IF) is found where the

warm Atlantic Water from the south meets colder water from the north. The front separates the two water masses. It is relatively close to the Faroe Islands, and the warm Atlantic Water flow north of the Faroes (the Faroe Current, FS) becomes a narrow eastward flow.

The main pattern of the southward overflow at greater depth from the north across the Greenland-Scotland ridge and into the North Atlantic is shown in Figures 4 and 5. It contains cold water from the deep layers in the north. In the Faroese area, the main overflow occurs in the bottom layer of the Faroe-Shetland channel in the east, between Shetland and the Faroe Islands. The overflow is part of the mass balance system between northward and southward water flow that again is part of the great conveyor belt known in oceanography, i.e. the thermohaline circulation in the world ocean (Figure 6).

Water masses and radioactivity

Ocean water is characterized by physical and chemical properties as density, temperature and salinity. The world ocean contains large water bodies that can be identified according to their physical and chemical properties. The water bodies are known as “water masses” in oceanography.

Figure 7 illustrates the average water mass distribution around the Faroe Islands. The boundaries between the masses will always be somewhat ambiguous. The water masses have different origins, according to the flow patterns in the open ocean, and this needs to be considered in the case of e.g. a submarine accident. A potential submarine accident would likely occur in a well defined water mass, and radioactivity from the accident would be detected and spread with the flow regime of the water mass in the world ocean.

Vertical profiles of Cs-137 and Sr-90 have been taken around the Faroe Islands. Results from a survey in August 1990 at a station north of the islands (Figure 8) are shown in Figure 9, together with the ratio between the activity concentrations (Dahlgaard *et.al.*, 1991). The position is at 63^{o}N20’N6^{o}05’W, where the bottom depth is 2400m. The origin of the samples as related to water mass specification was determined from hydrographical analyses. A notable maximum is observed in the profiles at 400m. The ratios indicate input of the isotopes from other sources than global fallout. The range of the isotope ratio is 2.1-3.0, and Dahlgaard *et al.* conclude that it corresponds to increased input from Sellafield/Chernobyl, and that the peak at 400m depth as based on results from their hydrographical measurements corresponds to input of seawater from the Greenland Sea (cf. Figure 5). The lowest ratio of 2.1 at 1000m may still be considered relatively high compared to the fallout ratio of about 1.5, as this water had not recently been in contact with the atmosphere.

Long term time series of radioactivity in Faroese waters are shown in Figures 10 and 11 (AMAP, 2010), together with measurements from off the west and east coasts of Greenland. The activity concentrations are generally observed to be lower off the Faroe Islands than off the Greenland coasts. A signal from the Chernobyl accident can be seen in the Faroese data set.

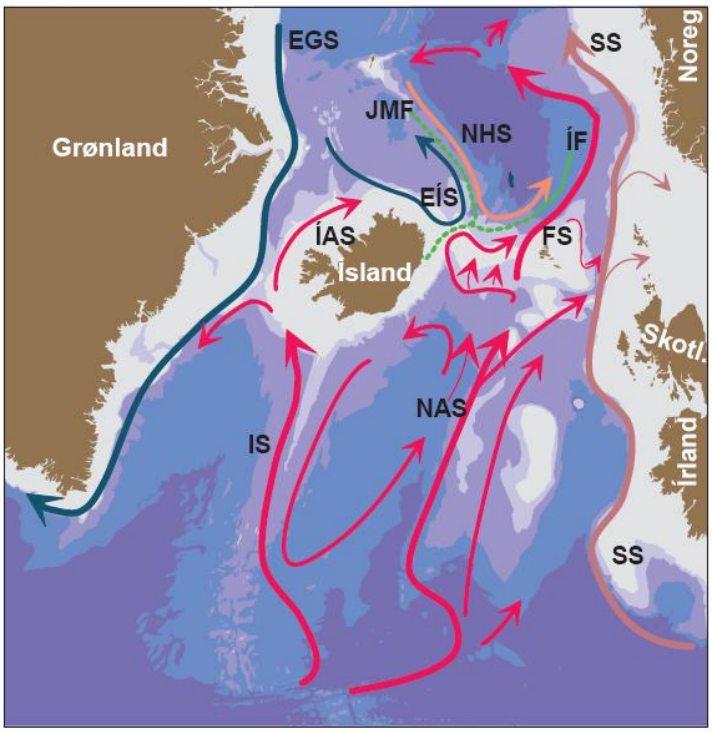

Fig. 3. Upper layer water flows. (Hansen, 2000).

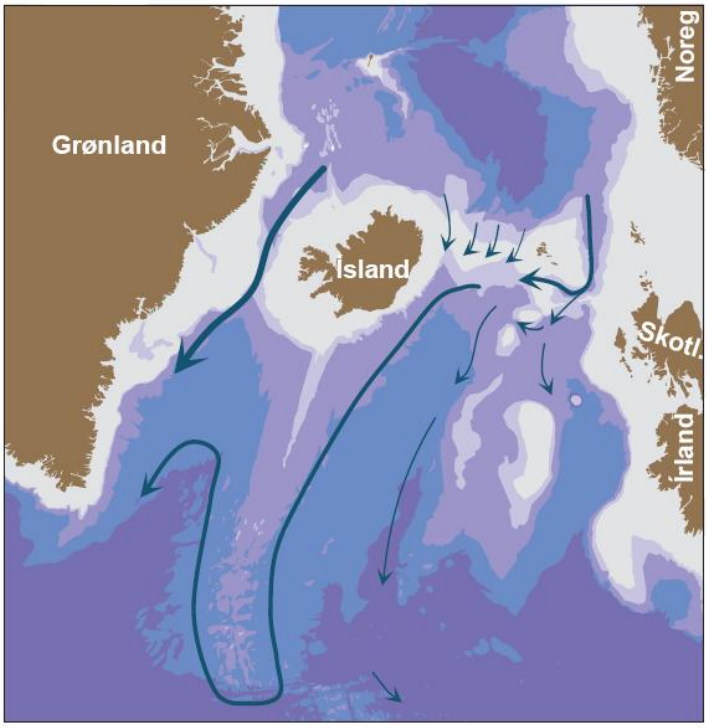

Fig. 4. Main pattern of overflow water. (Hansen, 2000).

Fig. 5. Cold southward flow over the Greenland-Iceland-Scotland ridge. The blue area illustrates the depth below 1000m (Hansen, 2000).

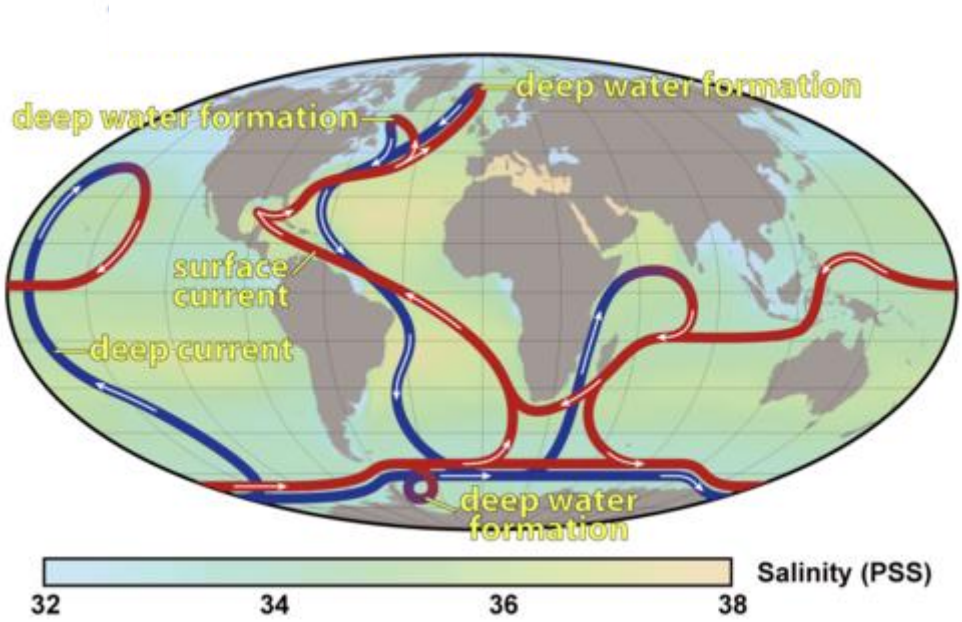

Fig. 6. The conveyor belt showing the thermohaline circulation in the world ocean (picture from internet).

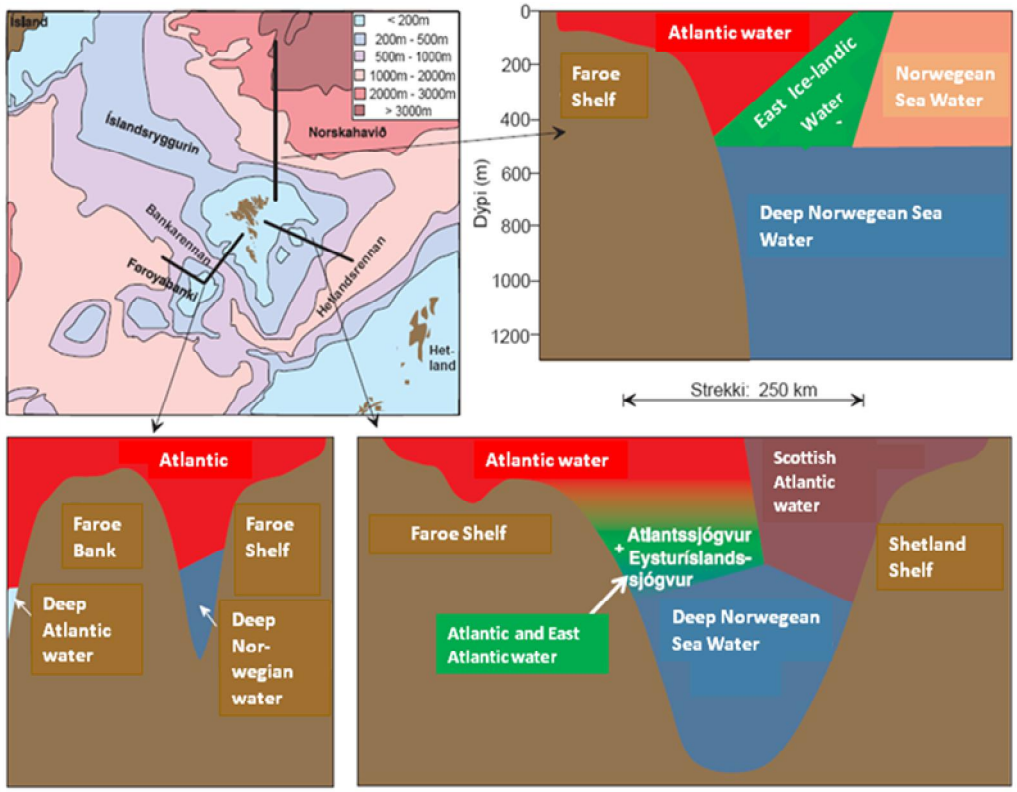

Fig. 7. Typical water mass distribution. (Hansen, 2000).

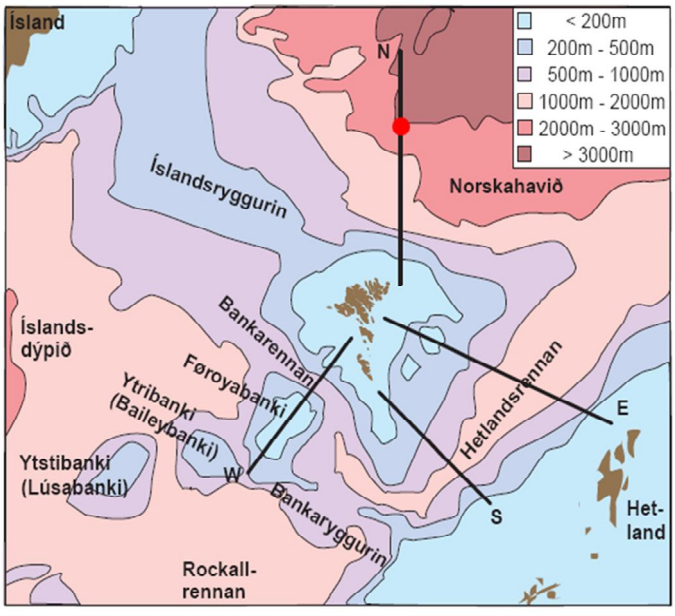

Fig. 8. Bottom topography. Depth profiles in Figure 9 were taken at the station marked with the red dot.

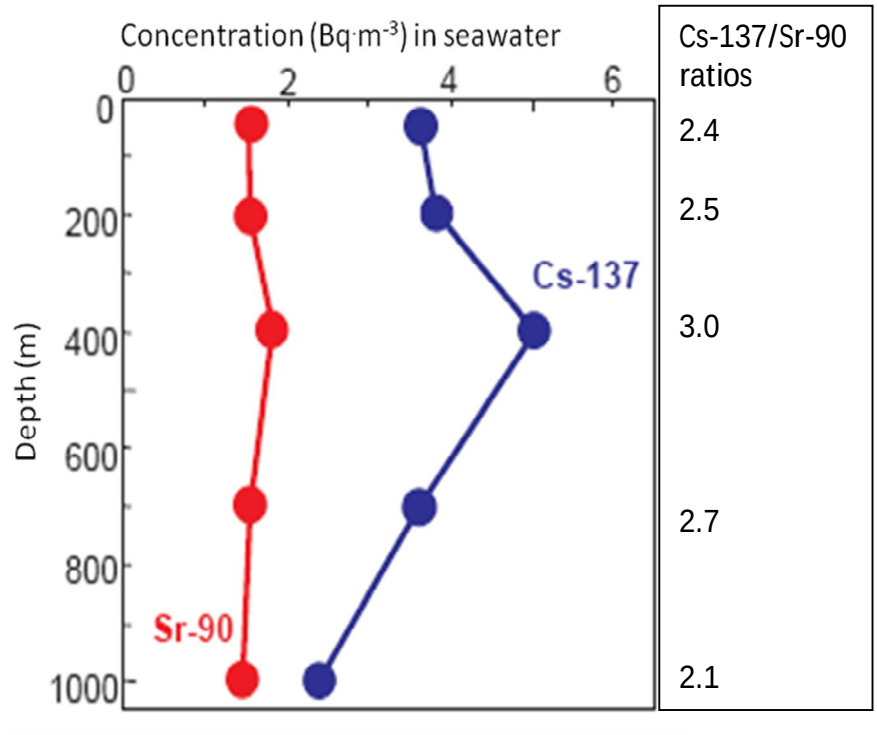

Fig. 9. Profiles of Cs-137 and Sr-90 north of the Faroes in August 1990(cf. Fig. 8).

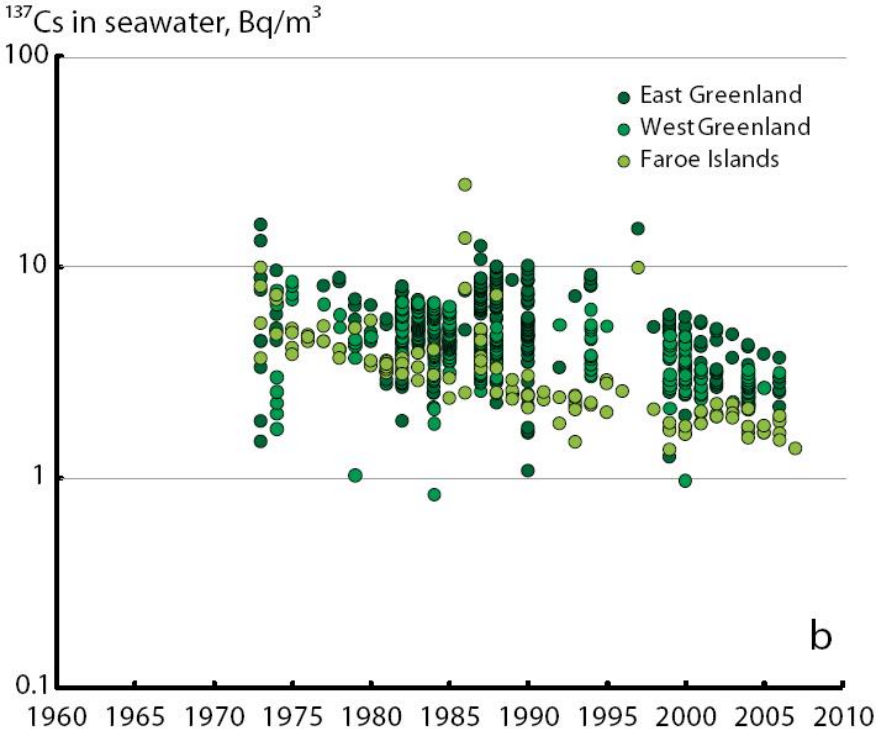

Fig. 10. Cs-137 in seawater off the coasts of the Faroe Islands and Greenland.

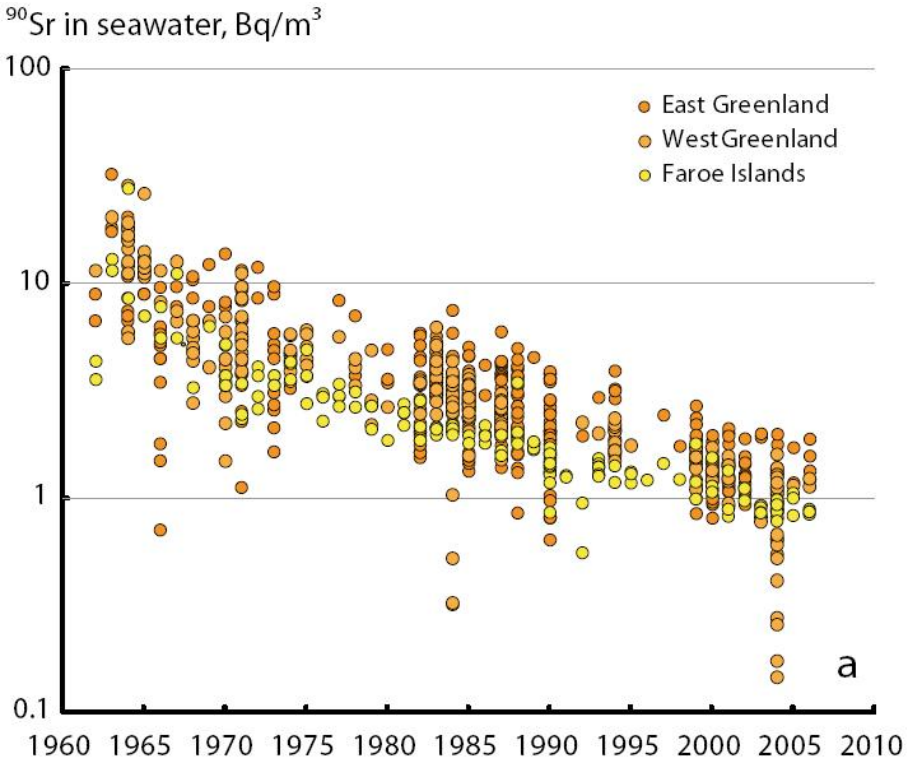

Fig. 11. Sr-90 in seawater off the coasts of the Faroe Islands and Greenland.

References

AMAP Assessment 2009: Radioactivity in the Arctic. Oslo 2010. ISBN 13 978-82-7971-059-2

Aure, J. et al., 1998. Havets miljø 1998. Fisken og havet, særnr. 2. Bergen: Havforskningsinstituttet. (In Norwegian)

Dahlgaard, H.; Hansen, B.; Joensen, H.P. Observations of radioactive tracers in Faroese waters. ICES, C.M. 1991/C:26

Hansen, B. 2000. Havið (*The Ocean*) ISBN: 99918-0-248-7. (In Faroese)

3.3 Iceland

Sigurður Emil Pálsson, Geislavarnir Rikisins, Iceland
Kai Logemann, School of Engineering and Natural Sciences, University of Iceland

The following are excerpts from the MARICE-E-report MER-13-2012, which give a glimpse of the structure of the marine model used at the University of Iceland and which has been used within COSEMA for analysing some untypical release and dispersion events in the North Atlantic.

Introduction

In order to simulate the hydrography of Icelandic waters the workgroup MARICE at the University of Iceland has developed the numerical ocean model CODE. With this report a detailed description of the recent model version CODE 9.221 is given and its output is presented: the hydrography of Icelandic waters during the time period 1992 to 2006. The model was forced by the 6 hourly NCEP/NCAR re-analysis atmospheric fields. Daily river discharge data of 58 Icelandic rivers, estimated by the hydrological model WaSiM operated by the Icelandic Meteorological Office, were included as well as all available CTD profiles recorded from 1992 to 2006 in Icelandic waters. The CTD data was assimilated into the simulation. I.e. with an iterative procedure correction terms were determined which minimised the deviation between simulated and observed temperature and salinity profiles.

The presentation of the model output is confined to charts of monthly mean flow, temperature and salinity at the depth of 50 m and to overall model error estimations. For a more profound analysis of the data set the reader is referred to the following publications of the authors.

Model description

CODE (Cartesian coordinates Ocean model with three-Dimensional adaptive mesh adaption and primitive Equations) is a three-dimensional, primitive equations, z-level, coupled sea ice/ ocean model. The basic idea behind CODE is the simulation of basin-scale ocean dynamics (length scale in the order of 10000 km) including the small-scale structures, with length scales less than 10 km, of selected areas of interest. Additionally the computational costs of the simulation should be minimised to enable the computation of multi-decadal runs within an acceptable length of time. Both points could be realised using the technique of adaptive mesh refinement. Though this involves more complicated numerical methods the disadvantages of conventional nesting (higher computational effort, missing coupling between several model runs, numerical errors at open boundaries) or finite element (higher computational effort) approaches could be avoided. The simulation presented here – entire North Atlantic/Arctic Ocean with highly resolved (1 km) Icelandic waters – was computed on an Intel Xeon 3.33 GHz CPU and needed 92 hours for the simulation of one year.

First CODE application in COSEMA

Based on topographic and hydrographic criteria nine compartment boxes, horizontally dividing the Icelandic waters, were defined (Figure 18 and Table 2). These definitions

were transferred into the ocean model and a series of model experiments were carried out. Within these experiments the mean current and diffusion fields averaged over the period 1992 to 2006 were used. At the beginning of each model run a mathematical tracer concentration was set to 1 within one of the boxes. Then the advective and diffusive spreading of this concentration was simulated. After the simulation time of 24 hours the model was stopped, and the according flux rates between the boxes were computed (Figure 19).

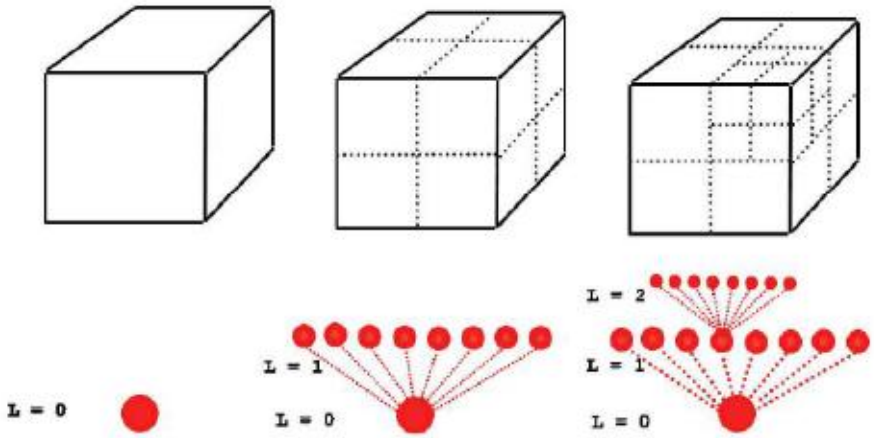

Fig. 12. Schematic process of adaptive grid refinement, following the algorithm of Khokhlov (1998). The large cube on the left side (adaption level 0) is split into 8 “children” of adaption level 1. Hence the model equations are no longer solved on the “parent cell”. However, the “parent cell” is not removed from the computer’s memory. It is obtaining the average properties of its children at each time step instead.

Overall view of model over the North Atlantic:

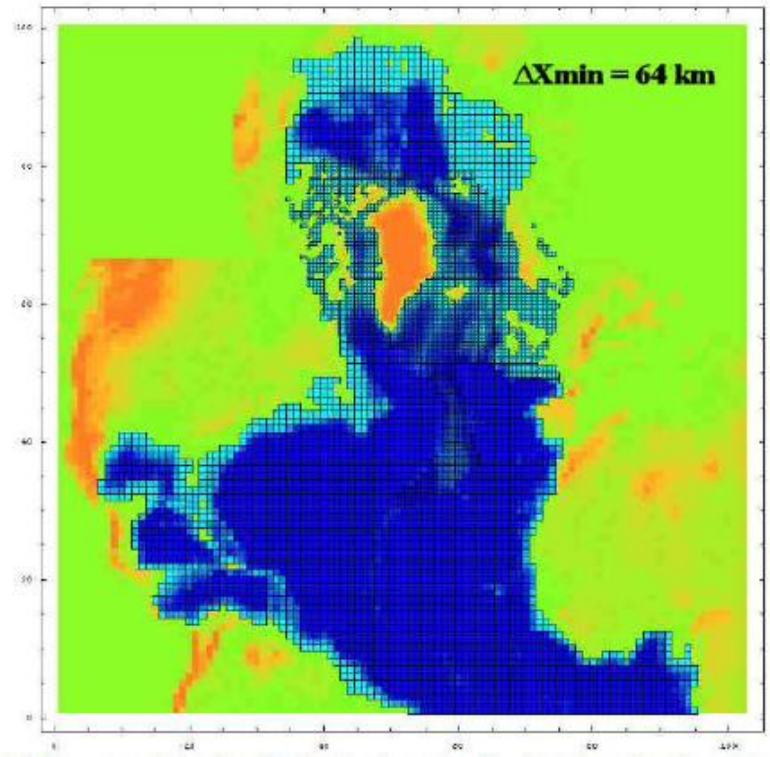

Fig. 13. The computational mesh after the first step of horizontal mesh refinement.

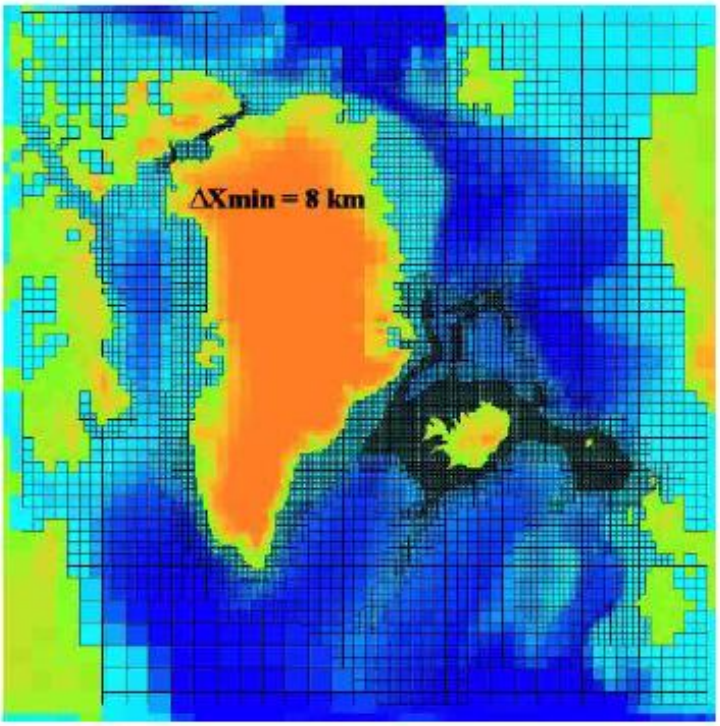

Fig. 14. The computational mesh after the fourth step of horizontal mesh refinement.

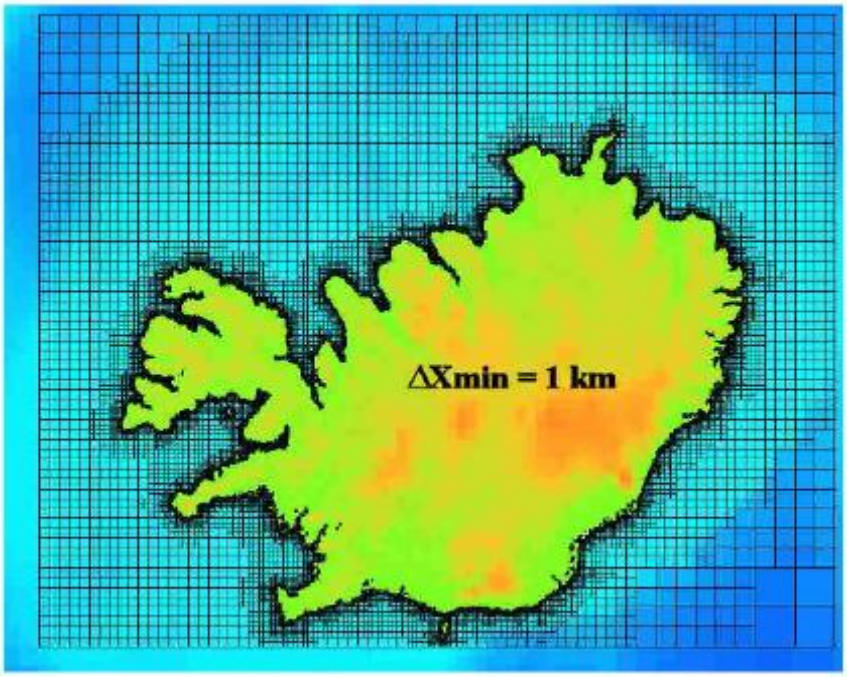

Fig. 15. The computational mesh after the final seventh step of horizontal mesh refinement.

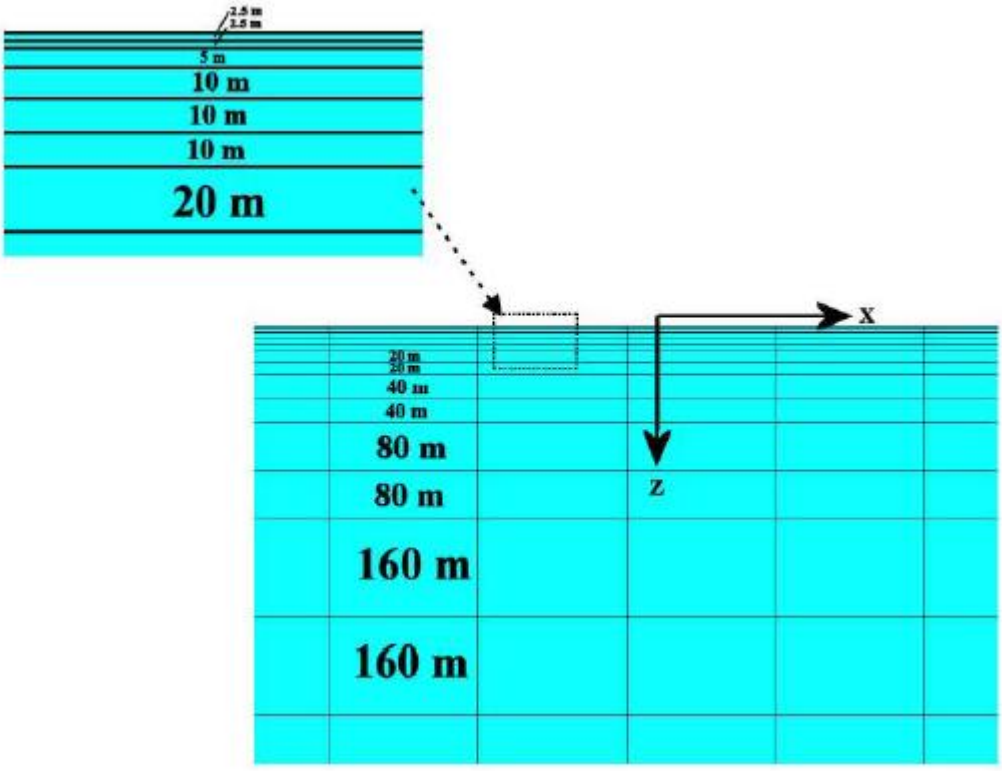

Fig. 16. The computational mesh's vertical structure.

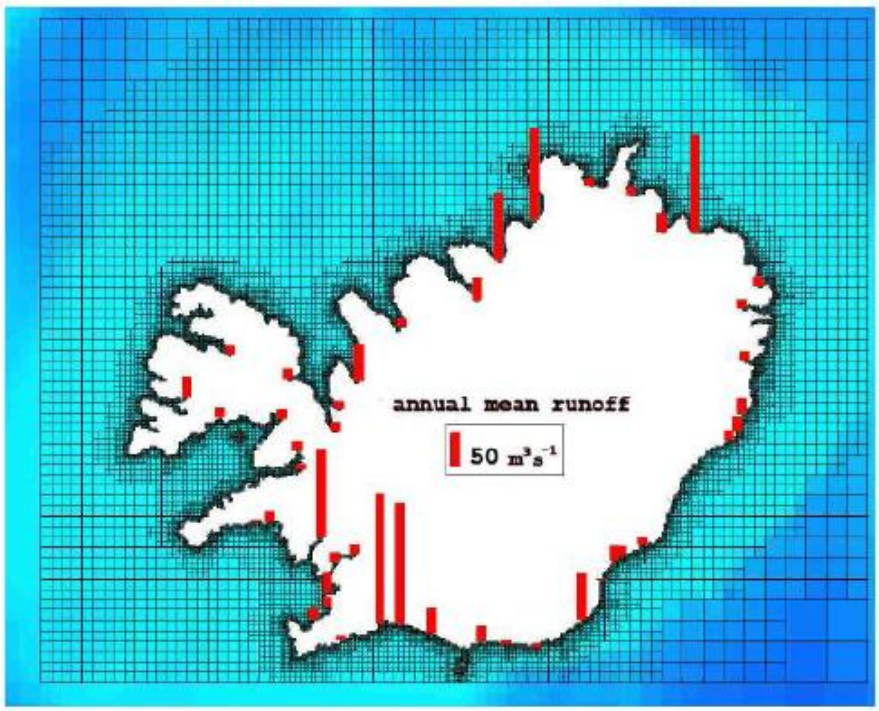

Fig. 17. The location and mean discharge of rivers included within the simulation.

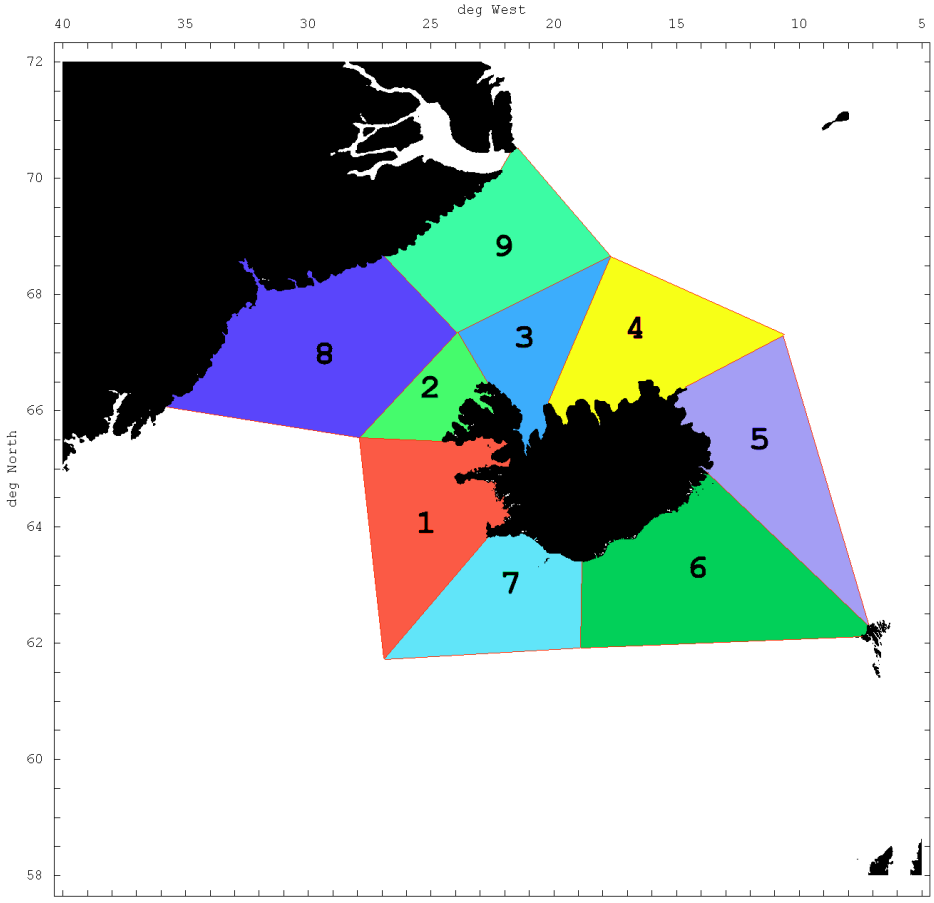

Fig. 18. Definition of compartmental boxes for modelling in COSEMA.

Table 2. Volume and depth of boxes.

box no.	volume (m^3)	mean depth (m)
1	0.30875736E+14	0.41388681E+03
2	0.45874487E+13	0.19979407E+03
3	0.14862981E+14	0.39440656E+03
4	0.42704377E+14	0.69592224E+03
5	0.50321238E+14	0.62822296E+03
6	0.11065060E+15	0.92798999E+03
7	0.69452649E+14	0.10830667E+04
8	0.40931894E+14	0.41316107E+03
9	0.51804176E+14	0.84404614E+03

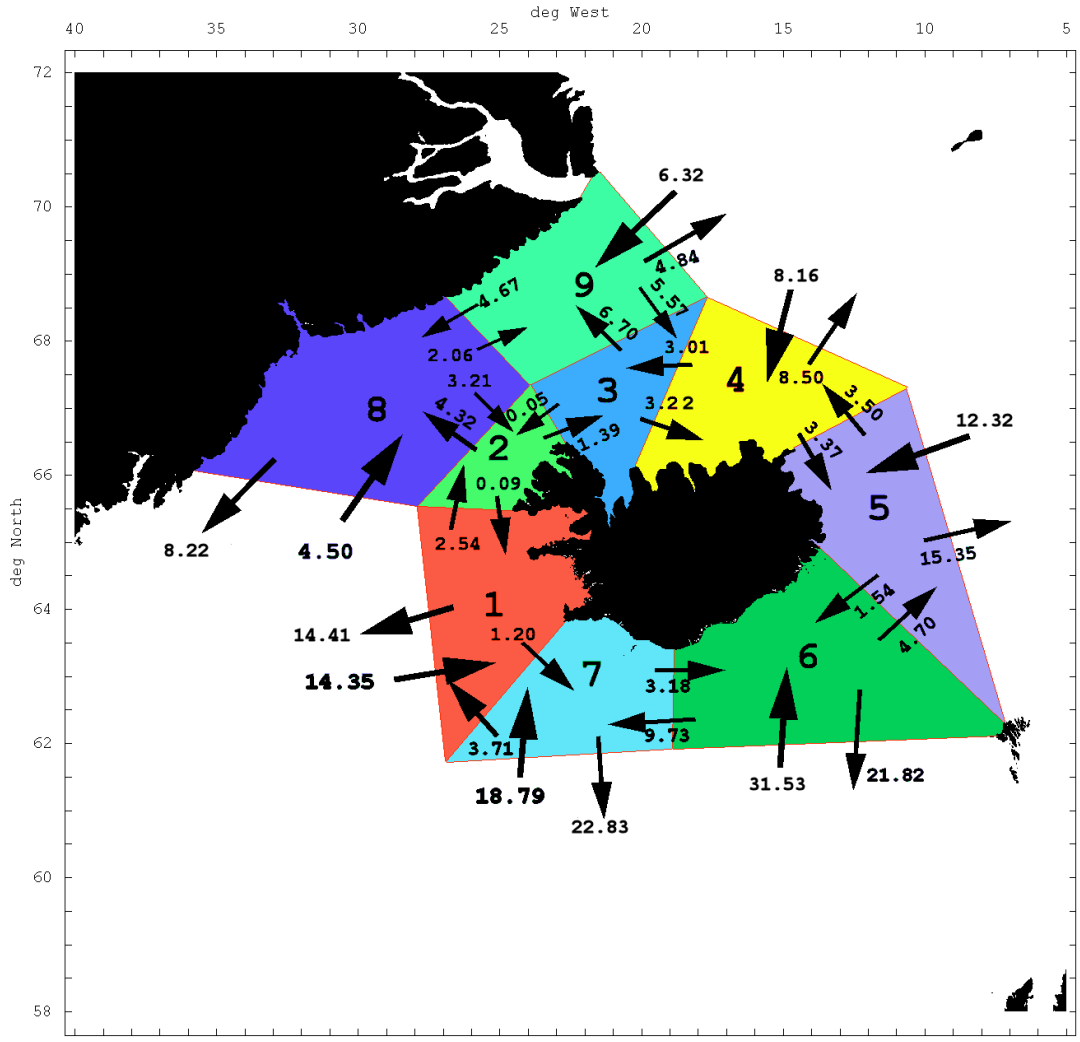

Fig. 19. Boxes with transfer parameters, flow rates between boxes in Sverdrup (1 Sv = 10^6 m^3 m^{-1}).

References

Logemann, K. and Harms, I.: High resolution modelling of the North Icelandic Irminger Current (NIIC), Ocean Sci., 2, 291-304, 2006.

Logemann, K., Olafsson, J., and Marteinsdóttir, G.: The ocean model CODE and its application to Icelandic waters, MARICE E-report MER-10-2010, University of Iceland, pp. 93, http://www.marice.is/ereports/MER-10-2010.pdf, 2010.

Logemann, K., Olafsson, J. & Marteinsdóttir, G. 2012. Modelling the hydrography of Icelandic waters from 1992 to 2006. MARICE-E-report MER-13-2012 (http://www.marice.is/ereports.htm)

4 RADIOACTIVE SOURCE TERM ANALYSES

4. 1 Nuclear power plant accident source term

Juhani Lahtinen, Radiation and Nuclear Safety Authority – STUK, Finland

4.1.1 Background

At the project meeting in March 2012 it was decided that the releases to the ocean in Fukushima should be used as a basis of the COSEMA source term. It is known that the situation in Fukushima was quite a complex one: there were three reactor facilities affected and there were planned and unplanned releases. In addition, deposition of airborne radioactive releases onto sea also constituted a source that – according to some estimates – is about the same order as (or for some nuclides even much bigger than) the direct releases to the ocean. Rain water washout of contaminated soils has also been mentioned but this contribution will become detectable in course of time as the concentrations along the coast have decreased.

Several papers and other documents addressing the marine source term of Fukushima have been published (see the list of references representing the situation in the autumn 2012). Some assessments rely mostly on measurements of concentrations in sea water, some on measurements and model calculations, and a few primarily on calculations. Most documents deal only with caesium (^{137}Cs, ^{134}Cs) and (sometimes) ^{131}I. Estimated quantitative values of direct releases to the ocean vary, although it is generally agreed that the planned release of waste water which was “slightly contaminated” is insignificant as compared to the unplanned releases:

- ^{137}Cs: from 3.5 to 27 PBq.
- ^{134}Cs: about the same as for ^{137}Cs.
- ^{131}I: from 11 to about 80 PBq.

Better and more reliable estimates are likely to be available after the UNSCEAR report (mentioned in Weiss, 2012) will be published.

STUK, which was responsible for defining the nuclear power plant source term to be used in COSEMA calculations, decided to use the paper of Bailly du Bois et al. (2011) as the basic source for source term estimation. It is likely that the source term – described originally in the project document “Marine source term of Fukushima nuclear power plant accident for NKS/COSEMA project” (Lahtinen; STUK, rev. 2, 9.5.2012) – is conservative; this was discussed briefly at the project meeting in Oslo in September 2012 but no changes were made.

One of the reasons to use the paper of Bailly du Bois as a corner stone was that it is based on measurements and that it considers also some other nuclides than caesium isotopes and ^{131}I.

4.1.2 Fukushima source term

Bailly du Bois et al. (2011) took the advantage of measurement results when estimating the marine source term of Fukushima (Figure 20). They derive the following conclusions:

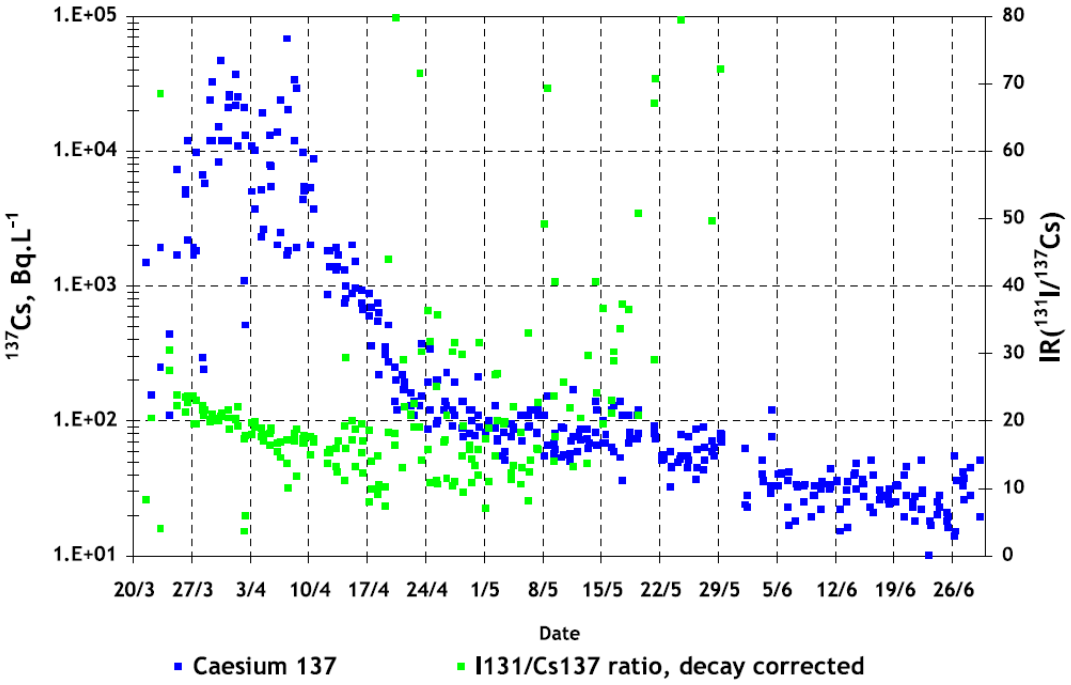

Fig. 20. Evolution of ^{137}Cs concentrations and ^{131}I/^{137}Cs ratios in sea water at less than 2 km from the Fukushima Dai-ichi power plant (Bailly du Bois et al., 2011).

- Release of 27 PBq (12 PBq – 41 PBq) of ^{137}Cs from March 21 to July 18.
- ^{134}Cs/^{137}Cs concentration ratio was close to 1 and the decay-corrected ^{131}I/^{137}Cs ratio close to the plant was 24–18 from March 26 to April 8.
- ^{90}Sr/^{137}Cs and ^{99}Tc/^{137}Cs concentration ratios were 0.02 and 0.01 respectively (rough estimates).

In order to define a source term utilizing the results given in Bailly du Bois et al. one can make the following assumptions:

- All measured activities result from direct releases to the sea.
- All contaminated water was released from the core of Unit 2 (BWR type, 760 MW_e, 2380 MW_{th}). (This of course is not true.)
- The release took place from March 26 to April 8.
- ^{134}Cs and ^{137}Cs activity concentrations in sea water were the same.
- Decay-corrected ^{131}I/^{137}Cs concentration ratio in water was 20.
- ^{90}Sr/^{137}Cs and ^{99}Tc/^{137}Cs concentration ratios in water were 0.02 and 0.01 respectively.
- Total ^{137}Cs release was 25 PBq.

From the above the released (decay-corrected for I-131) total activities can be estimated:

- ^{137}Cs: 25 PBq (corresponds approximately to a release fraction of 11 %)[1].
- ^{134}Cs: 25 PBq (11 %)[1]
- ^{131}I: 500 PBq (23 %)[1]
- ^{90}Sr: 0.5 PBq (0.3 %)[1]
- ^{99}Tc: 0.25 PBq (^{99}Tc activity originates apart from direct fission also from the decay of ^{99}Mo and ^{99m}Tc-99)[2]

If one follows here the same conventional procedure as in the case of releases to the atmosphere, the caesium release fraction given above can be applied to the caesium group (see Table 3), ^{131}I release fraction to the iodine group and ^{90}Sr release fraction to the strontium group. ^{99}Tc implies that nuclides in the ruthenium group were also released. This is supported by the fact that ^{58}Co was detected in the water too (TEPCO, 2011). In addition, tellurium (and ^{132}I originating from the decay of ^{132}Te) was found (IRSN, 2011a; IRSN, 2011c).

Table 3. Nuclide groups (NUREG, 1990)[3].

Inert gases	Kr-85, Kr-85m, Kr-87, Kr-88, Xe-133, Xe-135
Iodine	I-131, I-132, I-133, I-134, I-135
Cesium	Rb-86, Cs-134, Cs-136, Cs-137
Tellurium	Te-127, Te-127m, Te-129, Te-129m, Te-131m, Te-132, Sb-127, Sb-129
Strontium	Sr-89, Sr-90, Sr-91, Sr-92
Ruthenium	Co-58, Co-60, Mo-99, Tc-99m, Ru-103, Ru-105, Ru-106, Rh-105
Lanthanium	Y-90, Y-91, Y-92, Y-93, Zr-95, Zr-97, Nb-95, La-140, La-141, La-142, Pr-143, Nd-147, Am-241, Cm-242, Cm-144
Cerium	Ce-141, Ce-143, Ce-144, Np-239, Pu-238, Pu-239, Pu-240, Pu-241
Barium	Ba-139, Ba-140

[1] The nominal equilibrium inventory of the Olkiluoto BWR (2500 MW_{th}) is used as a reference. Note that the actual Fukushima inventory depends on the fuel burn-up and the power history before scram (and also partly on the fuel composition details).

[2] ^{99}Tc activities are normally not given in the lists of important radionuclides in a reactor.

[3] There also exist groupings that differ a bit from the one presented here.

4.1.3 Source term for COSEMA

The possible nuclear power plant sites of interest in COSEMA are Loviisa (PWR, 1500 MW_{th}), Olkiluoto (BWR, 2500 MW_{th}), Forsmark (BWR, 3300 MW_{th}), Ringhals (PWR, 3135 MW_{th}) and Oskarshamn (BWR, 3300 MW_{th}). There are several units at every site but those mentioned have the greatest thermal power. If actual inventories are not available, the inventories of the Loviisa and Olkiluoto reactors can be scaled and used in calculations.

As a very crude and probably conservative approximation one may assume that the release fraction for the tellurium group is the same as that for caesium and the release fraction for the ruthenium group is the same as that for strontium. Taking this and the reasoning in the preceding section into account the release fractions for the COSEMA studies can be chosen to be: iodine 20 %, caesium 10 %, tellurium 10%, strontium 0.5 %, ruthenium 0.5 %. Other groups with smaller release fractions can be considered if needed.

It is realistic to assume that there is a delay between the reactor shutdown and start of the release. A 10-hour delay could be used, for example.

Two release periods could be considered: three days and three weeks.

References

Bailly du Bois P., Laguionie P., Boust D., Korsakissok I., Didier D., Fievert B. (2011). *Estimation of marine source-term following Fukushima Dai-ichi* accident. Journal of Environmental Radioactivity (2011), doi:10.1016/j.jenvrad.2011.11.015. Available online 14 December 2011.

Buesseler K., Aoyma M., Fukasawa, M. (2011). *Impacts of the the Fukushima nuclear power plants on marine radioactivity*. Environmental Science & Technology 45; 23; 9931–9935.

EC (2012). *Rasff News. Food Information Exchange. News: 11-653-add30.* European Commission, Health & Consumers Directorate-General. January, 2012. http://ec.europa.eu/energy/nuclear/radiation_protection/doc/emergencypreparedness/20120103_infomsg.pdf.

IRSN (2011a). *Impact on marine environment of radioactive releases from the Fukushima-Daiichi nuclear accident.* IRSN, 13th May 2011. http://www.irsn.fr/EN/news/Documents/IRSN_Fukushima-Accident_Impact-on-marine-environment-EN_20110513.pdf

IRSN (2011b). *Synthèse actualisée des connaissances relatives à l'impact sur le milieu marin des rejets radioactifs du site nucléaire accidenté de Fukushima Dai-ichi*. IRSN, 26th October 2011. http://www.irsn.fr/FR/Actualites_presse/Actualites/Documents/IRSN-NI-Impact_accident_Fukushima_sur_milieu_marin_26102011.pdf.

IRSN (2011c). *Fukushima Ocean Release Study, Now In English*. English translation of the above document IRSN (2011b). http://www.simplyinfo.org/?p=3818.

IRSN (2012). *Summary of the Fukushima accident's impact on the environment in Japan, one year after the accident*. IRSN, 29rd February 2012. http://www.irsn.fr/EN/publications/thematic/fukushima/Documents/IRSN_Fukushima-Environment-consequences_28022012.pdf.

Katata G., Ota M., Terada H., Chino M., Nagai H. (2011). *Atmospheric discharge and dispersion of radionuclides during the Fukushima Dai-ichi Nuclear Power Plant Accident*. Journal of Environmentral Radioactivity 109; 1; 103–113.

Kawamura H., Kobayashi T., Furuno A., In T., Ishikawa Y., Nakayama T., Shima S., Awaji T. (2011). *preliminary numerical experiments on oceanic dispersion of ^{131}I and ^{137}Cs discharged into the ocean because of the Fukushima Daiichi nuclear power plant disaster*. Journal of Nuclear Science and Technology 48; 11; 1349–1356.

NERH (2011). *Report of the Japanese Government to the IAEA Ministerial Conference on Nuclear Safety. The Accident at TEPCO's Fukushima Nuclear Power Stations.* Nuclear Emergency Response Headquarters, Government of Japan. June 2011. http://www.kantei.go.jp/foreign/kan/topics/201106/iaea_houkokusho_e.html.

NUREG (1990). Severe Accident Risks: An Assessment for Five U.S. Nuclear Power Plants. Final Summary Report. U.S. Nuclear Regulatory Commission, NUREG-1150.

TEPCO (2011). http://www.tepco.co.jp/en/nu/fukushima-np/f1/index2-e.html.

Tsumune T., Tsubono T., Ayonoma M., Hirose K. (2011). *Distribution of oceanic ^{137}Cs from the Fukushima Dai-ichi Nuclear Power Plant simulated numerically by a regional ocean model*. Journal of Environmental Radioactivity (2011), doi:10.1016/j.jenvrad.2011.10.007. Available online 8 November 2011.

Weiss, W. (2012). *Preparing a scientific report to the General Assembly on 'Exposures due to the nuclear accident following the Great East-Japan earthquake and tsunami'*. Journal of Radiological Protection 32; 1; N113–N118. doi:10.1088/0952-4746/32/1/N113. Available online 6 March 2012.

In addition, a special issue of the Journal of Environmental Radioactivity (volume 111, September 2012) *Environmental Impacts of the Fukushima Accident (Part I)* contains some papers dealing with releases to the sea.

4.2 Submarine accident source term

Mikhail Iosjpe, Norwegian Radiation Protection Authority - NRPA

Inventory

The source term consists of an inventory of radionuclides, released as a function of time and a release point. Each of these elements will be described below.

The core inventory has primarily two components: the fuel matrix itself and the fuel burn-up. While the fuel matrix itself has only indirect influence on the amount of fission products, the amount of transuranics and release rates will depend directly on the type of matrix. In the current work, with its emphasis on a credible approach, the most probable representation of a Russian third-generation submarine core is a core load with 63% enriched fuel with 259.7 kg U-235 in a dispersion (UO_2-Al/ UO_2-Zr) or intermetallic configuration (UAl_x-Al) (Reistad, 2008). This composition has been verified to fit the only suggested core geometry for other than first-generation Russian submarines. However, as there exist an indefinite number of core configurations corresponding to various fuel volumes, the selection criterion has been to apply similar fuel density (4.5 Ug/cm^3) as that reported for Russian floating nuclear power plants under construction (Chuen and Reistad, 2007). A maximum credible inventory has been developed on the basis of a conservative approach to the average annual burn-up for third-generation reactors.

Average annual burn-up has been calculated to 30 effective full-power days (EFPD) and the maximum operational period hypothetically set to 20 years. At present, the average life-span for this class of vessels is 13.2 years. As the current decommissioning rate is higher than the commissioning rate, we may assume that this value will decrease slowly in the future. However, as the selection criterion has been a maximum credible burn-up, and normal vessel life is more than 13.2 years, we may assume 20 years of operation as a conservative estimate as a basis for calculating the radionuclide inventory at the time of the accident. The resultant burn-up is 114,000 MWd, or 269,000 MWd/tons of heavy metal. We have also assumed an operating power fraction of 0.5 at the time of accident, resulting in a high inventory of short-lived isotopes when the hypothetical accident occurs. The core inventory and core decay heat were developed using HELIOS 1.8 and SNF 1.2. HELIOS is a detailed reactor physics transport and burn-up code developed and supported by Studsvik Scandpower (Reistad, 2008).

Accident scenario

The hypothetical scenario forming the basis for this study, is if a core-melt / loss-of coolant accident (LOCA) (Reistad , 2008) was to occur together with another type of incident, such as an explosion. Then there would be a credible risk of substantial damage to all parts of the submarine. An explosion that ruptured the hull and provided water intrusion in the reactor compartment would also contribute to cooling the corium.

In this study, we will use the scenario described in Table 4, which corresponds to Scenario 1 from (Reistad, 2008).

Table 4. Release fractions for maximum credible accident for third-generation submarine.

	Phase 1: From t=0.1 days to t=1 year	Phase 2: From t=1 year
Coremelt release	Immediate release of release fraction as given in Table 4 (High flux reactor)	
Fuel corrosion	Constant release of fuel corrosion products: corrosion rate: 0.01 % of fuel material annually	

Release fractions

The main methodological problem here is the lack of relevant information on fuel materials, and secondly, on radionuclide behavior in fuel matrixes under extreme conditions (high temperature, saltwater intrusion etc.). However, a civilian nuclear system with potentially similar attributes to those of third-generation reactors – high power densities, high enrichment levels and moderate burn-up levels (50%) – is found in civilian research reactors. The hypothetical correspondence in fuel design and fuel properties has formed the basis for assessments of fuel consumption, as in (Reistad,2008). Few civilian research facilities have been analyzed on the basis of probabilistic methods; deterministic accident analysis remains the most applied method for these facilities. The source term evaluation for research facilities displays differences similar to those shown in Table 5, describing the release fractions for three HEU (highly enriched uranium) highly enriched uranium highly enriched uranium - fueled research reactors.

Table 5. Release fractions in the case of core meltdown following a LOCA (Abou Yehia and Bars, 2005).

	HIFAR	High flux reactor	SAFARI
Noble gases	1	1	1
I	0.3	0.8	1
Br		0.8	
Cs	0.3	0.8	0.163
Te	0.01	0.8	0.192
Rb	0.3	0.01	
Ru	0.01	0.1	0.005
Ba, Rh, Sr		0.1	
Actinides		0.01	0.1
Other		0.01	

The second component of the release fraction is fuel degradation and corrosion. Based on the hypothesis of the fuel matrix and the accident scenario, the corrosion processes of the uranium-loaded fuel component, UO_2 or UAl_x, starts immediately when the seawater enters the primary circuit. Experiments for long-term dissolution of fuel elements in seawater obtained dissolution rates from 0.1 to 1% of the fuel per year at temperatures from 10 to 20^{o}C (Petrov, 1991).

Release Scenario

The total and the individual releases of the radionuclides that had the most significant effect on the release rates during the initial and later phases of accidental releases are presented in Figure 21. As expected, the maximum release occurs during the initial period after the accident (the instant release fraction) with maximum values of $1.6 \cdot 10^{18}$ Bq at the beginning of release. Figure 20 shows that short-lived radionuclides of iodine and barium are most significant during the initial phase of release according to the present scenario, while ^{90}Sr and ^{137}Cs dominates in the final period of release.

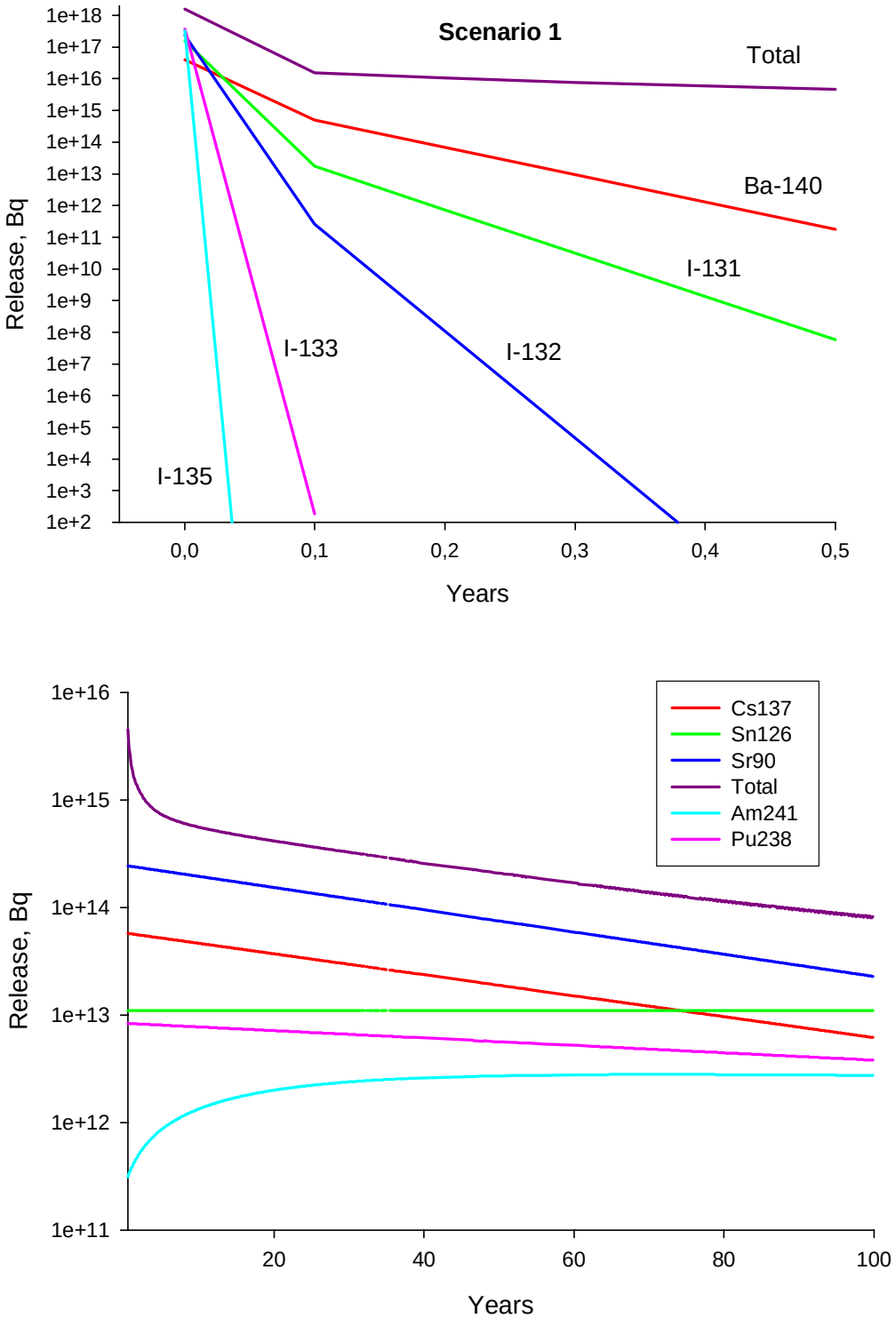

Fig. 21. The release scenario for the initial time of 0-0.5 year (top) and for the time 0.5-100 years (bottom)

References

Abou Yehia H. and G. Bars, 2005. Disparities in the safety demonstrations for research reactors and the need for harmonization. In: Joint Meeting of the National Organization of Test, Research, and Training Reactors and the International Group on Research Reactors, September 12-16, Gaithersburg, MD, 2005.

http://www.ncnr.nist.gov/trtr2005/Proceedings/Abou-Yehia%20-%20Disparities%20in%20safety%20Demonstrations.pdf

Chuen C. and O. Reistad (2007). Sea Fission – Russia's Floating Nuclear Power Plants. Jane's Intelligence Review 2007, 19(12), 48 – 52.

Iosjpe M., Reistad O., Liland A. (2011). Radioecological consequences after a hypothetical accident with release into the marine environment involving a Russian nuclear submarine in the Barents Sea StrålevernRapport 2011:3. Østerås: Statens strålevern, 2011.

Petrov, E., 1991. Estimation of the Nuclear Power Plant Condition and Radiation and Ecological Consequences of a Prolonged Stay of the SSN 'Komsomolets' on the Sea Bed and During Its Recovery, (unpublished), submitted from the Russian Central Design Bureau Marine Engineering "Rubin" to the Norwegian Government, November 15, 1991.

Reistad, O., S. Hustveit & S. Roudak, 2008. Operational and Accident Survey of Russian Nuclear Submarines for Risk Assessments using Statistical Models for Reliability Growth, *Annals of Nuclear Energy*, 35(11), 2126-2135.

Reistad O., 2008. Analyzing Russian naval nuclear safety and security by measuring and modeling reactor and fuel inventory and accidental releases. Doctoral thesis at NTNU, 2008:14.

5 CALCULATION SCENARIOS

5.1 Nuclear power plant accidents

Vesa Suolanen, Technical Research Centre of Finland - VTT , Nuclear Energy

5.1.1 Assumptions

As examples of consequences of severe nuclear power plant accidents in the Baltic Sea area, two hypothetical release scenarios were modelled: release from the 'Finnish coast' and release from the 'Swedish coast'. In the 'Finnish coast' release scenario radionuclides are released from a nuclear power plant to a local sea area and further transferred to the Gulf of Finland and to the Northern Baltic Proper. In case of the 'Swedish coast' release scenario, radionuclides are transferred via a local sea area directly to the Northern Baltic Proper. In both scenarios radionuclides are finally mixed to the entire volume of the Baltic Sea (Table 7). A nuclear power plant with two reactor units and a local sea area is shown in Figure 22 below. The considered accidental releases of this study are not directly related to any existing nuclear power plant in Nordic countries.

Fig. 22. Nuclear power plant and local sea area.

The radioactive source term to sea water was determined from the core inventory of the VVER-1000 reactor (Anttila, 2005) and applying further the element specific release fractions obtained in the source term analyses of this study (chapter 4.1, J. Iahtinen). The

used source strength in this study was the same for the both release scenarios, but the location of the release points were different for the two release scenarios. The used fuel burn-up was 50 MWd/kgU. Total released amounts of activity of the considered severe reactor accidents are presented in Table 6.

Table 6. Total amounts of activity released to sea in hypothetical severe accidents release scenarios. There is 71 tU in the core of the reactor (VVER-1000).

Nuclide	Specific activity at shutdown (GBq/tU)	Core activity at shutdown (Bq)	Release fraction	Total release to sea (Bq), t>10 h
C-14	$5.00 \cdot 10^{1}$	$3.55 \cdot 10^{12}$	0.2	$7.10 \cdot 10^{11}$
Co-60	$2.45 \cdot 10^{4}$	$1.74 \cdot 10^{15}$	0.005	$8.70 \cdot 10^{12}$
Sr-90	$3.96 \cdot 10^{6}$	$2.81 \cdot 10^{17}$	0.005	$1.41 \cdot 10^{15}$
Tc-99	$7.12 \cdot 10^{2}$	$5.06 \cdot 10^{13}$	0.005	$2.53 \cdot 10^{11}$
I-131	$3.56 \cdot 10^{7}$	$2.52 \cdot 10^{18}$	0.2	$4.85 \cdot 10^{17}$
Cs-134	$1.03 \cdot 10^{7}$	$7.29 \cdot 10^{17}$	0.1	$7.29 \cdot 10^{16}$
Cs-137	$5.87 \cdot 10^{6}$	$4.17 \cdot 10^{17}$	0.1	$4.17 \cdot 10^{16}$

Consequences of a short-term release (Figures 23 and 24) was considered. The highest activity release rate is obtained for iodine (I-131) which can be clearly seen from the linear scale Figure 23. Other important soluble release nuclides are C-134 and C-137.

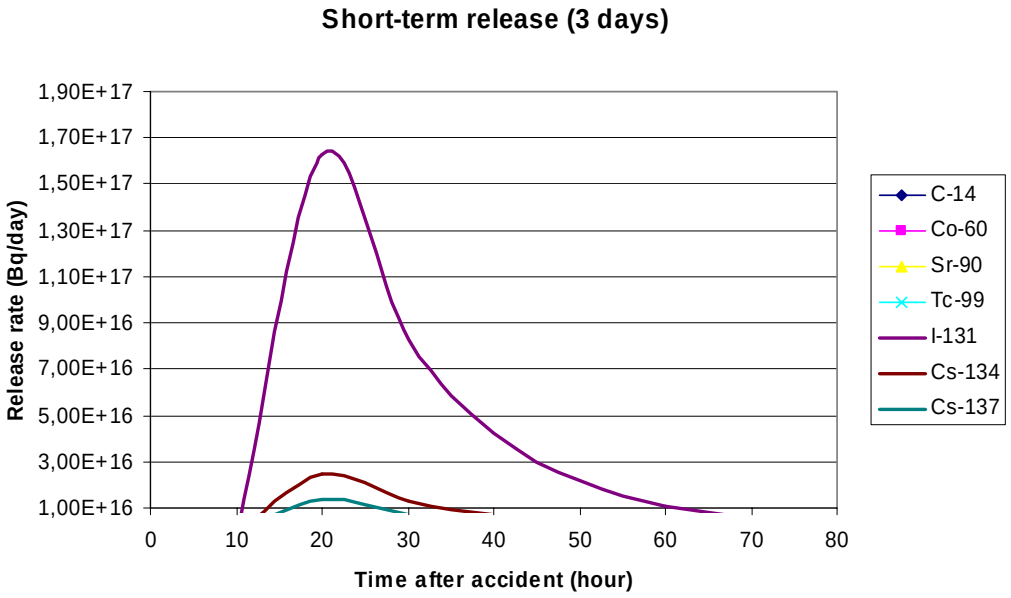

Fig. 23. Release rates temporal behaviour presented in linear scale for the most important radionuclides I-131, Cs-134 and Cs-137.

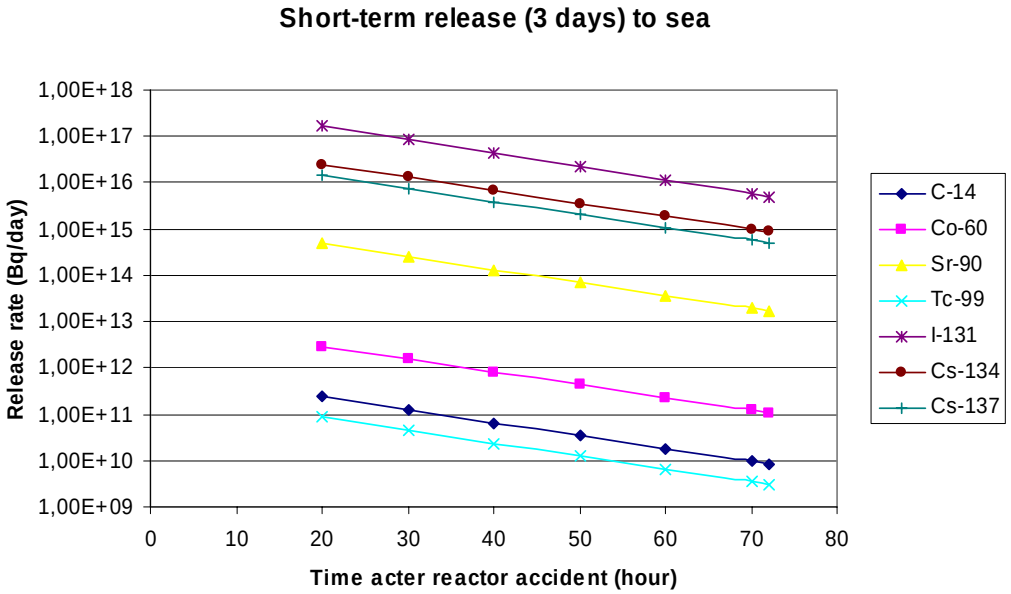

Fig. 24. Release rates of all important radionuclides in the short-term release assumption.

The aquatic transfer model consists of compartments for the local sea area close to nuclear power plant, the Gulf of Finland and the Baltic Sea dispersion area. Each water compartments has connection to bottom sediment layers (sedimentation term) and vice versa (resuspension term). The height of the well mixed surface sediment is 5 cm and for the buried sediment the height is 30 cm in the model. Some main parameter values used in model calculations with DETRA-code (Korhonen, R., et al., 1984(a); Korhonen, R., et al., 1984(b); Suolanen, V., 1994; Suolanen, V., 1996; Suolanen, V., et al., 1998) are presented in Table 7.

Table 7. Parameter values used in radionuclides transfer models for the hypothetical severe reactor accidents scenarios at the 'Finnish coast' and at the 'Swedish coast'.

Water comp. characteristics	Local sea area	Gulf of Finland	Baltic Sea
volume (m^3)	$1.0 \cdot 10^{8}$	$5.5 \cdot 10^{11}$	$1.4 \cdot 10^{13}$
water exchange rate (m^3/a)	$8.8 \cdot 10^{8}$	$6.0 \cdot 10^{11}$	$5.0 \cdot 10^{12}$
suspended sediment load (kg_s/m^3)	$5.0 \cdot 10^{-3}$	$3.0 \cdot 10^{-3}$	$4.0 \cdot 10^{-3}$
sedimentation rate ($kg_s/m^2/a$)	$1.7 \cdot 10^{-1}$	$1.7 \cdot 10^{-1}$	$4.0 \cdot 10^{-1}$

Sediment characteristics	surface sediment	buried sediment
volume fraction of water	90%	72 %
resuspension of sedimented material	10 % of total sedimentation	
water exchange rate	$1\ a^{-1}$	

K_d-values (liter/kg_s)	C_{fish} (Bq/kg_f)/(Bq/liter) ; (IAEA TRS 422 & 472)
C 100	2000
Co 5000	1000
Sr 10	2
Tc 5000	30
I 100	10
Cs 1000	250

5.1.2 Severe release from the Finnish coast

The activity concentrations obtained in the local sea area water after a severe accident are very high, over 10 kBq/liter (Figures 25, 27 and 28). Mixing and the large dilution capacity of the Gulf of Finland and the Baltic Sea will effectively decrease the radionuclide concentrations in time. For example Cs134 and Cs137 concentrations in the Baltic Sea reach the maximum of about 1 Bq/liter in seawater after about one year from a hypothetical release event at the Finnish coast. The radionuclide concentrations of the Gulf of Finland and the Baltic Sea waters reach the same level after homogenization at about one and a half year after a release event (Figure 25). The radionuclide concentrations in surface sediments reach typically 100 -1 000 times higher concentrations compared to seawater concentration values. The radionuclide concentrations of buried sediments build up after a certain delay related to diffusion of radionuclides and to the packing effect of sedimented material.

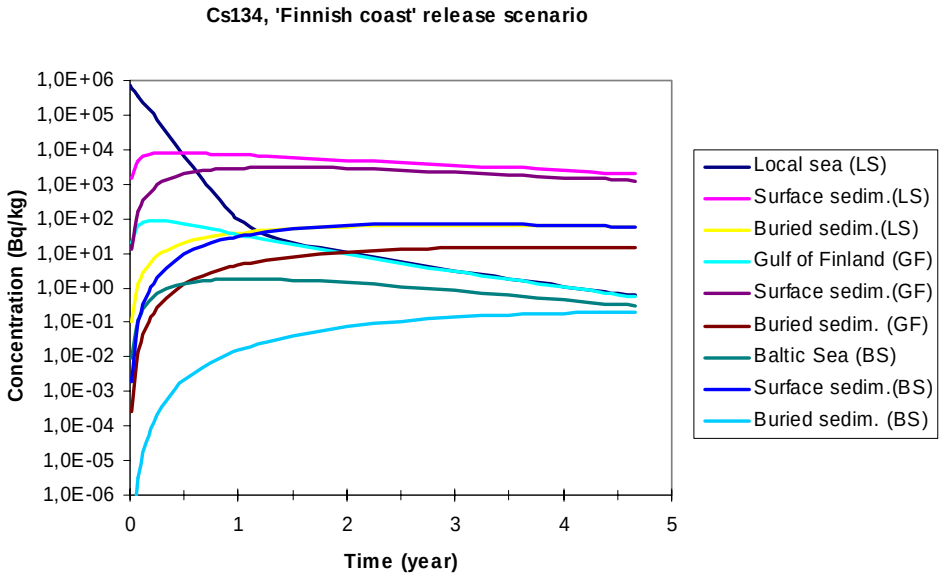

Fig. 25. Estimated temporal behaviour of Cs134 nuclide concentration in marine environment after a hypothetical severe release from the Finnish coast to the Gulf of Finland. (Legends of figure: LS=Local sea, GF=Gulf of Finland, BS=Baltic Sea)

The most higher concentrations of Cs134, Cs137 and of Sr90 nuclides were obtained after the 'Finnish coast' release scenario in seawater of the Baltic Sea (Figure 26). Although I131 has very high release rate in accident, the environmental concentrations in regional area are low and short duration due to the fast decay (radioactive half-life about 8 days) of I131 activity.

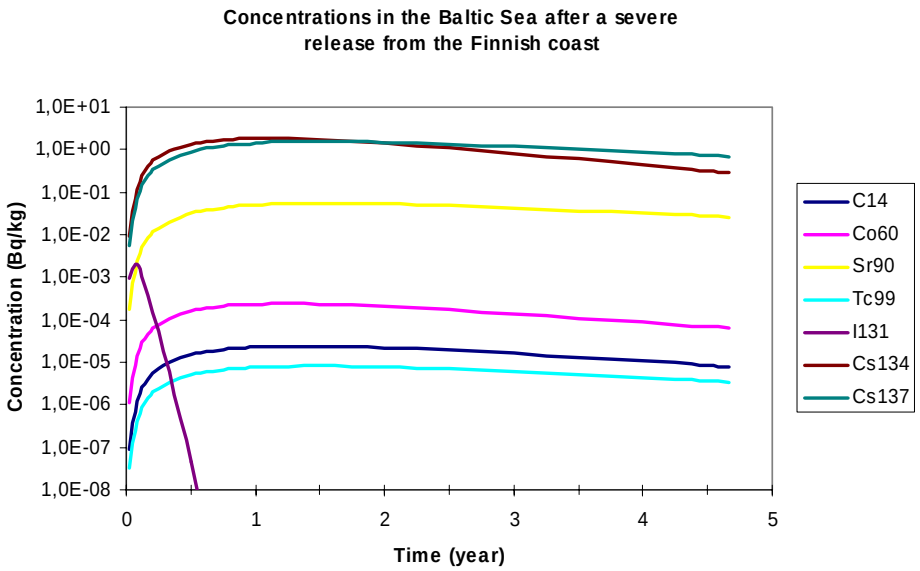

Fig. 26. Estimated radionuclide concentrations in the Baltic Sea for the 'Finnish coast' release scenario.

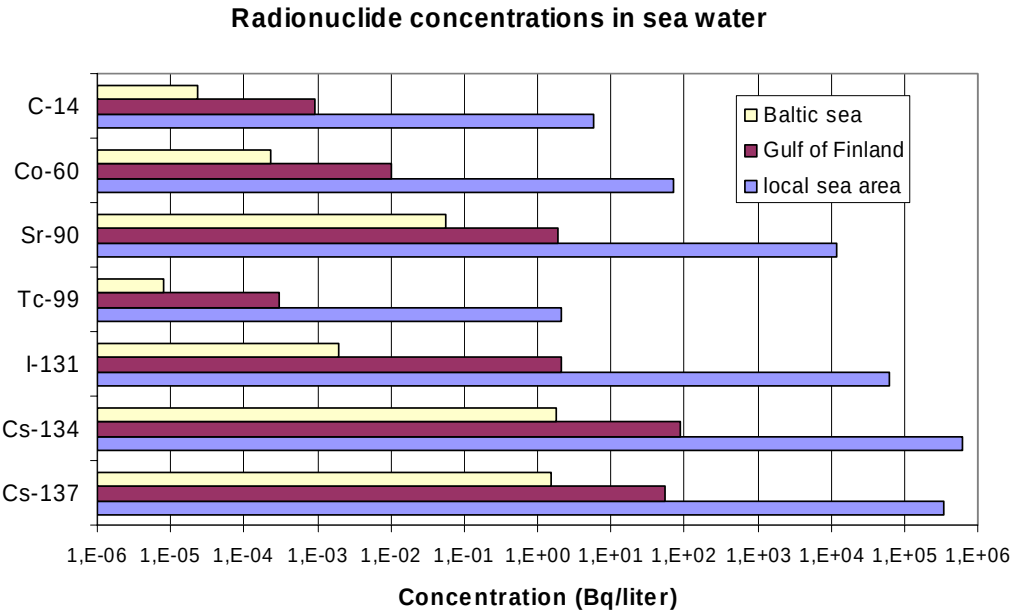

Fig. 27. Estimated maximum concentrations in sea water in local and areal scale after a hypothetical severe accident. Note that concentrations for local sea area are estimated with conservative basis. The time of maximum concentration varies depending on the considered nuclide and the temporal behaviour is presented in other figures of this report.

5.1.3 Severe release from the Swedish coast

The seawater concentrations increase faster (maximum at 0,33 year after release event) and to higher level in the Baltic Sea (Figure 28) compared to the 'Finnish coast' scenario results shown earlier in this report. This is due to the delay related to the mixing and dilution in the Gulf of Finland basin in the 'Finnish coast' scenario. Otherwise radionuclide concentration levels in the Baltic Sea Proper are about in the same level as in the 'Finnish coast' release scenario when considering longer term effects.

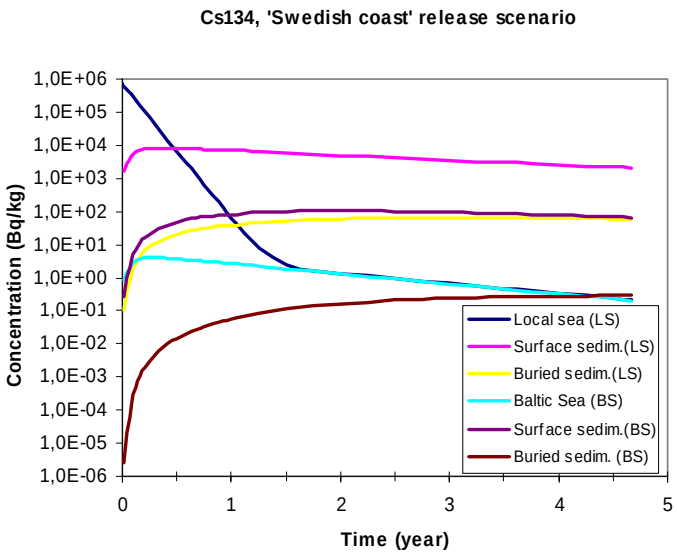

Fig. 28. Estimated temporal behaviour of Cs134 nuclide concentration in marine environment after a hypothetical severe release from the Swedish coast to the Baltic Sea via a local sea area near the release point.

5.1.4 Summary

In the study two release scenarios were considered: release from the Finnish coast and release from the Swedish coast. Based on the modelling results, the 'Swedish coast' release of radionuclides will reach the Northern Baltic Proper earlier causing faster increase of concentrations in the Baltic Sea water (Figure 29). Considering these two hypothetical severe release scenarios, it could be concluded that the maximum caesium concentrations in the Baltic Sea water seem to be 1- 2 Bq/liter after release.

The most exposed period from contaminated fish is the first four years after release, but in case of external exposure from shoreline sediments, the exposure period can continue for some decades after release. Also from crustaceans and molluscs the exposure period to human is long due to high concentrations in sediments.

The maximum individual total dose rate is $2 \cdot 10^{-5}$ Sv/year at the Baltic sea area (Figure 30). The fish pathway dominates during the two first years after release, but thereafter the external exposure from shoreline sediments seem to be the dominating component in the total dose rate. Exposure time-share of 0.1 was used in external dose calculations.

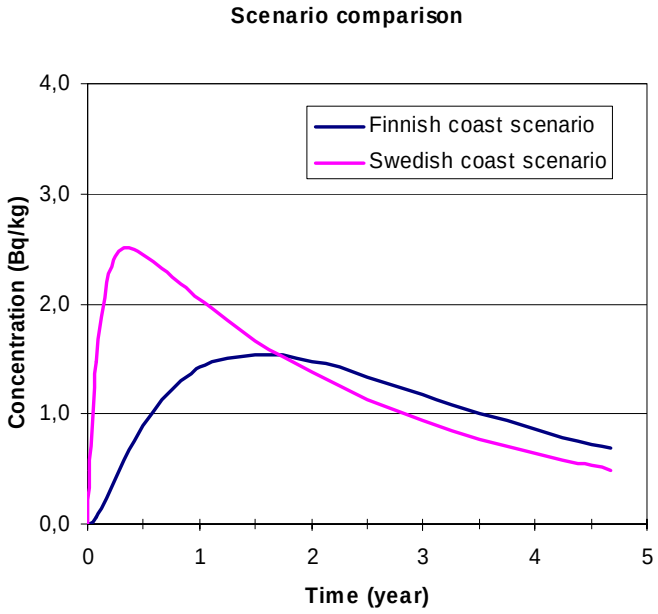

Fig. 29 Comparison of estimated Cs137 concentrations in the Baltic sea between the 'Finnish coast' and the 'Swedish coast' release scenarios.

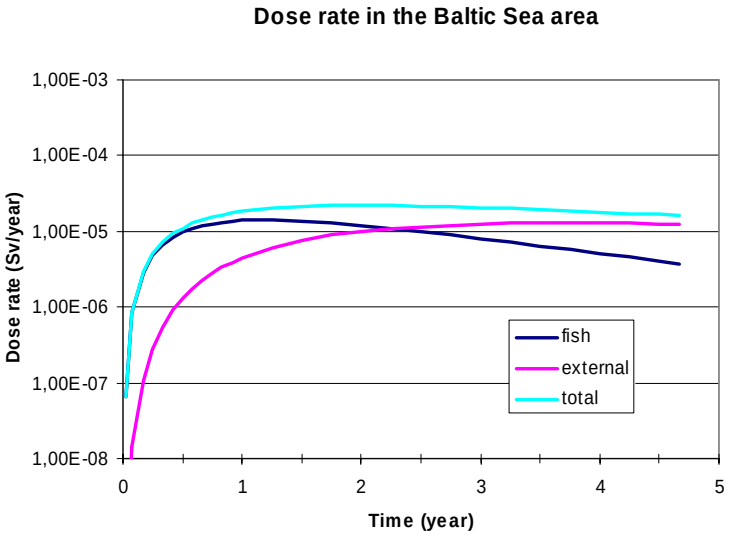

Fig. 30. Estimated individual dose rates from consumption of fish and from external exposure from shoreline sediments as well as total dose rate after a hypothetical severe nuclear power plant accident in the Baltic Sea area.

From individual dose rate results the time-integrated individual doses and collective doses were calculated. In the Baltic Sea area the estimated individual dose after a hypothetical severe accident is 0.01 mSv after one year and 0.1 mSv after five years from the release event. Total collective dose after one year is 98 manSv, and after five years

880 manSv (Table 8) which corresponds to about expected 20 detrimental effects to human in future.

Table 8. Estimated collective doses after a hypothetical severe nuclear power plant accident at the Baltic Sea northern coastal area. The exposed population of 10 milj. persons around the Baltic Sea was used in collective dose calculations.

	Collective dose (manSv)	
	after first year from release	after five years from release
fish consumption	82	422
external exposure from shoreline sediments	16	458
total	98	880

References

Anttila, M., Radioactive characteristics of the spent fuel of the finnish nuclear power plants, Posiva WR 2005-71.

IAEA TRS-422, Sediment distribution coefficients and concentration factors for biota in the marine environment, IAEA, Vienna, 2004, 93 p.

IAEA TRS-472, Handbook of parameter values for the prediction of radionuclide transfer in terrestrial and freshwater environments, IAEA, Vienna, 194 p.

Korhonen, R., Savolainen, I., Biospheric transfer model DETRA for assessment of radiation impacts, VTT Research Reports 323, 1984(a) (in Finnish).

Korhonen, R., Savolainen, I., Suolanen, V., Sensitivity analysis of biospheric behaviour of radionuclides released from nuclear waste repositories, Conf. of radioactive waste management, London, 27-29 Nov. 1984, (1984(b)).

Suolanen, V., Consequences of radioactive deposition on aquatic environments, Technical Research Centre of Finland, Research Notes 1612, 1994.

Suolanen, V., Model description and evaluation of model performance, Scenario S. Multiple Pathways Assessment of the IAEA/CEC co-ordinated research programme on the Validation of Environmental Model Predictions (VAMP). In: IAEA-TECDOC-904, Vienna 1996.

Suolanen, V., Ilvonen, M., Generic uncertainty model for DETRA for environmental consequence analyses. Application and sample outputs. In: STUK-YTO-TR 149, 1998.

5.2 Submarine accidents

5.2.1 Dispersal of near-surface radioactivity in the North Atlantic – three modelling experiments

Kai Logemann, School of Engineering and Natural Sciences, University of Iceland

5.2.1.1 Introduction

Within the frame of the COSEMA project three numerical experiments regarding oceanic dispersion are performed. The three experiments examine the Icelandic, the Faroese and the Norwegian coastal zone. Here, a radioactive source term is hypothesized which acts during the first 7 days of the simulation, thereby keeping the upper 40 m of the water column within a 4×4 km square, i.e. within a "source volume", at the concentration of 100%. This percentage, herein called concentration, describes the fraction of water molecules which have been within the source volume during the first seven days of the experiment. Thereafter, the source term is deactivated. I.e. the dispersal of a passive tracer cloud is simulated.

The physical basis of the simulation, i.e. the topography, the three-dimensional ocean currents and diffusion rates are taken from the CODE simulation of the time period September 2012 – August 2013 (Logemann et al. 2013) which includes the assimilation temperature and salinity data from the 3D-ARMOR analysis (Larnicol et al. 2006).

Based on the temporally averaged physical field three simulations with different source volume locations are performed:

1) The "Iceland" experiment with the location at 64.19°N, 22.23°W in the Faxaflói near Reykjavik.

2) The "Faroe Islands" experiment with the location at 61.89°N, 7.24°W southwest of the Vágafjøður.

3) The "Norway" experiment with the location at 58.96°N, 4.43°N southwest of Bergen.

Because of the adaptive computational mesh of the ocean model the different source volumes are differently resolved. In Faxaflói the horizontal gird spacing is at least 4 km, hence the signal is resolved with 100%. Around the Faroe Islands the resolution is 8 km, hence the initial concentration within the 8×8 km box is 25%. Along the Norwegian coast the model resolution is 64 km with leads to an initial concentration of only 0.4%.

5.2.1.2 Results

We have concentrated mainly on the maximum concentration found within the water column assuming this to be the crucial value regarding environmental threads by radioactivity. However, in order to obtain insights into a potential vertical spreading of the signal we selected certain locations downstream of the source regions where we analysed the time-dependent vertical concentration profile.

5.2.1.2.1 Iceland

The cloud is carried northwards, by the Coastal and Irminger Current, through the Faxaflói and further over the west Icelandic shelf towards Denmark Strait (Figure 31). Here, 300 km downstream, the main signal, a concentration slightly below 0.1%, arrives after around three months (Figure 32). Thereafter, the major part of the cloud is led eastwards over the north Icelandic shelf by the North Icelandic Irminger Current, whereas smaller parts are entrained into the southwards flowing East Greenland Current. Over the northern shelf maximum concentrations of around 0.02% appear after around 200 days. However, at that time the maximum concentration near the source region in Faxaflói is still 1.5% (Figures 31 and 33). Here, the concentration sinks below 1% only after 300 days. Highest values are found in near-bottom model cells which are effectively shielded from the ambient ocean current. These bottom-boundary values begin to dominate the overall maximum after 70 days which explains the bend of the maximum concentration curve at that time (Figure 33.)

5.2.1.2.2 Faroe Islands

The cloud is advected eastwards by the North Atlantic Current interacting with the Arctic Front. Thereby, the majority takes a path south of the Faroe Islands, whereas a smaller fraction follows the Faroese shelf in a northward direction. This way, after around 100 days, the entire Faroese shelf is affected by the cloud (Figure 34). At that time, the cloud, with a concentration of around 0.03%, has arrived at the western Shetland Islands; in the open ocean between both archipelagos the concentration goes up to 0.1%. Here, the vertical profile (Figure 35) indicates an effective mixing down to 150 m. Again, highest concentrations are found in the source region, west of the Faroe Island, around 0.7% after 100 days (Figure 36). In contrast to the Iceland case above the decrease of the overall maximum (Figure 36) concentration does not show the bend after a few months. This can be explained by the more exposed location of the source region compared to the rather shielded Faxaflói. After 300 days the cloud stretches out over large parts of the Norwegian Sea including the Norwegian coast. However, the maximum concentration, within the source region, is only 0.01% which points to significantly higher dispersion compared to the Iceland case above. Note that apart from the different hydrographic conditions (open shelf exposed to a direct flushing of the North Atlantic Current versus the shielded Faxaflói) the coarser model grid (8 km spacing versus 4 km) implies an immediate mixing right from the outset. This effect of numerical mixing because the model is not able to resolve the cloud sufficiently becomes even more noteworthy in the following case.

5.2.1.2.3 Norway

Here, already after 150 days, the cloud, which follows the Norwegian coast towards the north with the Norwegian Current (Figure 37), is dispersed down to a maximum concentration of 0.01% (Figure 39). The curve of concentration decrease shows two bends, after 15 and 90 days. The vertical profiles (Figure 38) point to a substantial downward mixing. Surprisingly we find the concentration maximum further north at 6°E, 63°N not at the sea surface but in a depth of 70 m 100 days after the release. This depth of maximum even increases with time and reaches 100 m after 200 days. The causes of this structure are probably a strong vertical shear of this mainly wind-driven flow off the Norwegian cost; but also downwelling along the slope or a strong vertical mixing seems to be responsible. After 300 days, in sharp contrast to the cases above, we find a clear signal arriving at the depth of 700 m.

5.2.1.3 Summary

We have performed three numerical experiments regarding the dispersion of 4 km × 4 km × 40 m = 640×10^6 m^3 of sea water being radioactively contaminated. We modelled this contamination by assigning a “concentration” of 100% to the water inside this volume. Here, the concentration is held constant at 100% during the first 7 days of the simulation whereas ocean currents and turbulent diffusion begin to spread the concentration signal over the adjacent sea. A scenario which may reflect an accident of radioactively contaminated water being led into the coastal ocean for several days. In this case, after having measured several values of contamination close to the accident location and having them extrapolated onto the 640×10^6 m^3 volume, our computations could help to estimate the likely spreading and dispersion of these values.

Unfortunately the computational mesh of the used ocean model CODE, being designed for Icelandic waters, shows different horizontal resolutions for the Icelandic (4 km), Faroese (8 km) and Norwegian (64 km) coastal waters. This causes a kind of numerical diffusion being the more effective the coarser the grid. Hence, the conclusion that the Norwegian waters show the highest dispersion rates should be waived. Instead, we should consider that the “Iceland” experiment may have produced the most realistic results, which also would be the most conservative estimations about the expected decrease of the contamination. Shortly these are: After 100 days the toxic cloud has spread 300 – 500 km downstream along the coast with a mean concentration of around 0.1% of the initial value whereas close to the accident location is the contamination is still at 2%.

However, apart from the effects of different resolution, the simulations have also revealed the dispersion’s high dependency on regional hydrographic structures: The slow dispersion within the shallow and shielded Faxaflói, the effective flushing west of the Faroe Islands, or the downward transport along the Norwegian coast. This clearly illustrates the need of operational regional ocean modelling being able to react to the specific circumstances for risk analysis related to an accidental release of radioactivity into the ocean.

5.2.1.4 Figures

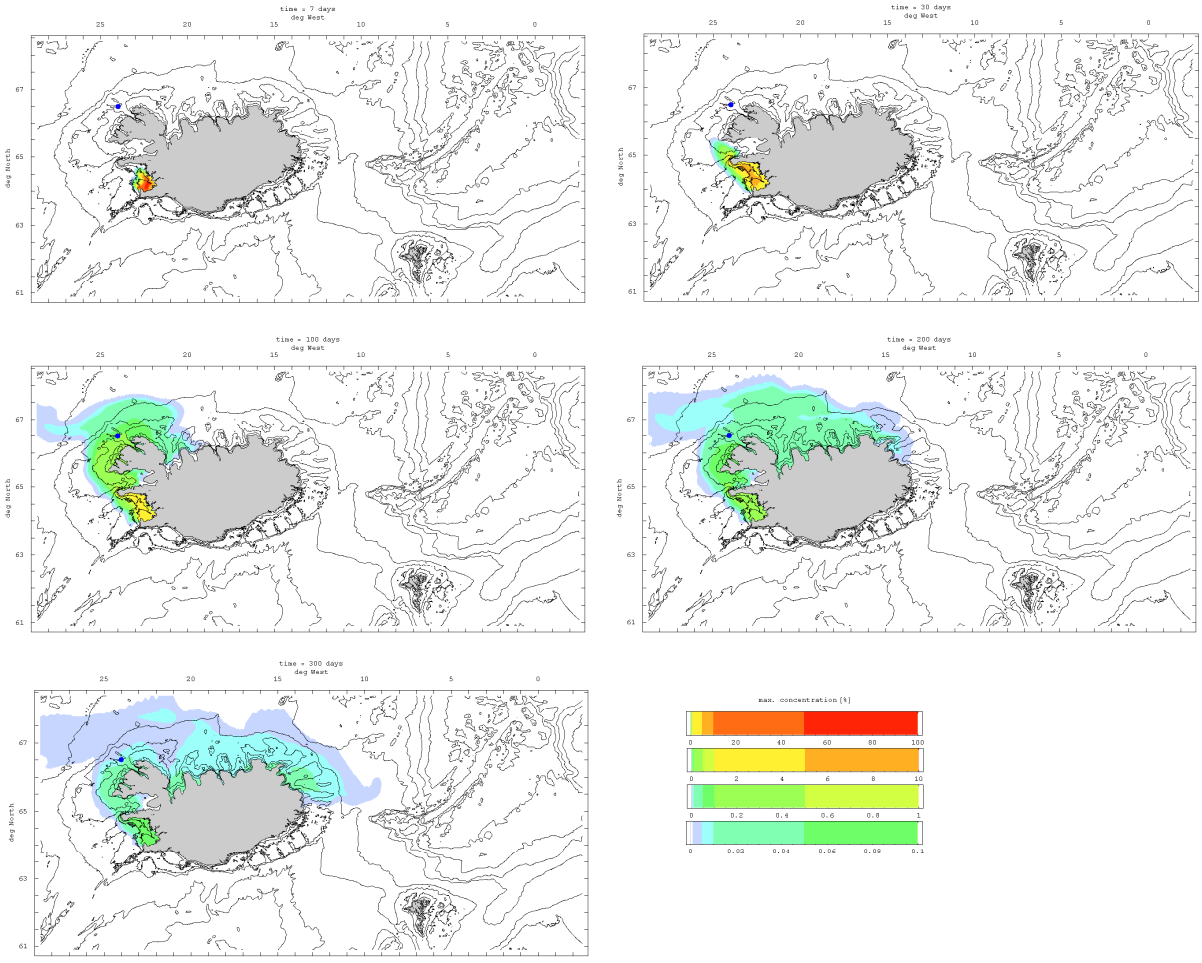

Fig. 31. Maximum concentration 7, 30, 100, 200 and 300 days after begin of the “Iceland” experiment. The blue point denotes the position (24°W, 66.5°N) of the vertical profiles shown in Figure 32.

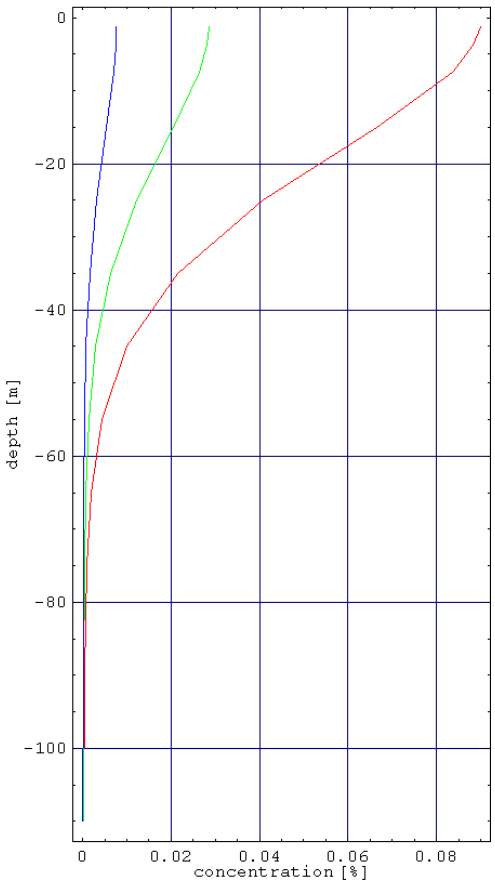

Fig. 32. Vertical profiles of concentration 100 (red), 200 (green) and 300 (blue) days after begin of the "Iceland" experiment at the position 24°W, 66.5°N.

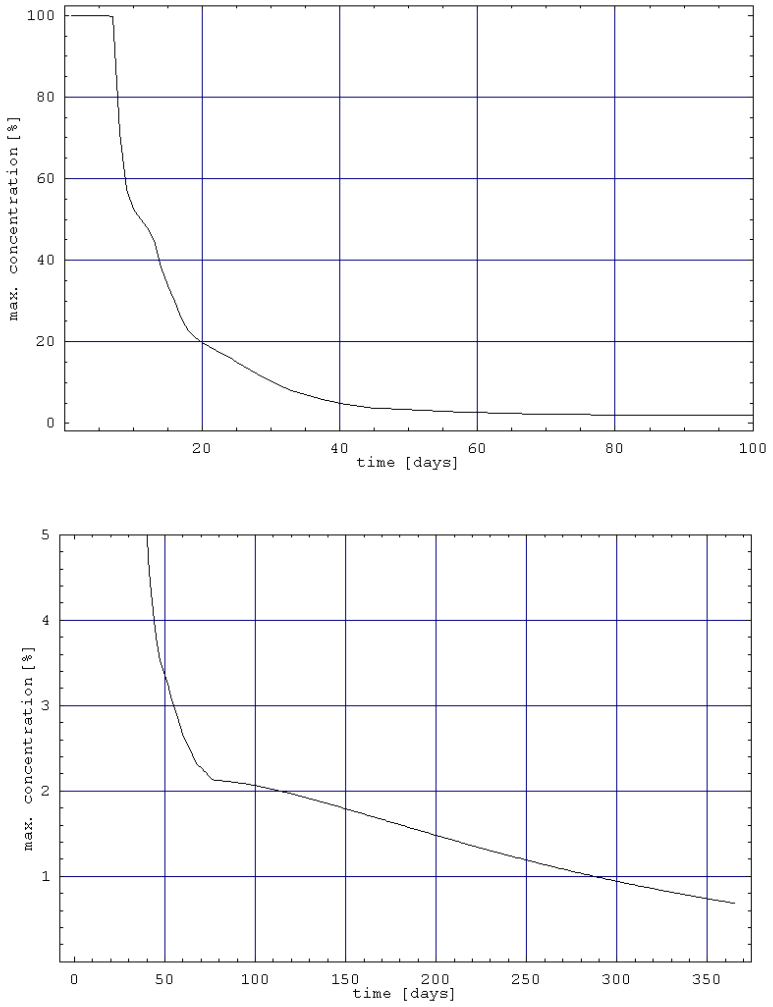

Fig. 33. Simulated time series of maximum concentration within the entire model domain (North Atlantic) in experiment “Iceland”.

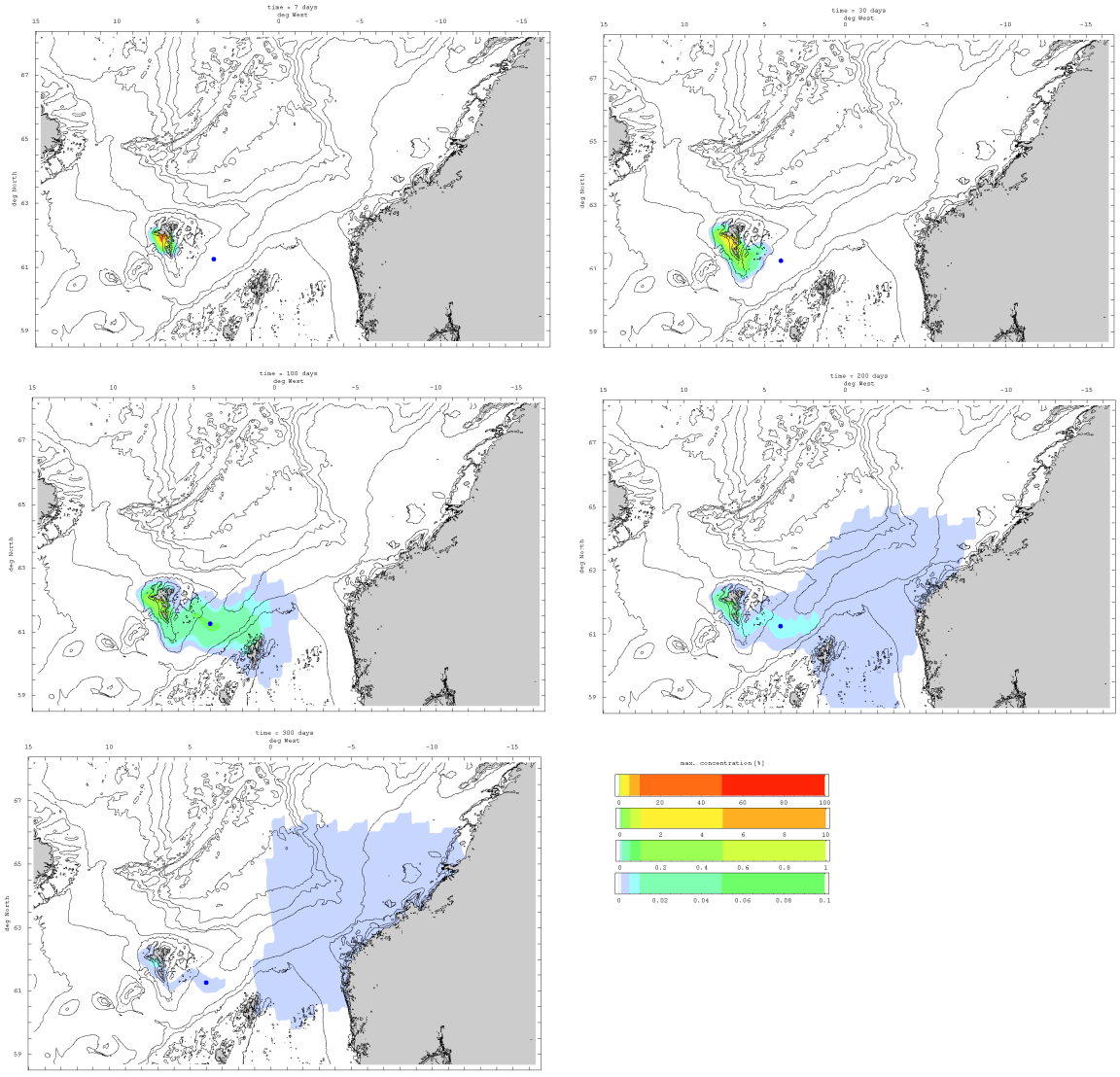

Fig. 34. Maximum concentration 7, 30, 100, 200 and 300 days after begin of the “Faroe Islands” experiment. The blue point denotes the position (4°W, 61.25°N) of the vertical profiles shown in Figure 35.

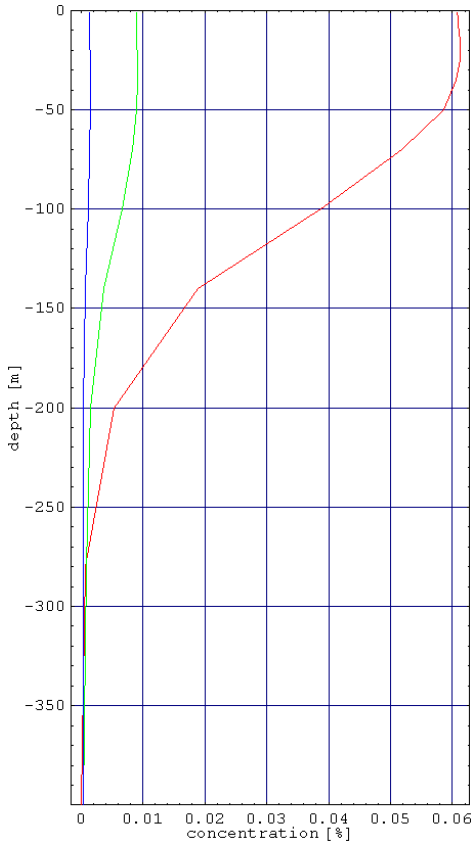

Fig. 35. Vertical profiles of concentration 100 (red), 200 (green) and 300 (blue) days after begin of the "Faroe Islands" experiment at the position 4°W, 61.25°N.

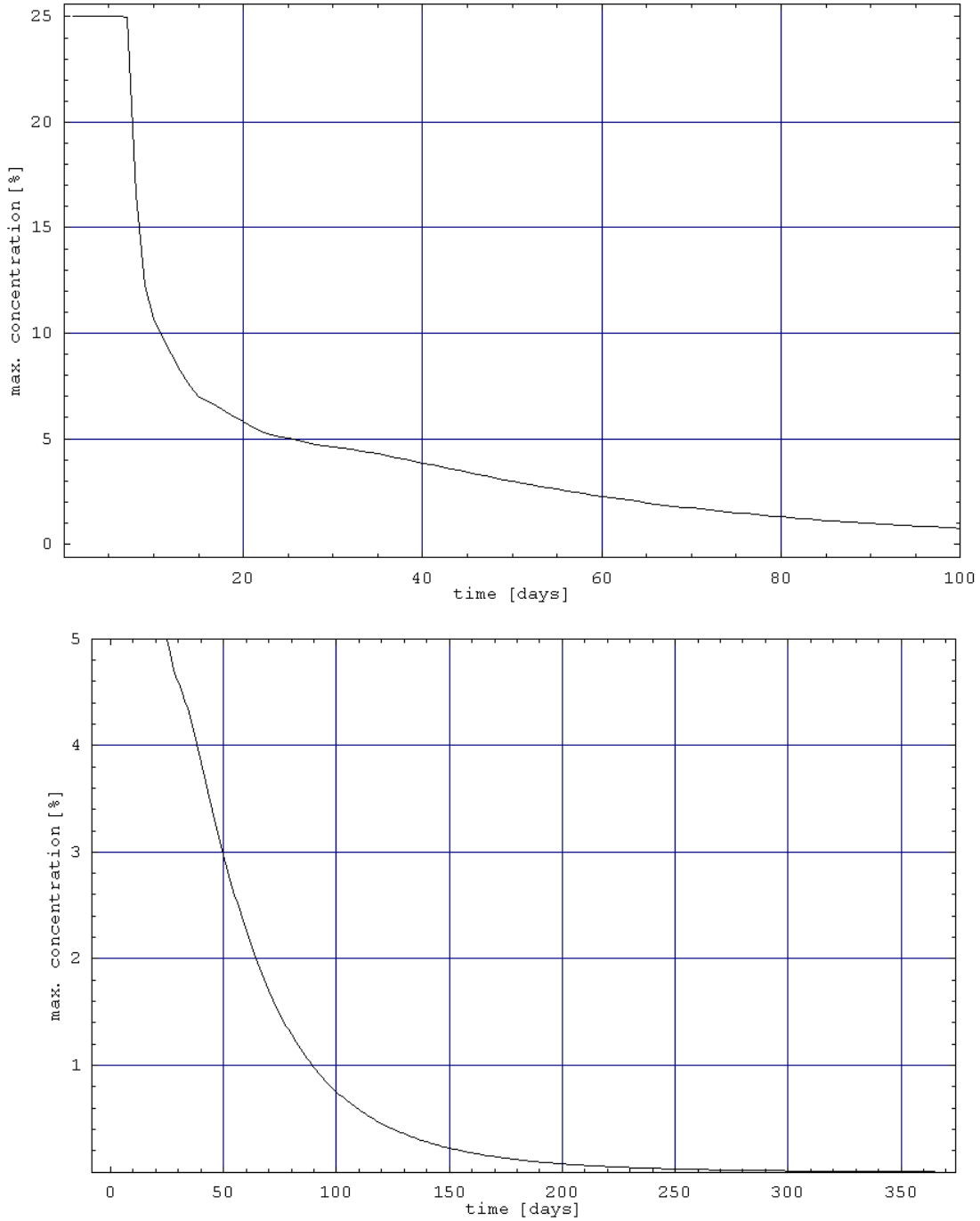

Fig. 36. Simulated time series of maximum concentration within the entire model domain (North Atlantic) in experiment “Faroe Islands”.

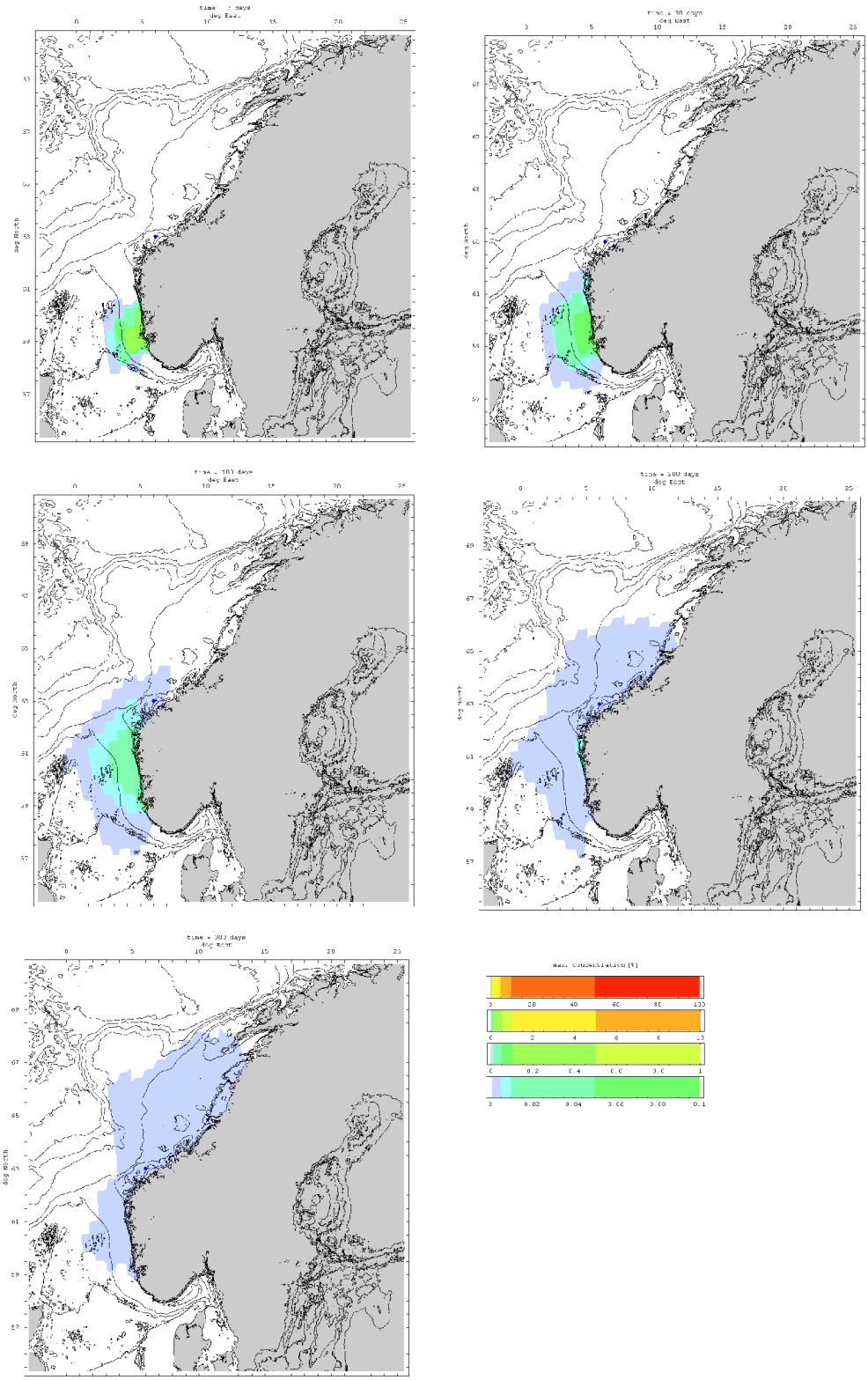

Fig.37. Maximum concentration 7, 30, 100, 200 and 300 days after begin of the “Norway” experiment. The blue point denotes the position (6°E, 63°N) of the vertical profiles shown in Figure 38.

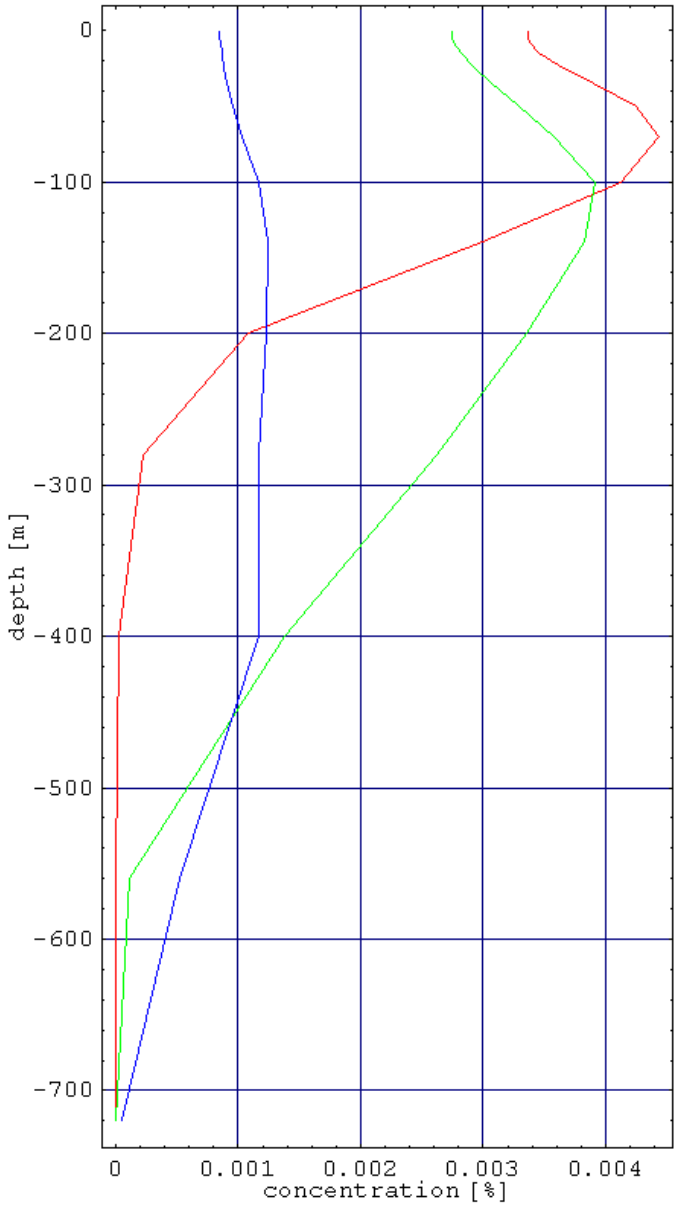

Fig. 38. Vertical profiles of concentration 100 (red), 200 (green) and 300 (blue) days after begin of the "Norway" experiment at the position 6°W, 63°N.

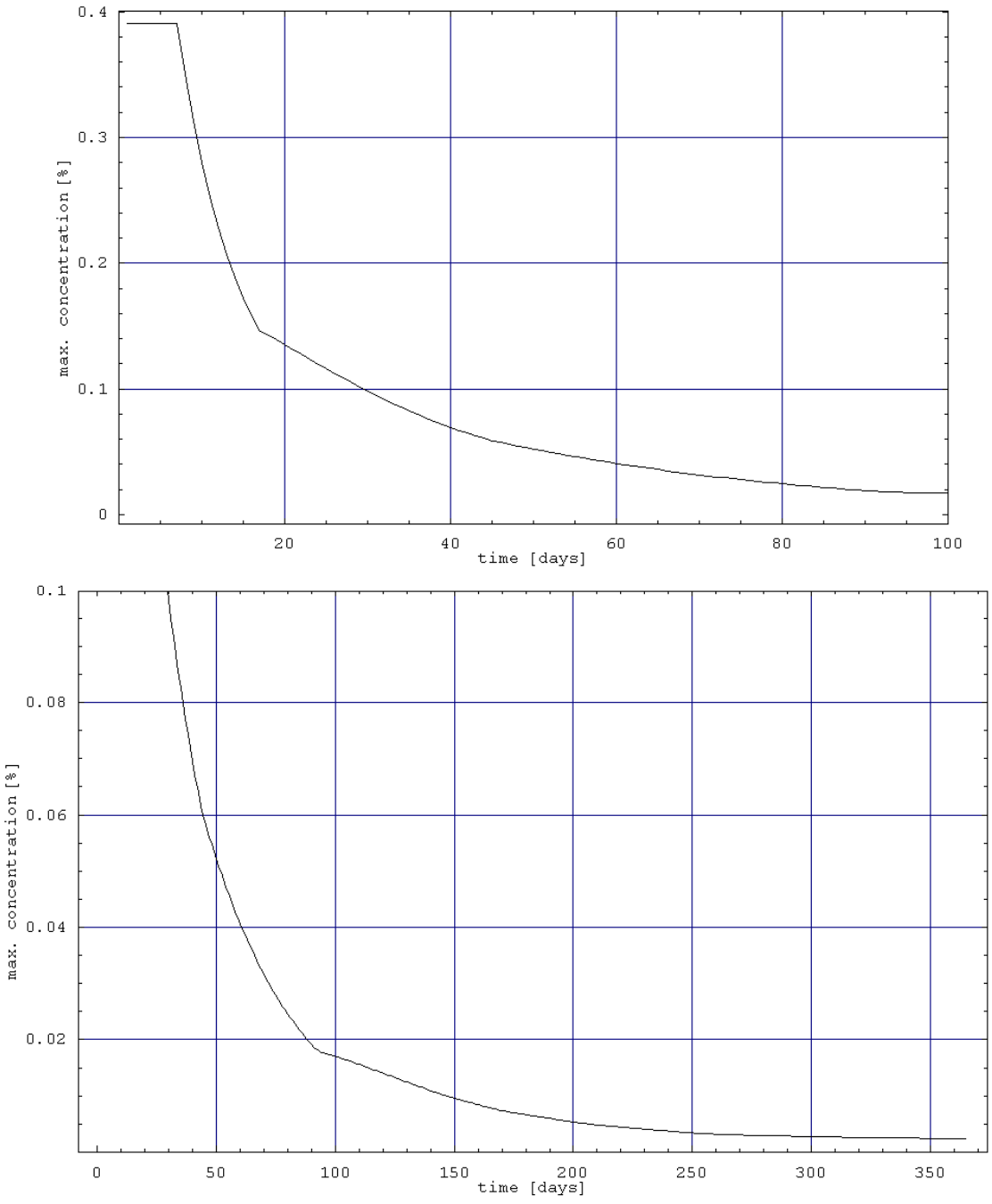

Fig. 39. Simulated time series of maximum concentration within the entire model domain (North Atlantic) in experiment “Norway”

References

Larnicol, G., Guinehut, S., Rio, M. H., Drevillon, M., Faugere, Y., & Nicolas, G. (2006, March). The global observed ocean products of the French Mercator project. In Proceedings of 15 Years of progress in radar altimetry Symposium, ESA Special Publication (Vol. 614).

Logemann, K., Ólafsson, J., Snorrason, Á., Valdimarsson, H., and Marteinsdóttir, G.: The circulation of Icelandic waters – a modelling study, Ocean Sci., 9, 931-955, doi:10.5194/os-9-931-2013, 2013.

5.2.2 Potential accident in the Icelandic coastal waters

Mikhail Iosjpe, Norwegian Radiation Protection Authority - NRPA

The present results in chapters 5.2.2 and 5.2.3 are based on two models: (i) the NRPA box model, which is detailed in Iosjpe, Brown & Strand (2002), Iosjpe (2006) and Iosjpe et al. (2009), and (ii) the present model, which is developed within COSEMA-project (Iosjpe, Pálsson, Logemann, 2013).

5.2.2.1 Brief description of the model

The present model is based on the methodology developed for the NRPA box model, which uses a modified approach for compartmental modeling (Iosjpe et al., 2002). This methodology allows for simulation of radionuclide dispersion over time.

The compartments, which include the volumes, mean depth and water exchanges between boxes for the Iceland coastal waters, were developed during the COSEMA-project by Geislavarnir Rikisins (Iceland). Additionally, two compartments surrounding the Iceland boxes were developed on the basis of the NRPA box model. The surface box structures for both models are shown in Figure 40.

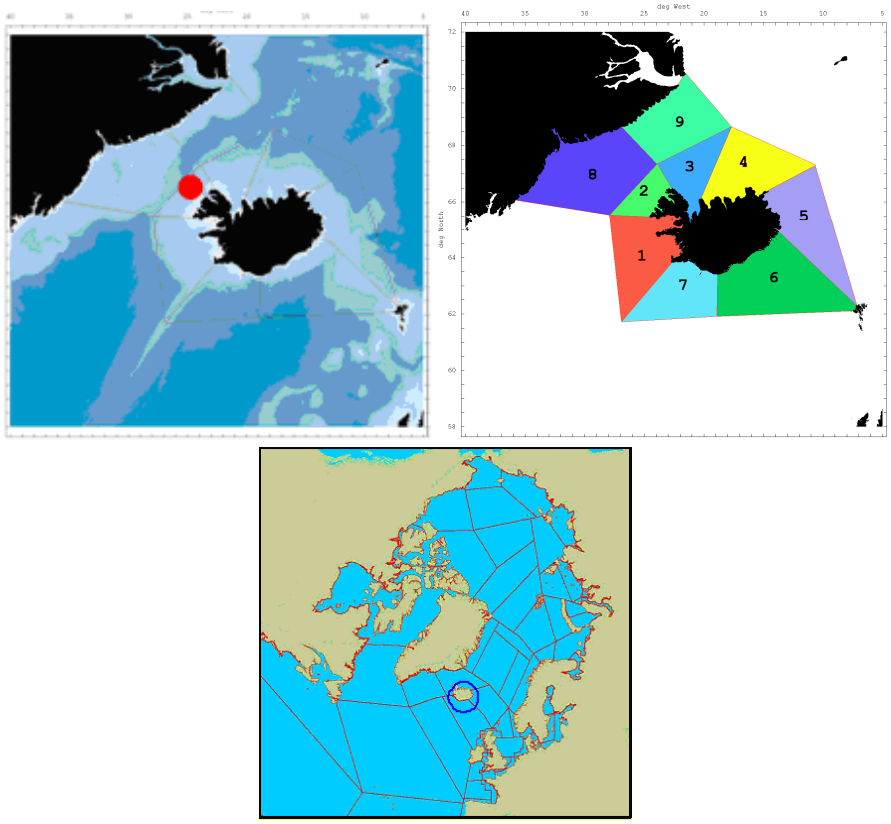

Fig. 40. The structure of the surface compartments in the present model (top) and the NRPA models (bottom) and location of the potential accident (red dot).

The present model developed in the COSEMA, adopts the sediment structure from the NRPA model, including the surface, mid-depth and deep sediment compartments for all

water regions. Water-sediment interactions include sedimentation, diffusion of radioactivity through pore water in sediments, resuspension, mixing due to bioturbation, particle mixing and a burial process for radionuclides in deep sediment layers. Radioactive decay is calculated for all compartments. The contamination of biota is further calculated from the known radionuclide concentrations in filtered seawater in the different water regions. Collective doses to the world population are calculated on the basis of seafood consumptions, in accordance with available data for seafood catches and assumptions about human diet in the respective areas (Nielsen et al., 1997; EC, 2000; IASAP, 2003).

The collective dose *D* (manSv) can be determined using the following expression:

$$D = \sum_{j=1}^{m} DCF_j \sum_{l=1}^{k} \varphi_l \cdot CF_{lj} \sum_{i=1}^{n} A_{il} \int_0^T C_{ij}(t)dt, \quad (1)$$

where [0, T] is the time interval (y); DCF_j (Sv/Bq) is the dose conversion factor for radionuclide *j* (j = 1,2,..., m); CF_{lj} (m^3/t) is the concentration factor for radionuclide *j* in seafood of type *l* (*l* = 1,2,..., k); A_{il} (t/y) is catch of seafood of type *l* in the model compartment *i*; (*i* = 1,2,...,n); C_{ij} (Bq/m^3) is the concentration of radionuclide *j* in filtered seawater in model compartment *i*; and φ_l is the edible fraction for seafood of type *l*. The following assumptions (CEC, 1990; EC, 2000; IASAP, 2003) for the edible fractions of marine produce to the human diet have been used: 50 % for fish, 35 % for crustaceans and 15 % for molluscs).

Collective dose rates DR can be defined using the following expression:

$$DR = \frac{D(t_2) - D(t_1)}{t_2 - t_1}, \quad (2)$$

where $D(t_1)$ and $D(t_2)$ are collective doses at times t_1 and t_2, respectively.

It is necessary to note that the model can also easily be used to provide information on impact doses/dose rates from different marine regions, and provide dose assessment to different population groups. Furthermore, the dose rate will be used in the present dose assessment because this parameter can easily indicate dose dynamic and is therefore widely used in recent investigations (EC, 2003; IASAP; 2003).

5.2.2.2 Validation of the model

Validation of the model is based on the global fallout of the $^{239+240}Pu$ after the testing of nuclear weapons in the atmosphere (UNSCEAR, 2000). The contamination by $^{239+240}Pu$ of the considered marine regions is strongly dominated by the global fallout, when compared to other sources of contamination (Green et al., 2013). Therefore, we have chosen to consider global fallout as a single source of $^{239+240}Pu$ contamination in the present project. Figure 41 shows the global fallout scenario from UNSCEAR (2000) (top figure) and the results of the model simulations for $^{239+240}Pu$ contamination compared with the experimental data (MARINA II, 2003) for the marine regions surrounding Iceland (bottom figure). The circles show the average values, while the error bars show

the minimum and maximum values of the experimental data. Figure 41 demonstrates that the model predictions are reasonably accurate.

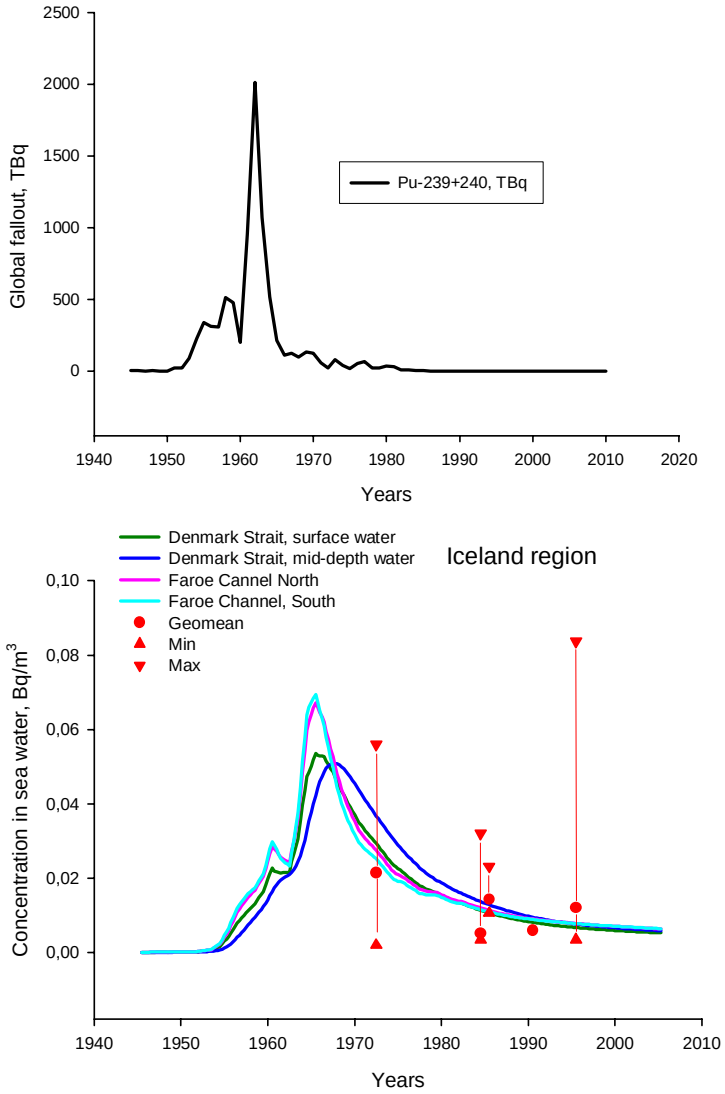

Fig. 41. Global fallout and comparison of the model simulations with experimental data.

5.2.2.3 Location of accident

The location (the compartment 2 in Figure 40) chosen for the accident was based on an evaluation of the radiological sensitivity of different marine areas. Radiological sensitivity analysis of Arctic marine regions shows that the shallow waters can be considered as the most vulnerable areas in the Arctic region, in terms of the effects of possible radioactive contamination (Iosjpe et al., 2003; Iosjpe, 2011; Iosjpe & Liland, 2012).

5.2.2.4 Results and discussion

The radioecological consequences of the potential scenarios leading to accidental releases of radioactivity have been evaluated on the basis of the calculated concentrations of radionuclides in typical sea foods, collective dose rates to man and individual doses for the critical groups and doses to marine organisms.

5.2.2.4.1 Concentrations of radionuclides in seafood

The Food and Agriculture organisation of the United Nations and World Health Organisation have provided recommendations (guideline levels) for the maximum permissible concentration of radionuclides in foods, when contaminated after an accidental release of radionuclides (CAC, 2006). According to the Codex Alimentarius Commission (CAC, 2006) radionuclides can be separated into four groups. Examples of some typical radionuclides for each group are presented in Table 9.

Table 9 Examples of international guideline levels for radionuclides in food.

Radionuclides in Foods		Guideline Level (Bq/kg)	
		Infant Foods	Other Foods
Group 1	^{238}Pu, ^{239}Pu, ^{241}Am	1	10
Group 2	^{90}Sr, ^{106}Ru, ^{129}I	100	100
Group 3	^{60}Co, ^{134}Cs, ^{137}Cs	1000	1000
Group 4	^{3}H, ^{14}C, ^{99}Tc	1000	10000

Following the CAC (2006) recommendations, the model calculations for fish, crustaceans and molluscs are provided separately for each group of radionuclides presented in Table 8.

It is clear that the highest level of sea food contamination is expected in box 2 (the accident location compartment). Results of the simulations of the radionuclide concentrations in seafood (fish, crustaceans and molluscs) for group 1 are shown in Figure 42. Results show the three most significant radionuclides in the group and the total concentration for the group.

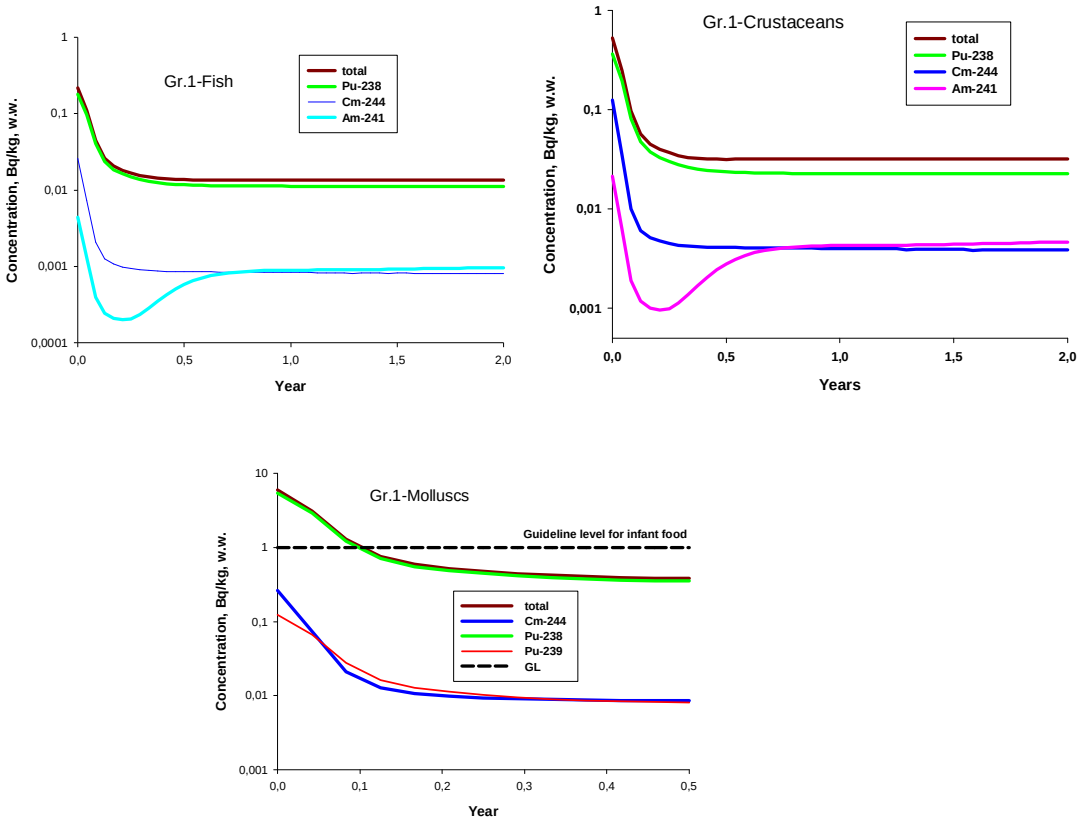

Fig. 42. Predicted concentration of radionuclides (Group 1) in sea food.

Results of the model calculations indicate that the concentration of radionuclides from group 1 in seafood lies significantly under the CAC guideline levels for fish and crustaceans, but considerably exceeding the CAC guideline level for molluscs for infant food during the first four weeks after the accidental release began. The total concentration level of radionuclides in seafood for group 1 is heavily dominated by ^{238}Pu. Therefore, it is interesting to note that the concentration of ^{238}Pu in compartment 2 is one to three orders of magnitude higher than in other boxes (results are presented in Figure 43).

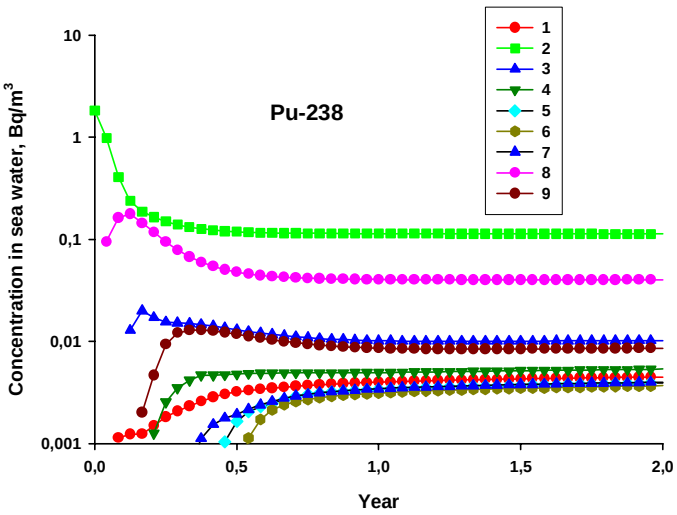

Fig. 43. Concentrations in sea waters in compartment 1-9.

Predicted concentration of Group 2 radionuclides in seafood is shown in Figure 44. The CAC guideline level is shown for comparison.

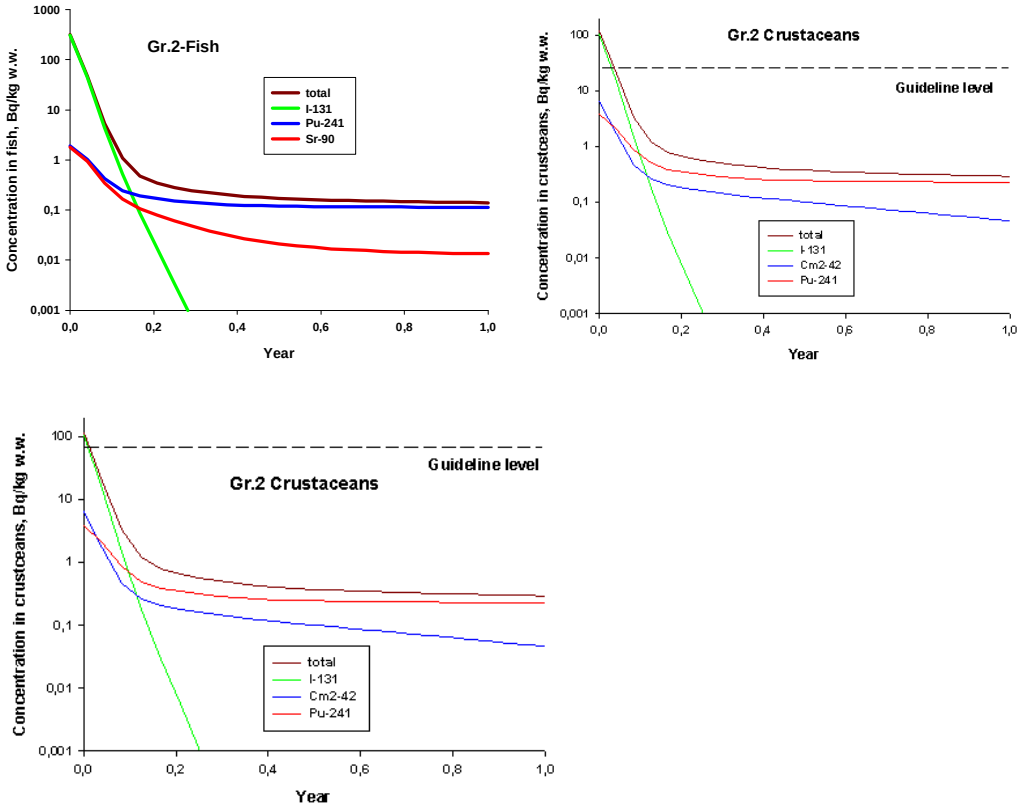

Fig. 44. Concentration of radionuclides (Group 2) in seafood.

The predicted concentration of radionuclides in fish is lower then the CAC guideline level for group 2 radionuclides. Results of the simulations for crustaceans and molluscs indicate that the radionuclide concentrations in the zone of the accident exceeds the CAC guideline level for a period of approximately one to two months after the accident. The predicted maximum values of the radionuclide concentration in crustaceans and molluscs are around 120 and 700 Bq/kg, respectively. The radionuclides that impacted the concentration levels in seafood (for group 2) the most were ^{131}I, ^{241}Pu and ^{106}Ru.

The concentrations of group 3 radionuclides in seafood are shown in Figure 45.

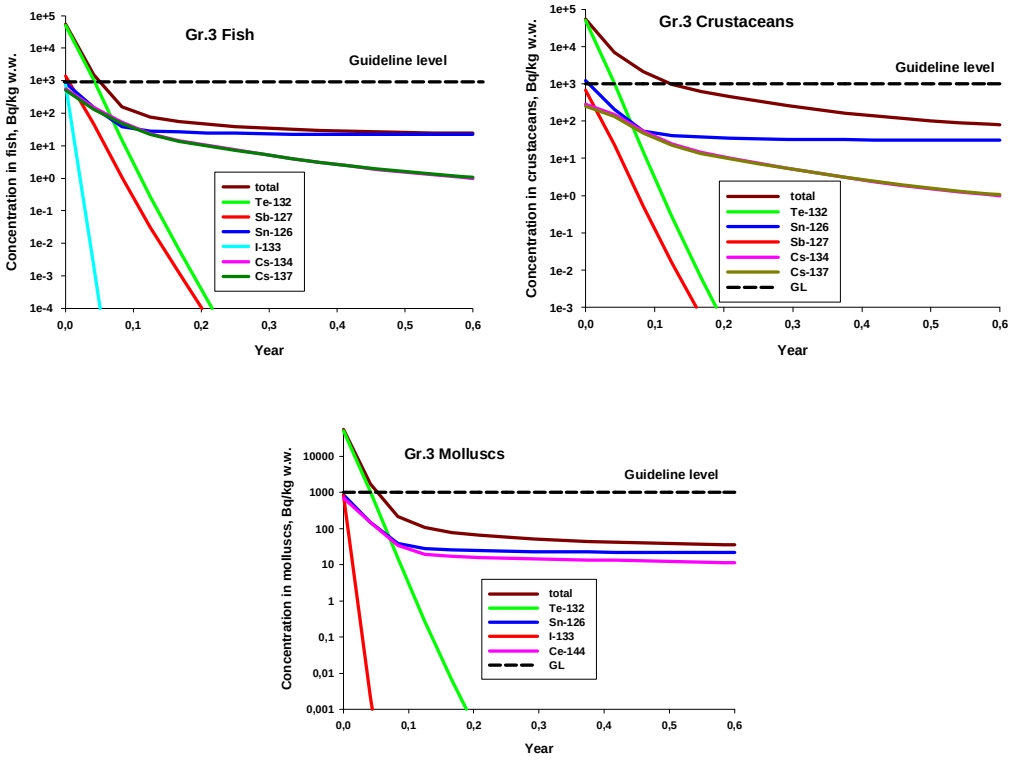

Fig. 45. Predicted concentration of radionuclides (Group 3) in seafood.

The results of the simulations for group 3 radionuclide concentrations in seafood indicate that the radionuclide concentrations in box 2 (the accident location) exceeds the CAC guideline value of 1000 Bq/kg for a period of approximately one-two weeks after the accident. The concentration of radionuclides is dominated by the level of ^{132}Te during these weeks. ^{126}Sn and ^{144}Ce (for molluscs) start to dominate the concentration level of group 3 radionuclides in seafood during the time following the two weeks after the accident.

Figure 46 shows that the contamination curves of seafood by group 4 radionuclides lies under the guideline levels for general food, but exceeds the guideline level for infant food for a period of approximately one week after the accident. ^{127}Te, ^{129m}Te dominate the radionuclide concentration during this initial time. During the time following this week, ^{125}Sb and ^{147}Pm have a significant impact on the total concentration of radionuclides in

fish, and ^{103}Ru and ^{147}Pm dominate the radionuclide concentrations in crustacean and molluscs.

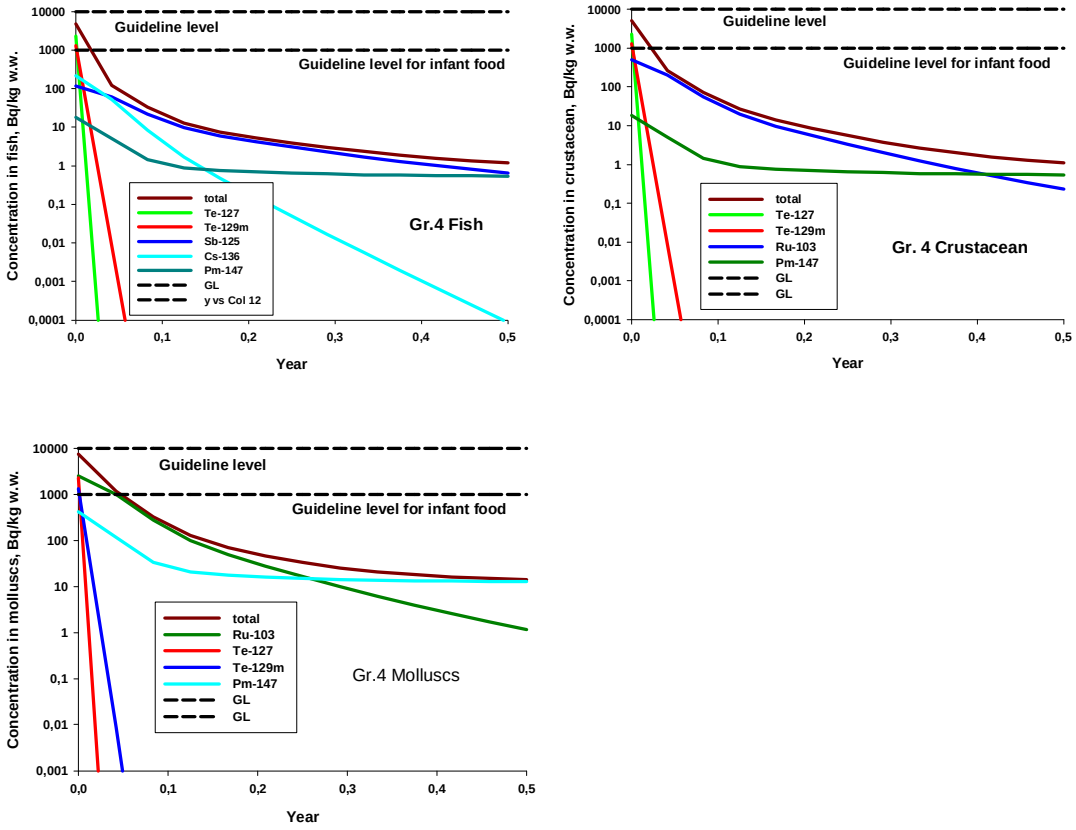

Fig. 46. Predicted concentration of radionuclides (group 4) in seafood.

5.2.2.4.2 Collective dose rates to man

The results presented in Figures 47 and 48 show that the maximum collective dose rates in the studied scenario, occur during the first year after the release of radioactivity. The maximum collective dose rate is approximately 58 manSv per year, with ^{134}Cs, ^{137}Cs and ^{126}Sn having the highest impact on the maximum collective dose rate.

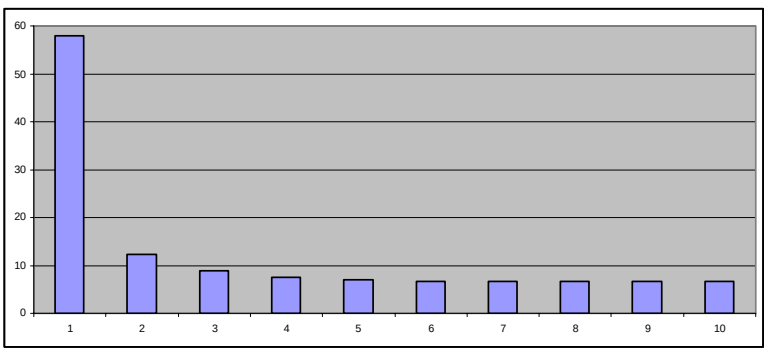

Fig. 47. Predicted collective dose-rates, manSv per year

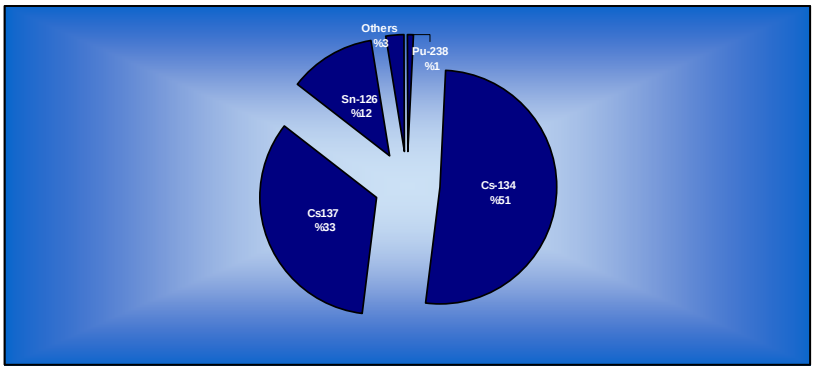

Fig. 48. Impact of radionuclides to the collective dose rate (the first year after the hypothetical accident)

5.2.2.4.3 Doses to the critical group

In the present study we assume that the critical group is a population living on the coast of the sea region nearest to the accident location. The evaluation of the doses for this group will be based on an investigation of consumption patterns for the population living on the Norwegian coast and inland (Bergsten, 2003), where maximum seafood consumption is 200, 40 and 4 g/day for fish, crustaceans and molluscs, respectively.

The individual dose rates for the ingestion pathway have been calculated on the basis of expressions (1) and (2), where catchments of seafood were replaced by consumptions for the critical groups.

The proportions of the total calculated dose attributable to the different types of seafood are presented in Figure 49, corresponding to the maximum dose rate. Figure 49 shows that for the present scenario ^{134}Cs, ^{137}Cs and ^{126}Sn were the three radionuclides that gave the most significant contribution to the doses received from ingestion of seafood for the critical group. It is also necessary to note that the impact of ^{144}Ce is significant for the doses from crustaceans and molluscs.

The calculated maximum dose-rate equals 110 μSv yr^{-1}, which is significantly lower than the average annual dose of 1-10 mSv from nature sources. At the same time, this dose-rate is significantly higher than range 1 - 10 μSv yr^{-1} for the negligible component to the annual individual dose from natural sources (UNSCEAR, 2000) and, therefore, has to be under consideration during evaluation of the accident consequences.

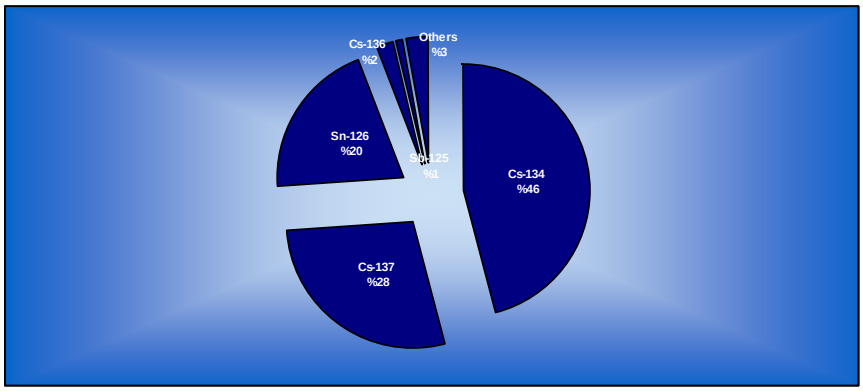

Fish (0.11 mSv per year)

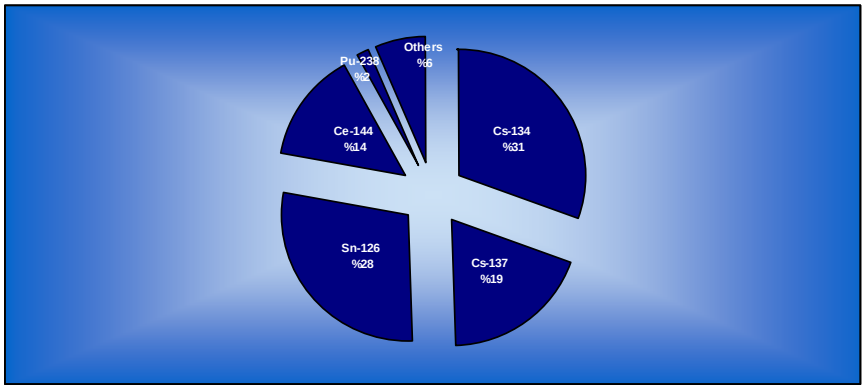

Crustacean (0.02 mSv per year)

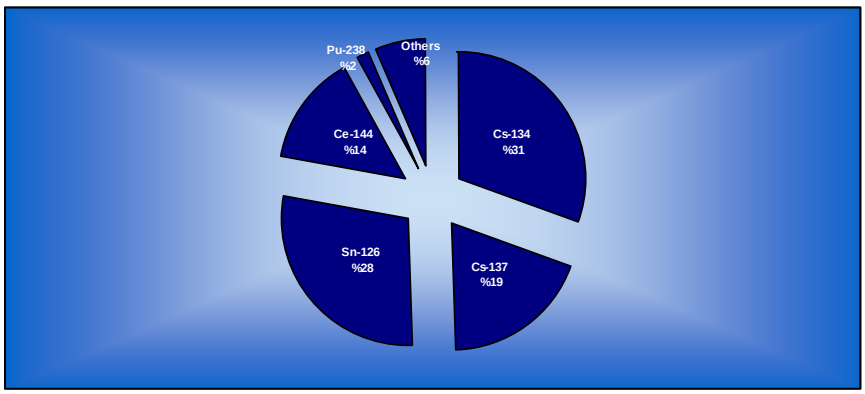

Molluscs (0.004 mSv per year)

Fig. 49. Potential dose impact to the critical group from fish, crustaceans and molluscs.

5.2.2.4.4 Doses to biota

Dose rates calculated for the different reference marine organisms (fish, crustacean and mollusks) in the sea region nearest the location of the hypothetical accident are presented in Figure 50. Figure 50 also indicates that the dose rates in fish, crustaceans and mollusks all follow the same pattern, with the maximum concentration of radionuclides corresponding to the initial period after the accidental releases began and with a following relatively fast decrease.

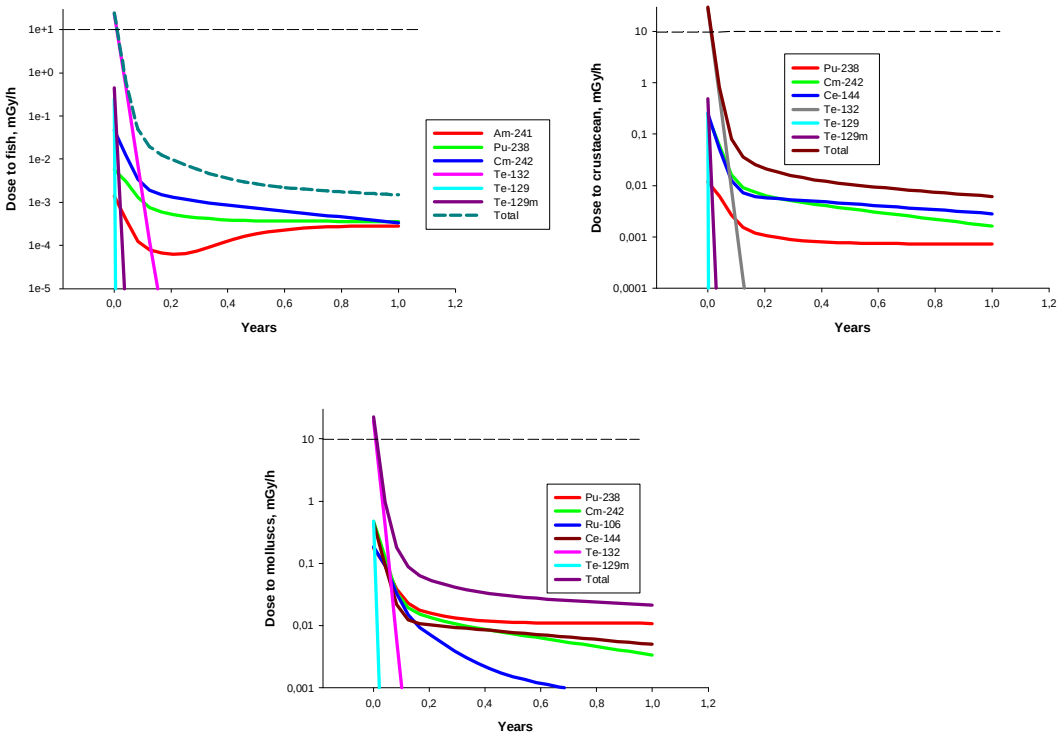

Fig. 50. Doses to fish, crustaceans and molluscs

There has previously been a consensus that the screening dose rate of 10 μGy h^{-1} or less is not harmful to marine biota (Brown et al., 2006). According to results presented in Figure 50, doses to the marine organisms are less than the screening dose except during the very short time period after the accident.

5.2.2.5 Sensitivity and uncertainty analysis

Different approaches are used for sensitivity and uncertainty analysis (Avila et al., 2004; Oughton et al., 2008; Hovard, 2002; Jørgensen, 1994; Till and Meyer, 1983). The following analysis have been provided on the basis of the local (S(L)) and global (S(G)) sensitivity indexes and (Jørgensen, 1994; Till and Meyer, 1983)

$$S^{(L)}(P) = \left(\frac{dV^{(S)}}{dP} \right)_{P_0} \frac{P_0}{V_0^{(S)}},$$

(3)

$$S^{(G)}(P) = 1 - \frac{V_{min}^{(S)}}{V_{max}^{(S)}},$$

where $V^{(S)}$ and P correspond to state variables (for example, concentrations of radionuclides in water and sediment phases, doses to man and biota, *etc.*) and parameters which are under evaluation; P_0 and $V_0^{(S)}$ correspond to the basic values of the parameter P and the state variable $V^{(S)}$; indexes $V_{min}^{(S)}$ and $V_{max}^{(S)}$ correspond to the minimum and maximum absolute values of the state variable $V^{(S)}$ within the range of parameter P.

This approach for sensitivity and uncertainty analysis is chosen mainly because the results of such analysis come up against the problem of complexity. Some results of the preliminary analysis are shown in Figure 51. The results show that the concentration of radionuclides in the environment and the doses to marine organisms can either increase or decrease with a given increase of the evaluated parameters. It is also shown that the results can strongly depend on the chosen time of analysis (Iosjpe, 2011a; Iosjpe, 2012).

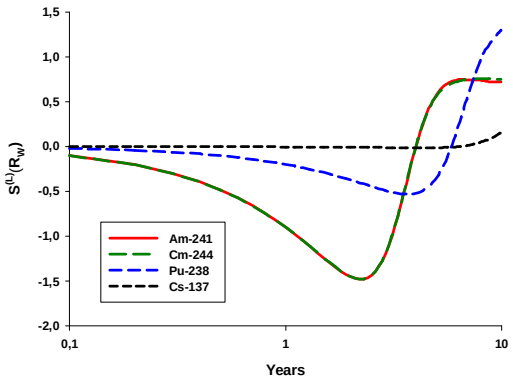

Fig. 51. Dynamics of the local sensitivity index $S^{(L)}$ of the sediment reworking rate (R_W) for the bottom water compartment of the southern part of the Norwegian Current.

5.2.2.5.1 State variables and environmental parameters (end points)

The results described in section 5.2.2.4.3 indicate that doses to the critical group (high consumption of seafood) is one of the most vulnerable end points for the simulated scenario. Therefore, the dose to the critical group has been selected for the following analysis.

In the present sensitivity and uncertainty analysis the concentration of radionuclides in biota and dose to critical group will be considered as state variables. The following parameters are selected for the analysis: *fl* - water exchange for the compartment, *Ta* - time of availability for the initial compartment (compartment 2), *SR* - sedimentation rate, *SSL* - suspended sediment load in water column, R_W - sediment reworking rate, k_d - sediment distribution coefficient, *CF* - radionuclide concentration factors for biota and ω - porosity of the bottom sediment.

The following radionuclides, which belong to all four groups described in Table 1, that have been selected for the analysis are: ^{238}Pu, ^{239}Pu, ^{240}Pu, ^{241}Am, ^{241}Pu, ^{244}Cm, ^{131}I, ^{90}Sr, ^{106}Ru, ^{134}Cs, ^{137}Cs, ^{133}I, ^{126}Sn, ^{110m} Ag, ^{127}Sb, ^{132}Te, ^{136}Cs, ^{129}Te, ^{129m}Te, ^{127}Te, ^{125}Sb, ^{135}I, ^{103}Ru, ^{147}Pm, ^{242}Cm and ^{144}Ce.

5.2.2.5.2 Results

Figure 52 shows some of the results of the local sensitivity index calculations, during the first year of radionuclide dispersion, for initial compartment of the model (this time corresponds to the maximum dose to the critical group).

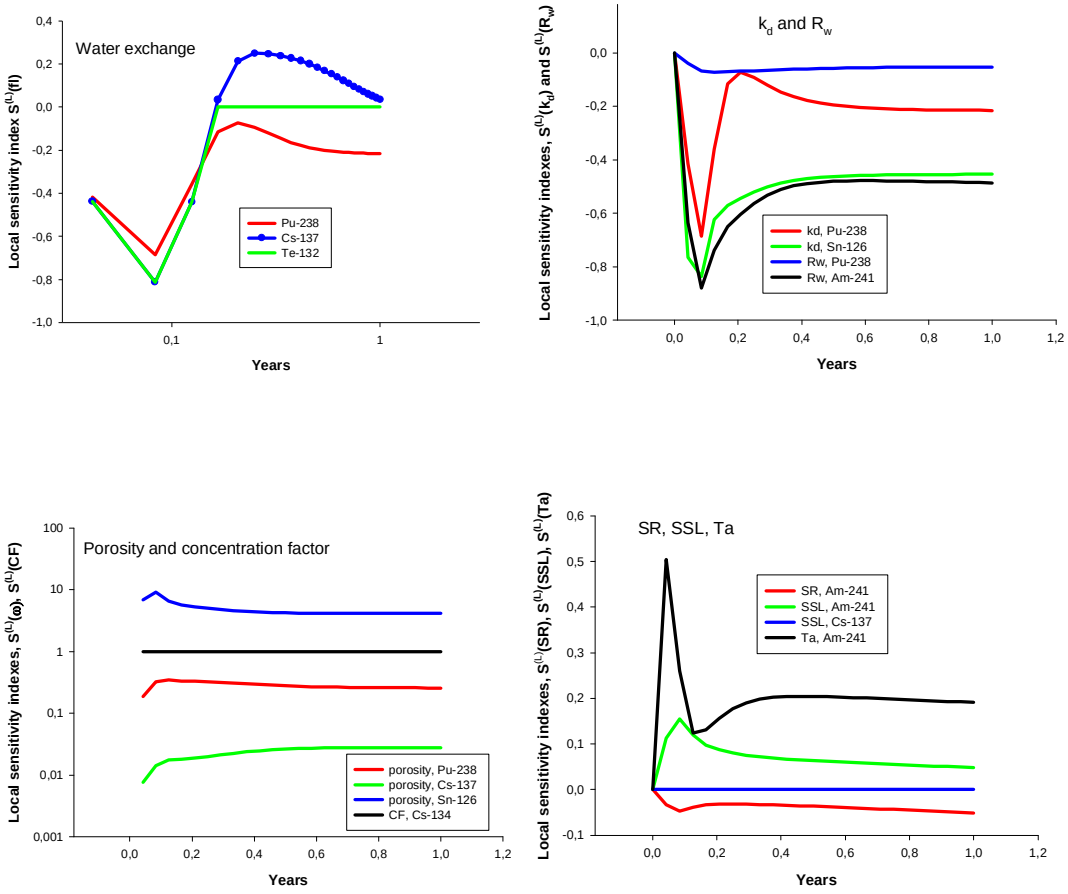

Fig. 52. The local sensitivity indexes $S^{(L)}$ for the fish concentration in compartment 2, which is shown in Figure 40.

The analysis of the results indicates which parameters have the most significant influence on the state variables. Furthermore, the analysis shows, whether the state variables will increase or decrease by a given change of a parameter. For instance, if the local sensitivity index equals 1, this means that state variable and a given parameter have a direct proportional relationship (for example, the concentration factor for ^{134}Cs, *CF*, in the bottom left of Figure 42). If the local sensitivity index equals 0, the selected parameter has no influence on the state variable (for example, the suspended sediment load in the water column for ^{137}Cs, *SSL*, in the bottom-right of Figure 52).

The basic values for the parameters selected in the present sensitivity analysis are: The sediment reworking rate (R_W) waters are chosen as R_W=5·10^{-3} m y^{-1} (Mitchell et al., 1999; MARINA II, 2003). The basic values of the sediment distribution coefficient (k_d) and concentration factors (*CF*) are chosen according to (IAEA) 2004 recommendations. Values for the suspended sediment load (*SSL*) and the sediment rate (*SR*) for the compartment 2 are chosen as 1.0E-07 t m^{-3} and 1.0E-04 m^{-2} y^{-1}, respectively (Nielsen et al., 1995; Nielsen et al., 1997). The value of the porosity of the bottom sediment (ω) is chosen as 0.7 (Nielsen et al., 1997). The value of the time of availability for the initial compartment 2, *Ta*, ware evaluated as 0.02 y.

Sediment distribution coefficients (k_d) and concentration factors (*CF*) can be defined according to IAEA (2004) within a factor of 10. The sediment reworking rates (R_W) and pore-water turnover rates (R_T), which describe the intensity of water-sediment interactions, may be defined as part of the optimization of the model parameters, by fitting the parameters to the experimental data. It is apparent that the parameter values can be chosen within a wide range during the optimization process. For instance, for the same equations describing the water-sediment interactions, the same regions (the Irish Sea) the parameters R_W can differ within a factor of 20 (MacKenzie and Nicholson, 1987; Mitchell et al., 1999). The sedimentation rate (*SR*), can generally differ with a factor of 3 according to (Mitchell et al., 1999). The suspended sediment load (*SSL*) can differ widely, but for this region it can differ with a factor of 3 according to (Nielsen et al., 1997; MARINA II, 2003). A range for the porosity of the bottom sediment (ω) can be defined as 0,3 - 0,75 according to MacKenzie and Nicholson (1987) and MARINA II, (2003). Water fluxes can differ with a factor of 1.2 for this region according to Drange et al., (2005). The time of availability for compartment 2 can vary in the interval [0, 0.05] as defined by the model graph structure.

Uncertainties were calculated on the basis of expression (3) for the global sensitivity index:

$$S^{(G)}(\{P_i\}) = 1 - \frac{D_{min}^{(CG)}}{D_{max}^{(CG)}} = 0.996.$$

Here $\{P_i\}$ is a set of all selected parameters, i=1,.., *n*, where n is the number of selected parameters; $D^{(CG)}_{min}$= 0.009 mSv and $D^{(C)}$ = 2.4 mSv are the minimum and maximum doses, respectively.

The minimum and maximum doses to the critical group were calculated in the same way as in section 5.2.2.4.3 for all selected parameters and for all radionuclides within their respective range.

The global sensitivity index is very close to 1. This means that in our evaluation all significant parameters were under consideration.

The maximum value 2.4 mSv per year correspond to the average annual dose of 1-10 mSv from nature sources.

Impact of different radionuclides to the maximum dose to the critical group is shown in Figure 53. Dose is dominated by radionuclides ^{126}Sn, ^{134}Cs and ^{137}Cs.

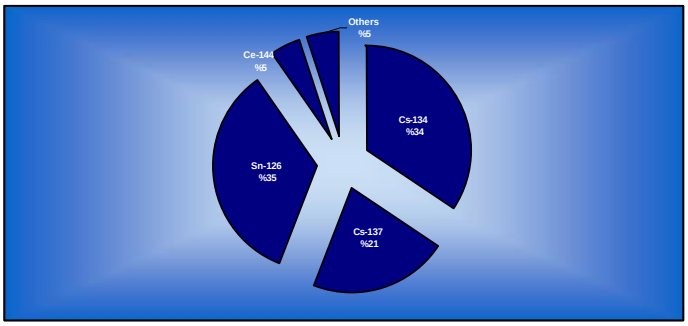

Fig. 53. Impact of radionuclides to the maximum dose rate (the first year after the hypothetical accident) to the critical group

5.2.3 Potential accident in the Kattegat region. Environmental sensitivity of marine regions

Mikhail Iosjpe, Norwegian Radiation Protection Authority - NRPA

The term “environmental sensitivity of marine regions” describes the vulnerability of different marine areas to harmful effects of radionuclide releases (Tracy et al., 2013). The present report will provide a comparison of environmental sensitivity for the Iceland coastal waters and the Kattegat region (the red spot in Figure 54) based on a study of the radioecological consequences after a hypothetical accident scenario involving a nuclear submarine, where a wide set of radionuclides is released into the marine environment.

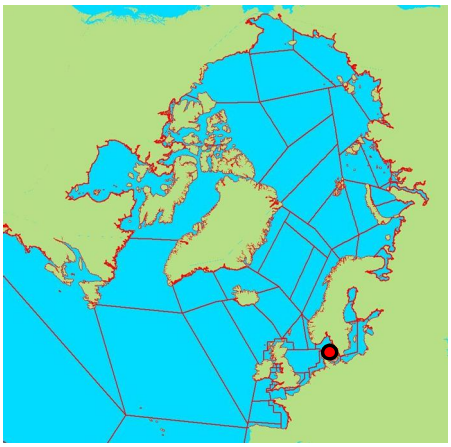

Fig. 54. The Kattegat region

5.2.3.1 Validation of the model

Validation of the NRPA model is based on the description of the global fallout after the testing of nuclear weapons in the atmosphere, releases from European nuclear facilities and the Chernobyl accident (UNSCEAR, 2000, StrålevernRapport, 2006; 2007; 2008; 2009; 2011; AMAP, 1998; White Book, 2005; Green et al., 2012; 2013). Releases of $^{239+240}$Pu and ^{137}Cs are shown in Figure 41 (top figure) and in Figure 55.

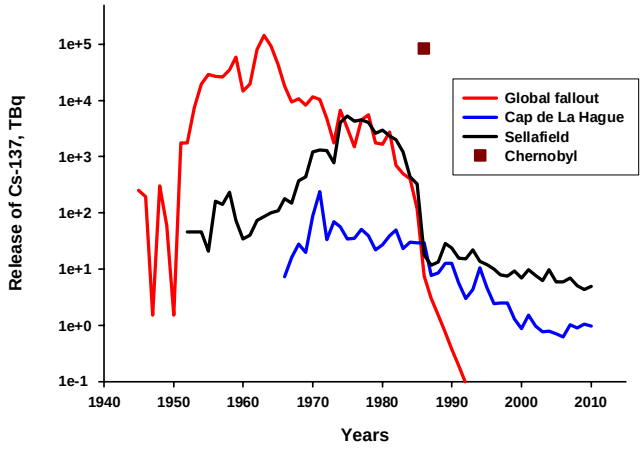

Fig. 55. Sources of ^{137}Cs

In Figures 56-58, the results of the model calculations of the concentration of $^{239+240}$Pu and ^{137}Cs in the Baltic Sea and surrounding waters are compared with the experimental data. This experimental data are collected from StrålevernRapport (2006 - 2011), Marina-Balt (2000) and Ikäheimonen (2009).

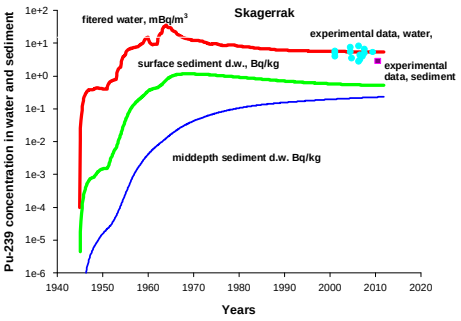

Fig. 56. $^{239+240}$Pu in the Skagerrak

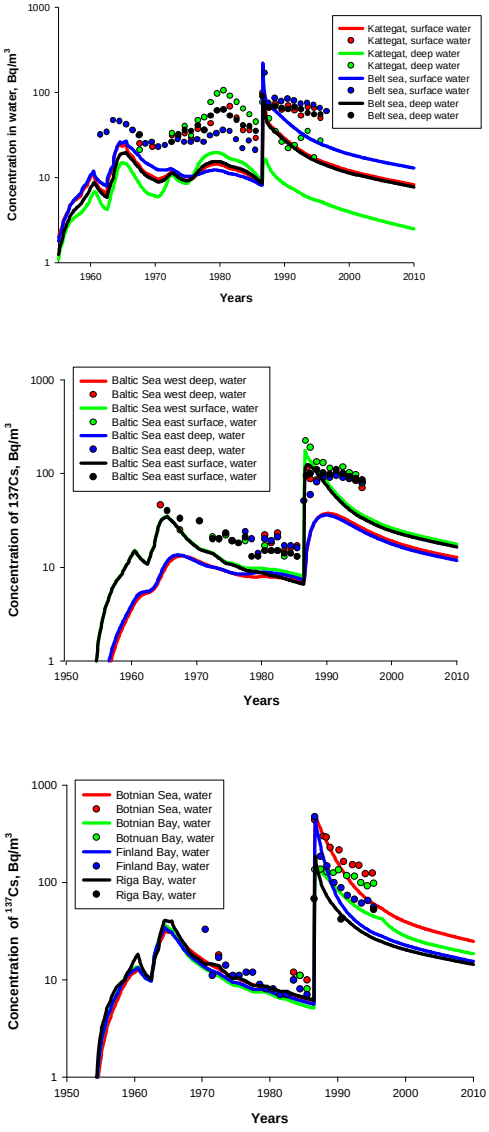

Fig. 57. ^{137}Cs in the Baltic Sea regions

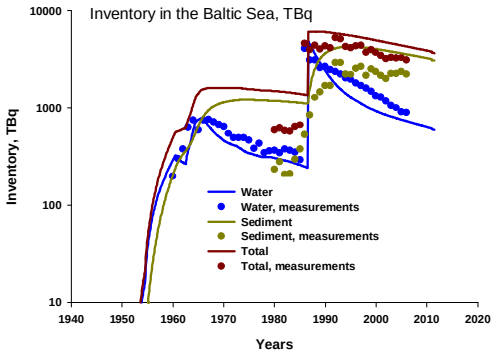

Fig. 58. Inventory of ^{137}Cs in the Baltic Sea regions

The circles show the average values of the experimental data. Generally, Figures 56-58 demonstrate that the model predictions for $^{239+240}$Pu and ^{137}Cs are reasonably accurate, but for the deep waters there is underestimation of the concentration by a factor of up to 3-5 (Figure 57). Calculations of ^{137}Cs inventory in Figure 58 slightly underestimate and overestimate the inventory in water and sediment, respectively. This might suggest that the set of parameters for the description of the water-sediment interactions in the Baltic Sea regions still have some room for improvement (the present version of the model uses parameters that have been optimized for the Irish Sea regions). Additionally, the results can be improved by optimization of the model parameters similar to the optimization process, described in (Nielsen, 1995).

5.2.3.2 Environmental sensitivity indexes

The environmental sensitivity of the marine regions have been described in the present study with the help of two parameters: (i) collective dose rates to man and (ii) individual doses for the critical group with the following index for the environmental sensitivity (ESI):

$$\mathrm{ESI} = \frac{\mathrm{D_{r1}}}{\mathrm{D_{r2}}}, \qquad (4)$$

where D_{r1} and D_{r2} are collective doses (or doses to the critical group) for the marine regions 1 and 2, respectively.

Thus, according to the present formulation of the environmental sensitivity index (4), when ESI > 1 the radioecological consequences to humans in region 1 are greater than in region 2, and region 1 is then recognized as the more vulnerable marine area of the two.

5.2.3.3 Results of calculations

Similar to the release of radionuclides into the Icelandic coastal waters, the results presented in Figures 59 and 60 show that the maximum collective dose rates in the studied scenario, occur during the first year after the release of radioactivity, and ^{134}Cs, ^{137}Cs and ^{126}Sn have the highest impact on the maximum collective dose rate. The maximum collective dose rate is approximately 609 manSv per year. So, the calculation of the environmental sensitivity index gives us the following result:

ESI_c= 609 manSv / 58 manSv ≈ 10.5

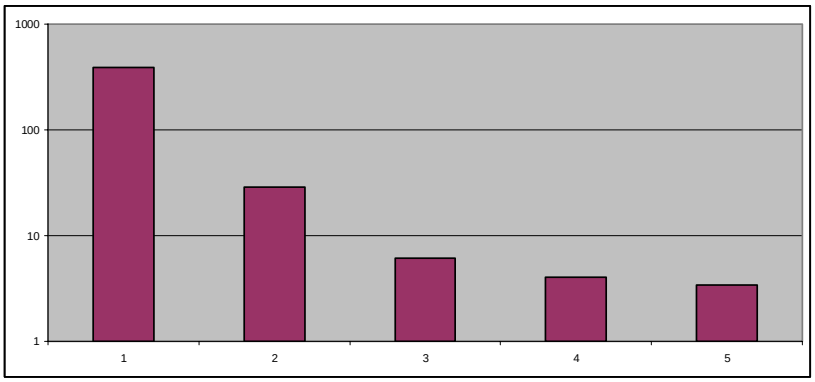

Fig. 59. Collective dose-rates (the Kattegat region), manSv per year

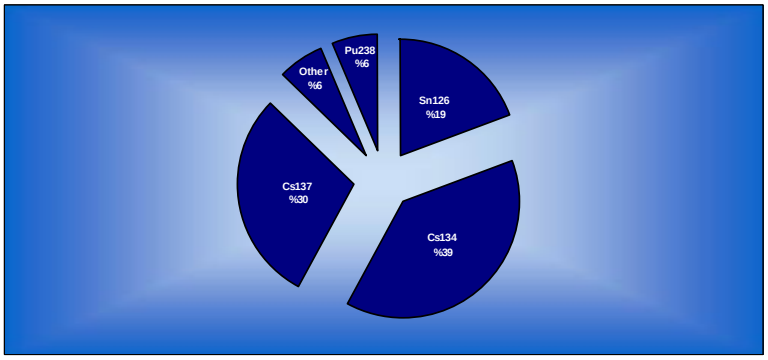

Fig. 60. Impact of radionuclides to the collective dose rate (the first year after the hypothetical accident in the Kattegat region)

Doses to the critical group after a hypothetical accident in the Kattegat region have been calculated here in the same way as described in the section 5.2.2.4.3 of the present report.

Similarly to the description in section 5.2.2.4.3, the proportions of the total calculated dose attributable to the different types of seafood are presented in Figure 61, corresponding to the maximum dose rate. As for the Icelandic coastal waters, Figure 61 shows that for the present scenario ^{134}Cs, ^{137}Cs were the radionuclides that gave the most significant contribution to the doses received from ingestion of seafood for the critical group. When compared results to the Kattegat to the results for the Icelandic coastal waters, ^{126}Sn has less of an impact, probably because ^{126}Sn has a very high k_d, and the suspended sediment load in the water column for the Kattegat region is up to order of magnitude higher than for the Icelandic region. This leads to much lower concentration of ^{126}Sn in filtered water and marine organisms.

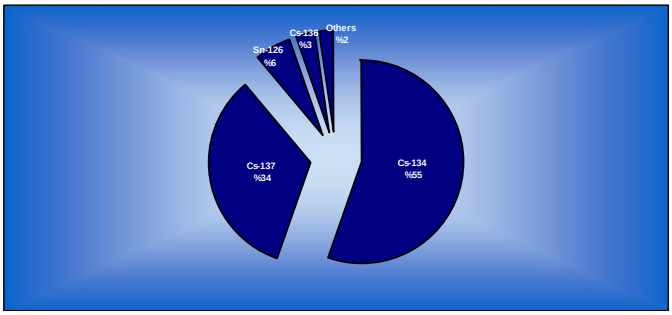

Fish (7.2 mSv per year)

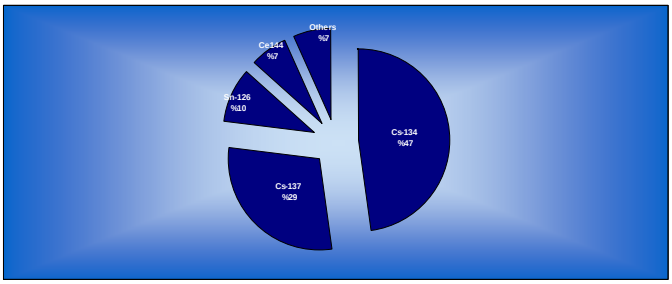

Crustacean (0.8 mSv per year)

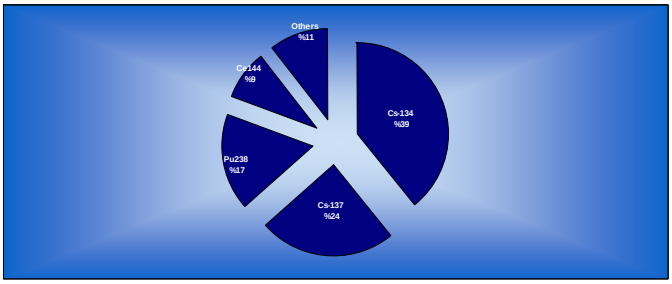

Molluscs (0.1 mSv per year)

Fig. 61. Dose impact to the critical group from fish, crustaceans and molluscs

The calculated maximum dose-rate equals 8.1 mSv yr^{-1}, which is significant in comparison to the average annual dose of 1-10 mSv from nature sources.

The calculation of the environmental sensitivity index gives the following result:

ESI_{cg}= 8.1 Sv / 0.11 Sv ≈ 73.6

Thus, the Kattegat region is much more vulnerable to the releases of radionuclides into marine environment than the Icelandic coastal waters (from 10 to 70 times according to the selected end point).

It is necessary to note that for the Kattegat region elevated levels of radionuclides in marine food products in comparison to CAC guidelines can be observed for a relatively

long period (up to 5 months). Examples for the total concentrations for molluscs (group 1) and fish (group 3) are shown in Figure 62.

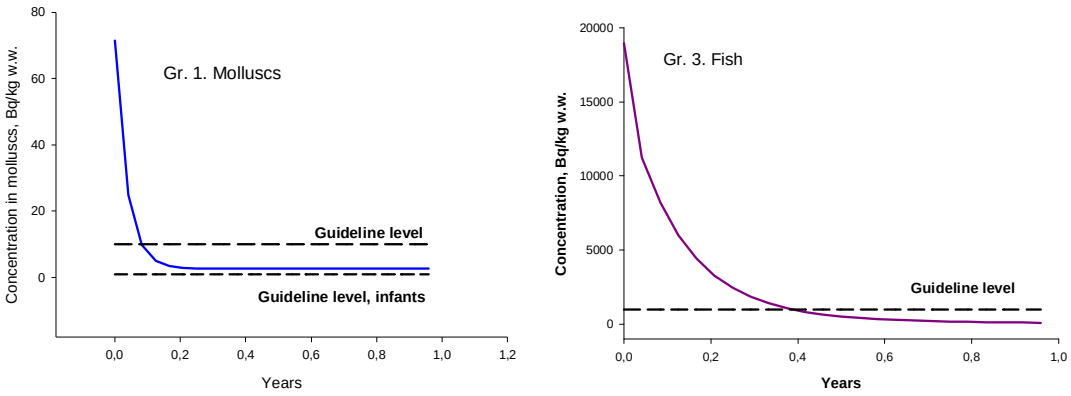

Fig. 62. Predicted concentration of radionuclides in seafood.

Conclusions

The consequences of an accident with a modern Russian submarine for the Icelandic and Kattegat marine regions were calculated on the basis of the most conservative scenario from the ones were under consideration in the present investigation.

Validation of the models was provided by comparing the results of the calculations with the available experimental data.

Calculations indicate that, generally, concentration of radionuclides in seafood would be under the international guideline levels for different groups of radionuclides. Simultaneously, results of calculations indicated that concentrations of radionuclides for some marine organisms during initial time of release near the accident location exceeded guideline levels. In the Kattegat region this time can be up to five months. Elevated levels of radionuclides in marine food products may lead to economical consequences in a market very sensitive to contaminants, even if they don't exceed guideline levels.

Calculated collective dose rates to man as well as doses to a critical group are significantly lower than doses from natural sources for the Icelandic coastal waters, but for the Kattegat region they can be equal or higher than the annual individual dose from natural sources and, therefore, have to be taken into consideration during the evaluation of the accident consequences.

Calculations of doses to biota for the Icelandic coastal waters show that doses are less than the screening dose, except for a very short period immediately after the accident.

This sensitivity and uncertainty analysis demonstrates that the results of such an analysis come up against the problem of complexity. Further, the sensitivity analysis shows that the relations between state parameters and parameters that are selected for the evaluation are dynamic. It is also shown that the uncertainties for the present calculations can change the result of the calculations up to several orders of magnitude.

Finally, the estimation of vulnerability of the Iceland and Kattegat regions were compared. Calculations show that the Kattegat region is much more sensitive to the release of radionuclides into the marine environment.

References

AMAP, 1998. AMAP assessment report: Arctic pollution issues. Oslo: Arctic Monitoring and Assessment Programme, AMAP, 1998.

Avila R., Beresford N.A., Agüero A., Broed R., Brown J., Iosjpe M., Robles B. and Suañez A., 2004. Study of the uncertainty in estimation of the exposure of non-human biota to ionising radiation, J. Radiolog. Protect., 24 A105-A122.

Bergsten, C., 2005. Fish and Game Study, part B: "The consumption of foods that may be important when assessing the dietary intake of mercury, cadmium and PCB/dioxins, with a focus on population groups living on the coast and in the inland of Norway." Oslo: Norwegian Food Safety Authority, 2005.

Brown, J.E., A. Hosseini, P. Børretzen & H.Thørring, 2006. Development of a methodology for assessing the environmental impact of radioactivity in Northern Marine environments, *Marine Pollution Bulletin*, vol. 52, no. 10, pp. 1127– 1137.

Drange, H, Gerdes, R, Gao, Y, Karcher, MJ, Kauker, F, Bentsen, M, 2005. Ocean General Circulation Modelling of the Nordic Seas, in: The Nordic Seas: An Integrated Perspective, Drange, Dokken, Furevik, Gerdes and Berger (Eds.), AGU Monograph 158,American geophysical Union, Washington DC,199-220.

CAC, 2006. Codex Alimentarius Commission: Joint FAO/WHO Food Standards Programme. Appendix 31. ftp://ftp.fao.org/codex/Alinorm06/al29_41e.pdf (09.01.07)

CEC, 1990. The radiological exposure of the population of the European community from radioactivity in North European marine waters. Project ´Marina´, Commission of the European Communities. Bruxelles: EUR 12483.

EC, 2000. The radiological exposure of the population of the European Community to radioactivity in the Barents Sea. MARINA-Balt project. EC, Radiation Protection Series 110, EUR 19200 EN.

EC, 2003. Update of the MARINA Project on the radiological exposure of the European Community from radioactivity in North European marine waters. EC, Radiation Protection 132 Luxembuourg, 2003.

Fiocchi A., Assa'ad A., Bahna S., 2006. Food allergy and the introduction of solid foods to infants: a consensus document. Adverse Reactions to Foods Committee, American College of Allergy, Asthma and Immunology. Annals of Allergy, Asthma and Immunology, 2006 Jul; 97(1):10-20; quiz 21, 77.

Green N.W., Skogen M., Aas W., Iosjpe M., Måge A., Breivik K., Yakushev E., Høgåsen T., Eckhardt S., Ledant A.B., Jaccard P.F., Staalstrøm A., Isachsen P.E., Frantzen S., 2013. Tiførselprogrammet 2012. Overvåkning av tilførsler og miljøtilstand i Barentshavet og

Lofotenområdet. Klima og forurensningsdirektoratet, ISBN 978-82-577-6279-7 (in Norwegian).

Hertel-Aas, T., Oughton, D., Jaworska, A., Bjerke, H., Salbu, B., and Brunborg, G., 2008. Effects of chronic gamma irradiation on reproduction in the earthworm *Eisenia fetida* (Oligochaeta). The international conference on radioecology & environmental radioactivity. Proceedings, Oral and oral poster presentations, Part 2 (Eds. P. Strand, J. Brown and T. Jølle), NRPA, Østerås, Norway, June 2008, 183-186.

Hovard, B.J. (Ed.), 2002. Radioecological sensitivity, Final report., Centre for Ecology & Hydrology.

Høibråten S., Haugan A. and Thoresen P., 2003. The environmental impact of the sunken submarine Komsomolets. FFI/Rapport-2003/02523. Kjeller, 2003.

IAEA (1997). Predicted radionuclide release from marine reactors dumped in the Kara Sea: Report of the Source Term Working Group of the International Arctic Seas Assessment Project (IASAP). IAEA Tec-Doc-938.Vienna: International Atomic Agency, 1997.

IAEA, 2004. *Sediment distribution coefficients and concentration factors for biota in the marine environment.* IAEA Technical reports series no. 422. Vienna: International Atomic Energy Agency, IAEA.

IASAP, 2003. Modelling of the radiological impact of radioactive waste dumping in the

Arctic Seas. IAEA-TECDOC-1330. Vienna: International Atomic Energy Agency, IAEA.

ICPR, 2007. The recommendations of the international commission on radiological protection. Annals of the ICRP, Publication 103, Exeter, UK.

Ikäheimonen T.K., Outola I., Vartti V.-P., Kotilainen P., 2009. Radioactivity in the Baltic Sea: inventories and temporal trends of 137Cs and 90Sr in water and sediments. J Radioanal Nucl Chem (2009) 282:419–425.

Iosjpe, M., 2006. Environmental modeling: Modified approach for compartmental models, In: Povinec P.P., Sanchez-Cabeza J.A., eds. *Radionuclides in the environment: International conference on isotopes in environmental studies,* Monaco 2004. Radioactivity in the Environment, vol.8. Amsterdam: Elsevier, 2006: 463– 476.

Iosjpe M., 2011. Radioecological sensitivity of the shallow marine environment. *Radioprotection*, 46, nº 6, S189-S193.

Iosjpe M., 2011a. A sensitivity analysis of the parameters controlling water-sediment interactions in the coastal zone: Consequences to man and environment, Journal of Marine Systems 88 (2011), 82-89.

Iosjpe M., 2012. Dose assessment to marine biota: evaluation of key environmental parameters, IRPA 13, P11.38,http://www.irpa13glasgow.com/information/downloads/.

Iosjpe, M., J. Brown & P. Strand, 2002. Modified approach for box modeling of radiological consequences from releases into marine environment, *Journal of Environmental Radioactivity* 2002, 60, 91– 103.

Iosjpe M., M. Karcher, J. Gwynn, I. Harms, R. Gerdes and F. Kauker, 2009. Improvement of the dose assessment tools on the basis of dispersion of the ^{99}Tc in the Nordic Seas and the Arctic Ocean. *Radioprotection*, vol. 44, n° 5, 531-536.

Iosjpe M. & Liland A., 2012. Evaluation of environmental sensitivity of the marine regions. Journal of Environmental Radioactivity 108 (2012) 2-8.

Iosjpe M., Pálsson S. E., Logemann K., 2013. Evaluation of consequences of the potential accident with the modern operative nuclear submarine in the Iceland coastal waters. ERR2013 conference, Abstract, Session 10 – Radiation Protection of the Environment, O10.4.

Iosjpe M., Perianez R, Aldridge J. & Børetzen P. (2003). Radionuclide dispersion models for Arctic, Atlantic and Mediterranean seas. Estimation of radiological sensitivity of marine areas. A deliverable report for REMOTRANS, Project FIGE-CT-2000-00085, December 2003.

Jørgensen S.E., 1994. Fundamentals of ecological modelling. Developments in Environmental Modelling, 19, Elsevier, Amsterdam-London-New York-Tokyo, 1994.

Karcher, M.J. & I.H. Harms, 2000. Estimation of water and ice fluxes in the Arctic for an improved box structure of the NRPA box model, In: Iosjpe, M. [ed.] Transport and fate of contaminants in the Northern Seas. Østerås: Norwegian Radiation Protection Authority, NRPA.

Khlopkin N.S., 1994. Assessment and prognosis of the state of nuclear installation of submarine “Kosmomolets”. Report of the Working Group of RRC Kurchatov Institute. Moscow 1994.

Kobayashi T., Togawa O., Odano N. and Ishida T., 2001. Estimates of collective doses from a hypothetical accident of a nuclear submarine. Journal of Nuclear Science and Technology, 2001, 38(8), 658-663.

Kull I., Bergström A., Lilja G., Pershagen G., Wickman M., 2006. Fish consumption during the first year of life and development of allergic diseases during childhood, Allergy. 61(8), 1009-15.

Lewis, B. J. & J.J.M.R. Morgan, 1999. Source Term Analysis for A Nuclear Submarine Accident. In conference proceedings *Sixth International Conference on CANDU Fuel, September 26– 30*, Niagara Falls, Canada, 1999, 153– 168.

Lynn N et al., 1995. Scenarios for potential radionuclide release from marine reactors Dumped in the Kara Sea. (unpublished, undated), p. 4.

MacKenzie J. and & Nicholson S., 1987. COLDOS – A computer code for the estimation of collective doses from radioactive releases to the sea. SRD R 389, UK Atomic Energy Authority.

MARINA II, 2003. Update of the MARINA Project on the radiological exposure of the European Community from radioactivity in North European marine waters, European Commission, Radiation Protection 132, Contract B3-4305/2000/304957/MAR/C4.

Marina-Balt, 2000. The radiological exposure of the population of the European Community to radioactivity in the Baltic Sea Marina-Bait project Proceedings of a seminar held at Hasseludden Conference Centre, Stockholm, 9 to 11 June 1998. Edited by S. P. Nielsen. Directorate-General Environment, EUR 19200 EN.

Mitchell P. I., Condren O. M., León Vintró L., & McMahon C. A., 1999. Trends in plutonium, americium and radiocaesium accumulation and long-term bioavailability in the western Irish Sea mud basin. J. Environ. Radioact. 44, 221-249.

NATO, 1998. NATO CCMS Pilot Study. Cross-border environmental problems emanating from defence-related installations and activities: Final report, volume 4: Environmental risk assessment for two defence-related problems. Phase II: 1995-1998. NATO report 227. Oslo, 1998.

Nielsen, S.P., 1995. A box model for North-Atlantic coastal waters compared with radioactive tracers. Journal of Marine Systems, 6, 545-560.

Nielsen, S.P., Iosjpe M., Strand P., 1995. A preliminary assessment of potential doses to man from radioactive waste dumped in the Arctic Sea. NRPA report 1995:8, ISSN 0804-4910, Østerås, Norwegian Radiation Protection Authority, 1995.

Nielsen, S.P., Iosjpe, M. and Strand, P., 1997. Collective Doses to Man from Dumping of Radioactive Waste in the Arctic Seas. *The Science of the Total Environment*, 202, 135-147.

Oughton D.H., Agüero A., Avila R., Brown J.E., Copplestone D., Gilek M., 2008. Addressing uncertainties in the ERICA Integrated Approach, J. Environ. Radioact. 99, 1384-1392.

Petrov, E., 1991. Estimation of the Nuclear Power Plant Condition and Radiation and Ecological Consequences of a Prolonged Stay of the SSN 'Komsomolets' on the Sea Bed and During Its Recovery, (unpublished), submitted from the Russian Central Design Bureau Marine Engineering “Rubin” to the Norwegian Government, November 15, 1991.

Smith, K. and Jones, A., 2003. Generalised Habit data for radiological assessment. NRPB report W41.

StrålevernRapport, 2005.. Radioactivity in the marine environment 2003. Results from the Norwegian national monitoring programme (RAME). Østerås: Statens strålevern, 2005:20.

StrålevernRapport, 2006. Radioactivity in the marine environment 2004: Results from the Norwegian national monitoring programme (RAME). Østerås: Statens strålevern, 2006:14.

StrålevernRapport, 2007. Radioactivity in the marine environment 2005: Results from the Norwegian national monitoring programme (RAME). Østerås: Statens strålevern, 2007:10.

StrålevernRapport, 2008. Radioactivity in the marine environment 2006: Results from the Norwegian national monitoring programme (RAME). Østerås: Statens strålevern, 2008:14.

StrålevernRapport, 2009. Radioactivity in the marine environment 2007: Results from the Norwegian national monitoring programme (RAME). Østerås: Statens strålevern, 2009:15.

StrålevernRapport, 2011. Radioactivity in the marine environment 2008 and 2009: Results from the Norwegian national monitoring programme (RAME). Østerås: Statens strålevern, 2011:4.

Tracy B.L., Carini F., Barabash S., Berkovskyy V., Brittain J.E., Chouhan S., Eleftheriou G., Iosjpe M., Monte L., Psaltaki M., Shen J., Tschiersch J., Turcanu C., 2013. The sensitivity of different environments to radioactive contamination. Journal of Environmental Radioactivity 122 (2013) 1- 8.

Till J.E. and Meyer H.R. (Eds.), 1983. Radiological Assessment. A Textbook on Environmental Dose Analysis. NVREG/CR – 3332, ORNL – 5968. Washington, D.C. 20555, NRC FIN BO766.

US DoHHS, 1998. Accidental radioactive contamination of human food and animal feeds: recommendations for state and local agencies. Food and drug administration, Rockville.

UNSCEAR, 2000. Sources and effects of ionizing radiation. UNSCEAR 2000 Report to the General Assembly with Scientific Annexes. Volume I: Sources. UN, New York, 2000.

White Book, 2005. Sivintsev, Yu.V., Vakulovskiy, S.M., Vasiliev, A.P., Vysotskiy V.L., Gubin A.T.,Danilyan V.A., Kobzev V.I., Kryshev I.I., Lavkovskiy S.A.,Mazokin B.A., Nikitin A.I., Petrov O.I., Pologih B.G., Skorik Yu.,I. Technogenic Radionuclides in the Seas Surrounding Russia ("White Book-2000"), Moskow, IzdAT, 2005.

6 VALIDATION CONSIDERATIONS

6.1 Review report on measured data of the Baltic Sea marine environment

Vesa-Pekka Vartti, Radiation and Nuclear Safety Authority - STUK

6.1.1 Introduction

This draft report will concentrate on measured radioactivity data in the Baltic Sea. The data presented here is mainly based on HELCOM MORS Environmental Database [1]. While most of the radioactivity in the marine environment is due to naturally occurring radionuclides, this draft will concentrate on man-made radioactive substances.

6.1.2 Sources of radioactivity in the Baltic Sea

The man-made radioactive substances in the Baltic Sea are due to four major events [2]:

1. The atmospheric nuclear weapons test of Soviet Union and United States in the northern hemisphere during 1950s-1960s.
2. Chernobyl nuclear power plant accident in 1986
3. Discharges from the spent nuclear fuel reprocessing plants, Sellafield in the United Kingdom and La Hague in France
4. Authorised discharges of radioactivity in the sea from routine operation of nuclear installations in the Baltic Sea region

Two man-made radionuclides, ^{90}Sr and ^{137}Cs, are considered to be of special concern to man. Both have relatively long physical half-lives (28.80 and 30.05 years, respectively [3]) and are readily transported through food chains because of chemical similarities to calcium (strontium) and potassium (caesium).

The direct input of ^{137}Cs from the Chernobyl accident into the Baltic Sea was estimated to be 4700 TBq [4], in addition the amount of Chernobyl-derived ^{137}Cs carried into the Baltic Sea by river runoff has been estimated to be 300 TBq during 1986-1996 [5]. The Chernobyl accident is the main source for ^{137}Cs in Baltic Sea (83% of the total). The total injection of ^{137}Cs in Baltic Sea from the nuclear weapons test fallout is estimated to be 800 TBq [6] and 13% of the total inventory. The remaining 4% of the total inventory of ^{137}Cs (250 TBq) comes mainly from Sellafield and La Hague [3]. The share of the discharges from local nuclear installations into Baltic Sea is very small, 0.04% (2.4 TBq) of the total inventory of ^{137}Cs.

For ^{90}Sr, the main source of contamination was the fallout from the nuclear weapons tests (81%, 500 TBq), while the proportion from the Chernobyl fallout was smaller (13%, 80 TBq). The remaining 6% (40 TBq) comes mainly from sources outside the Baltic Sea, mainly Sellafield and La Hague. The share of the discharges from local nuclear installations into Baltic Sea is small, 0.2% (1.04 TBq).

6.1.3 Radionuclides in seawater

In the HELCOM MORS Environmental Database the Baltic Sea is divided into 15 sub-basins (Figure 63).

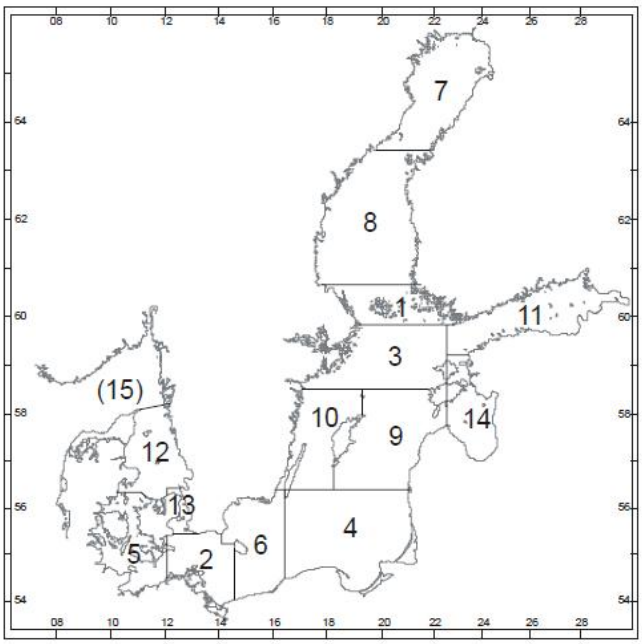

1. Archipelago Sea
2. Arkona Sea
3. Northern Baltic Proper
4. Southern Baltic Proper
5. Belt Sea
6. Bornholm Sea
7. Bothnian Bay
8. Bothnian Sea
9. Gotland East
10. Gotland West
11. Gulf of Finland
12. Kattegat
13. Sound
14. Gulf of Riga
15. Skagerak

Fig. 63. The division of Baltic Sea area into sub-basins.

In 2011 altogether 103 results of ^{137}Cs and 46 results of ^{90}Sr from surface water samples and 75 results of ^{137}Cs and 25 results of ^{90}Sr from near bottom water samples were reported to the HELCOM MORS Environmental Database.

The highest measured ^{137}Cs activity concentration in 2011 was 39.1 Bq/m^3 in surface water and 41.3 Bq/m^3 in near bottom water and the lowest activity concentrations were 3.2 Bq/m^3 in surface water and 3.7 Bq/m^3 in near bottom water. The highest mean values of sub basins in surface water samples were reported in Bothnian Sea, 36.4 Bq/m^3 and lowest in Skagerak, 20.0 Bq/m^3. In near bottom water samples the highest mean values were reported in Bothnian Bay, 37.2 Bq/m^3 and the lowest in Kattegat, 9.5 Bq/m^3. Activity concentration data of ^{137}Cs from 2011 are presented in Table 10.

For ^{90}Sr the highest activity concentration in 2011 was 9.8 Bq/m^3 in surface water and 15.4 Bq/m^3 in near bottom water and the lowest activity concentrations were 5.0 Bq/m^3 in surface water and 2.4 Bq/m^3 in near bottom water. The highest mean values of sub basins in surface water samples were reported in Gotland East, 9.8 Bq/m^3 and lowest in Belt Sea, 6.3 Bq/m^3. In near bottom water samples the highest mean values were reported in Gotland East, 9.6 Bq/m^3 and the lowest in Kattegat, 2.4 Bq/m^3. Activity concentration data of ^{90}Sr from 2011 are presented in Table 11.

For other man-made nuclides in sea water only few results have been reported. Pu-239,240 activity concentrations were below 0.01 Bq/m^3, the main source being the nuclear weapons tests. From Bornholm Sea, the Arkona Sea, the Kattegat and the Sound in 2007-2010 few results of ^{99}Tc activity concentrations were also reported, these values varied between 0.06 to 0.09 Bq/m^3. The main source of ^{99}Tc is the inflow of contaminated waters from the North Sea originating from the Sellafield nuclear reprocessing plant.

		Cs-137 in surface water [Bq/m³]				Cs-137 in near bottom water [Bq/m³]			
Basin	Basin name	number of values	min	max	mean	number of values	min	max	mean
1	ARCHIPELAGO SEA	1	33,0	33,0	33,0				
2	ARKONA SEA	18	3,2	35,9	28,2	11	17,3	33,9	28,1
3	NORTHERN BALTIC PROPER	1	31,8	31,8	31,8	1	30,9	30,9	30,9
4	SOUTHERN BALTIC PROPER	10	18,3	35,7	29,8	12	26,4	37,1	31,1
5	BELT SEA	28	21,5	32,4	26,3	28	7,2	24,8	16,7
6	BORNHOLM SEA	6	31,2	37,2	34,2	6	25,4	33,4	29,6
7	BOTHNIAN BAY	4	21,6	35,1	26,3	2	33,0	41,3	37,2
8	BOTHNIAN SEA	3	33,2	39,1	36,4	1	35,8	35,8	35,8
9	GOTLAND EAST	1	34,0	34,0	34,0	1	32,8	32,8	32,8
10	GOTLAND WEST	1	22,0	22,0	22,0				
11	GULF OF FINLAND	16	12,0	31,2	20,6	2	28,2	30,9	29,6
12	KATTEGAT	6	17,0	25,0	21,8	5	3,7	16,1	9,5
13	SOUND	6	22,2	31,3	26,4	6	5,8	30,8	18,5
15	SKAGERAK	2	15,0	25,0	20,0				

Table 10. ^{137}Cs activity concentration data in sea water in 2011 in the HELCOM MORS Environmental database.

		Sr-90 in surface water [Bq/m³]				Sr-90 in near bottom water [Bq/m³]			
Basin	Basin name	number of values	min	max	mean	number of values	min	max	mean
2	ARKONA SEA	11	6,4	8,4	7,5	2	8,0	8,0	8,0
3	NORTHERN BALTIC PROPER	1	9,7	9,7	9,7	1	9,0	9,0	9,0
4	SOUTHERN BALTIC PROPER	10	5,0	9,6	7,8	12	4,6	13,1	8,5
5	BELT SEA	6	5,1	7,3	6,3				
6	BORNHOLM SEA	5	7,6	8,4	8,2	5	6,1	15,4	8,6
7	BOTHNIAN BAY	1	6,8	6,8	6,8	1	7,4	7,4	7,4
8	BOTHNIAN SEA	1	9,8	9,8	9,8	1	9,6	9,6	9,6
9	GOTLAND EAST	1	9,0	9,0	9,0	1	8,2	8,2	8,2
11	GULF OF FINLAND	10	5,0	8,2	6,8	1	8,9	8,9	8,9
12	KATTEGAT					1	2,4	2,4	2,4

Table 11. ^{90}Sr activity concentration data in sea water in 2011 in the HELCOM MORS Environmental database.

6.1.4 Radionuclides in sediments

Due to the slow exchange of water between the Baltic Sea and the North Sea and the relatively rapid sedimentation rates, radionuclides have prolonged residence times in the Baltic Sea [7]. Most of the long lived artificial radioactivity is due to ^{137}Cs and is mostly found in the bottom sediments in the Bothnian Sea and in the eastern part of the Gulf of Finland (Figure 64). The amounts of ^{137}Cs have been relatively even in different monitoring stations of the Baltic Sea, although showing spatial variation during the reporting period (Figure 64). However, due to local or areal accumulation, transportation and erosion rates at some monitoring stations (especially in the Southern Baltic Proper, the Western Baltic and the Gulf of Finland) show a more fluctuant trend of

radioactivity concentration of ^{137}Cs. The sedimentation rate is relatively high in the Baltic Sea and varies widely (between 0.2 and 29 mm/year (HELCOM 2000)) depending on the area and local environmental factors, which is clearly seen by the vertical profiles in Figure 65. In addition to the geological conditions, the differences in sampling techniques increase the variability of the results.

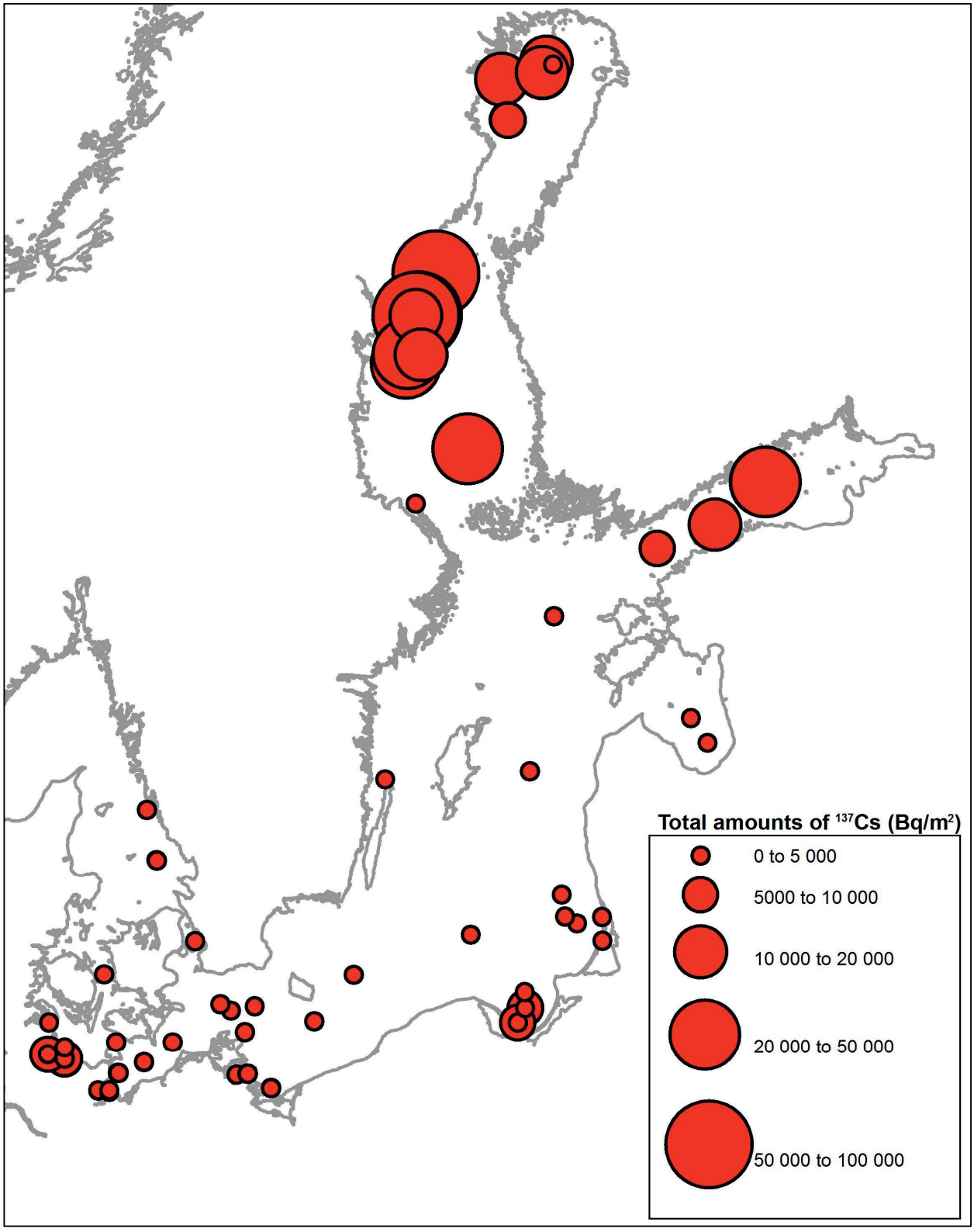

Fig. 64. Total amounts of ^{137}Cs Bq/m^2 at different sampling stations in 2007-2010. [2]

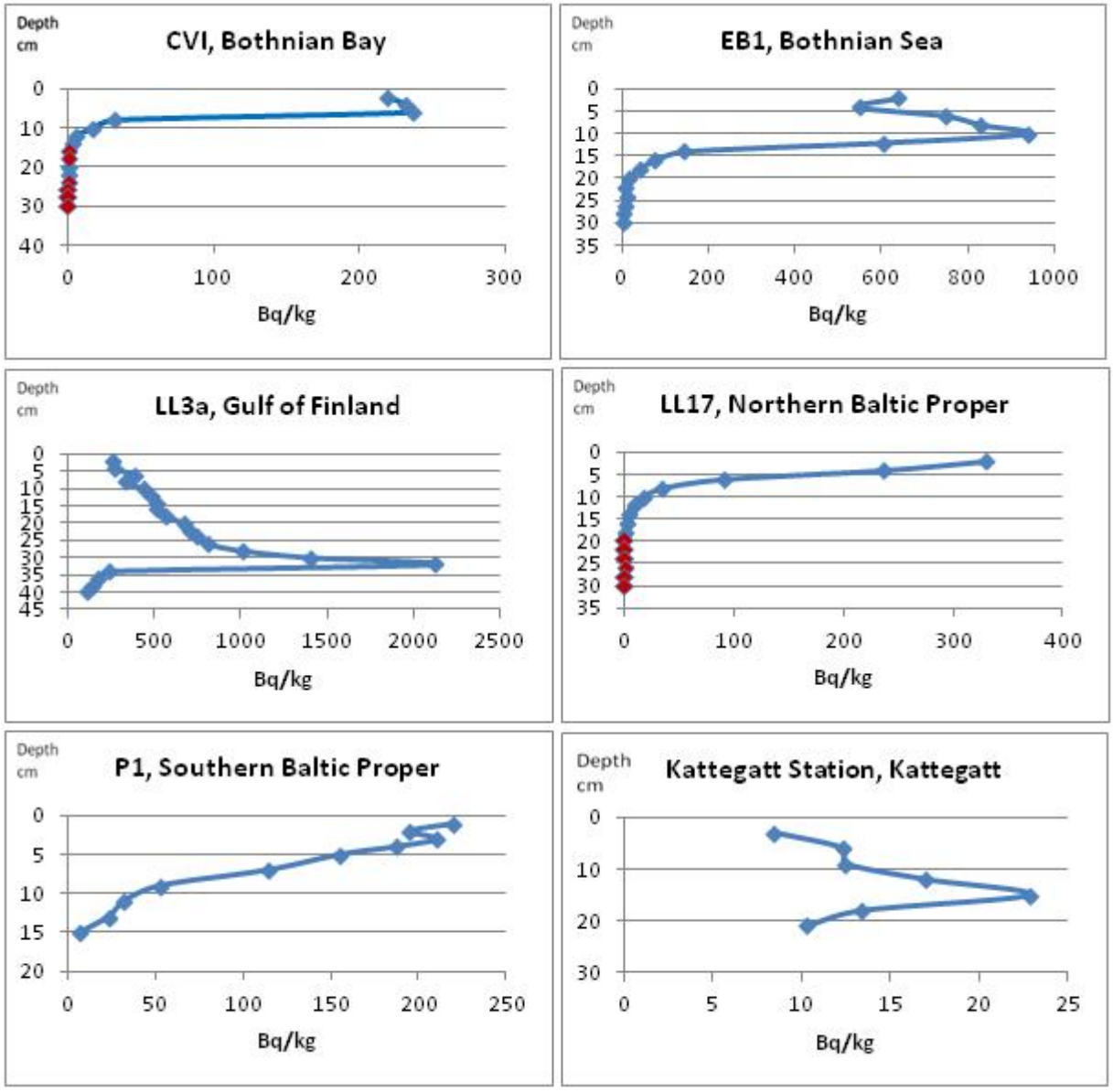

Fig. 65. Concentrations of ^{137}Cs (Bq/kg dry weight.) as a function of depth at some monitoring stations in the Baltic Sea in 2010. The measured values under the detection limits are marked in red.[2]

The total amount of ^{137}Cs activity in the Baltic Sea sediments has estimated to be about 2150-2480 TBq [2]. The highest concentrations reported to the HELCOM Environmental database were over 2000 Bq/kg d.w. Changes of ^{137}Cs concentrations in surface sea water [Bq m^{-3}] and total inventory in sediments [Bq m^{-2}] during 1980-2012 at three monitoring stations are presented in Figure 66.

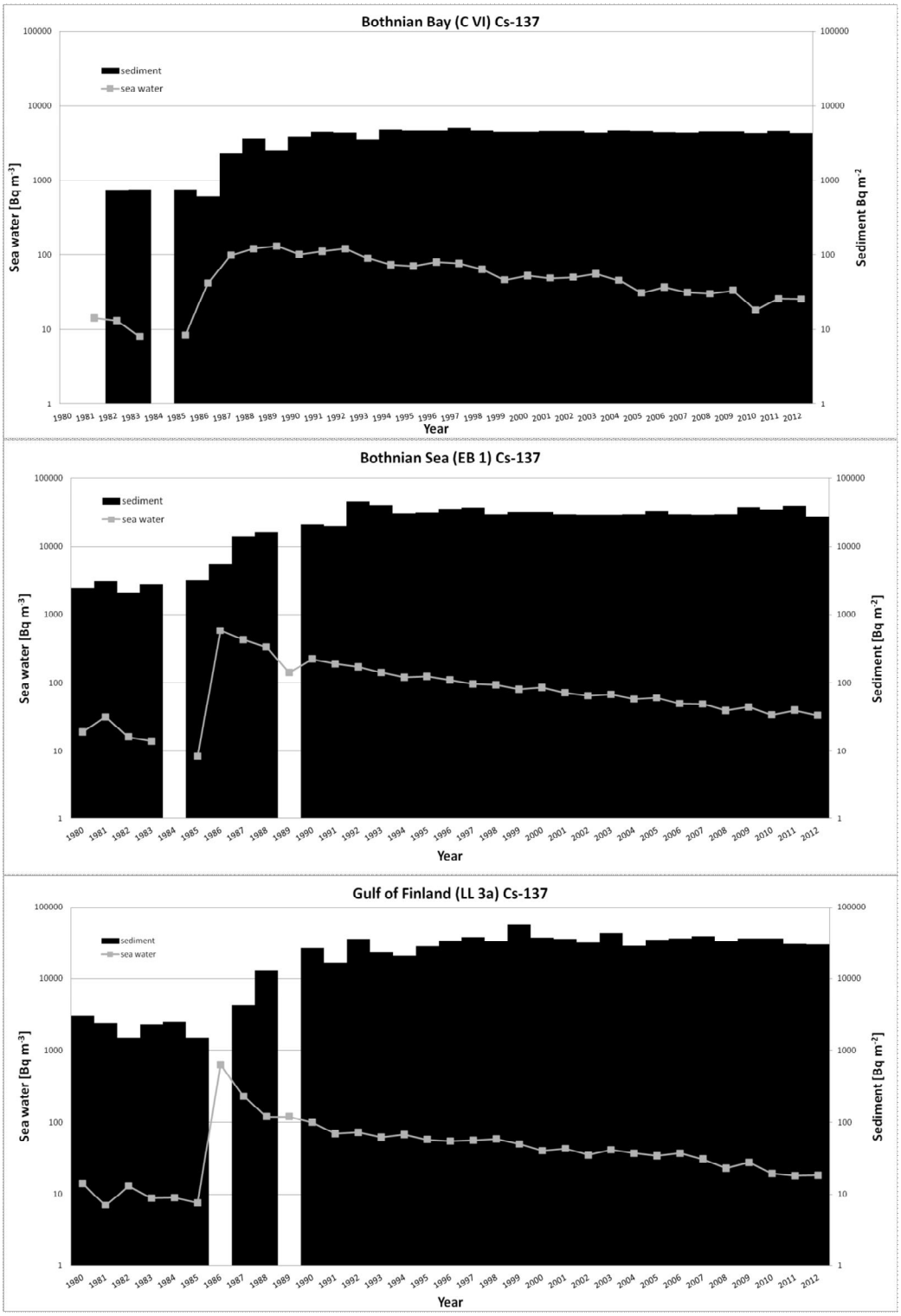

Fig. 66. Cs-137 concentrations in surface sea water [Bq m^{-3}] and total inventory in sediments [Bq m^{-2}] during 1980-2012 at three monitoring stations; C VI (Bothnian Bay), EB 1 (Bothnian Sea) and LL 3a (Gulf of Finland). Note the logarithmic scale in the graphs.

A rough estimate of total inventory of ^{90}Sr in Baltic Sea sediments is 21 TBq.[8]. This is mostly due to the global fallout. In the surveillance of the marine sediments of Finnish nuclear power plants, the measured values of ^{90}Sr activity concentrations have ranged between 0.6 and 8.5 Bq/kg d.w. [2]. The highest reported activity in the HELCOM database during 1999-2010 was 73.8 Bq/kg d.w.

In the surveillance of the marine sediments of Finnish nuclear power plants, the measured values of $^{239,240}Pu$ activities have ranged between 0.5 and 3.9 Bq/kg d.w.[2]. The highest reported activity concentrations in the HELCOM database during 1999-2010 was 14.1 bq/kg d.w. Due to the limited data, the present total amounts of plutonium activities are difficult to estimate. In the years 1999-2010, the reported ^{241}Am concentrations in the HELCOM database have ranged from 0.03 to 4.8 Bq/kg d.w.[2]. Recent rough estimate of the total inventory of ^{241}Am in the Baltic Sea sediments was 8.4 TBq [8].

6.1.5 Radionuclides in biota

The Chernobyl derived ^{137}Cs is the most dominant man-made radionuclide in Baltic Sea fish. In 2010 the mean activity concentrations of ^{137}Cs in the group of marine round fish (cod, herring, whiting) were between 0.7 and 7 Bq/kg w.w. (wet weight), in marine flat fish (plaice, flounder, dab) between 1.5 and 5 Bq/kg w.w. and in freshwater fish (pike) in Finnish coastal areas up to 15 Bq/kg w.w. [2].

The ^{90}Sr activity concentrations in Baltic Sea fish flesh are more than two orders of magnitude lower than those of ^{137}Cs. The highest activity concentration of ^{90}Sr reported to the HELCOM database in 2011 was 0.056 Bq/kg w.w. in herring and 0.018 Bq/kg w.w. in pike. The activity concentration in herring was higher because the sample included the whole fish without head and entrails and thus small bones which accumulate the bone-seeking ^{90}Sr more than fish flesh [2].

The highest measured activity concentrations of $^{239,240}Pu$ and ^{241}Am in Baltic Sea fish were one to two orders of magnitude lower than those of ^{90}Sr [2].

In *Fucus Vesiculosus* (bladder wrack) the activity concentrations of ^{137}Cs in the years 2009-2011 varied widely in the sub basins of the Baltic Sea. In the Bothnian Sea the values were between 16 and 25.4 Bq/kg d.w., in the Gulf of Finland between 12.4 and 25 Bq/kg d.w., in the Southern Baltic Proper, Bornholm Sea and Sound between 1.9 and 17.9 Bq/kg d.w. and in Kattegat between 0.25 and 5.1 Bq/kg d.w. [1].

In mussels *Mytilus Edulis* (Blue mussel) and *Macoma Baltica* the activity concentrations of ^{137}Cs in the years 2009-2011 varied between 0.6 and 9.8 Bq/kg d.w. [1].

References

[1] HELCOM MORS Environmental Database, http://www.helcom.fi/stc/files/Data/MORS/MORS2012_DISCHARGE.zip

[2] HELCOM 2013, Thematic assessment of longterm changes in radioactivity in the Baltic Sea, 2007-2010, Baltic Sea Environ. Proc. No. 135

[3] Decay Data Evaluation Project, Recommented Data, updated 9th September 2013, http://www.nucleide.org/DDEP_WG/DDEPdata.htm

[4] Nielsen, S.P., Bengtson, P., Bojanowski, R., Hagel, P., Herrmann, J., Ilus, E., Jakobson, E., Motiejunas, S., Panteleev, Y., Skujina, A. and Suplinska, M., 1999. The radiological exposure of man from radioactivity in the Baltic Sea, The Science of the Total Environment 237/238 (1999) 133-141

[5] Ilus, E, Ilus, T., 2000. Sources of Radioactivity. In: S.P.Nielsen (ed.), The radiological exposure of the population of the European Community to radioactivity in the Baltic Sea, Marina-Balt project, Radiation Protection 110, (2000) 9-76, EUR 19200, European Commission, Luxembourg.

[6] Nies, H. Bojanowski, R., Karlberg, O., Nielsen, S.P.,1995. Sources of radioactivity in the Baltic Sea, Baltic Sea Environment Proceedings No. 61 (1995) 6-18, Helsinki Commission.

[7] Ikäheimonen, T., Outola I., Vartti V-P., Kotilainen P., 2009. Radioactivity in the Baltic Sea: inventories and temporal trends caesium-137 and strontium-90 in water and sediments, J Radioanal Nucl Chem (2009) 419-425

[8] Hutri, K-L., Mattila, J., Ikäheimonen, T. K., Vartti, V-P., Artificial radionuclides 90Sr and 241Am in the sediments of the Baltic Sea: Total and spatial inventories and some temporal trends, Marine Pollution Bulletin, Volume 70, Issues 1–2, 15 May 2013, Pages 210-218.

6.2 Model validation against measured data

In the consideration of model validation related to the Baltic Sea area, measured data presented in previous chapters, were qualitatively and quantitatively shortly compared with modelling results of nuclear power plants release scenarios.

Qualitatively the temporal concentrations in seawater and in sediments seem to behave similarly between measured and modelled values: seawater concentrations increase first and sediment concentrations build up in later phase. After maximum, the seawater concentration starts decreasing. For sediments the maximum value is reached later than in seawater, but in the sediment the concentration maximum is broad and the concentrations stay at high level for a very long period of time.

Radionuclide concentrations in seawater and in sediments were also quantitatively studied. For a three years period after maximum, the measured values in seawater decreased about 55% and in model calculations the corresponding decrease was 50%. The measured concentration ratios sediment/seawater were 500 – 1000, and 200 – 1000 in model estimates correspondingly. Additionally, for example to the Gulf of Finland, where measured ratio sediment/seawater is high, the model estimate is there likewise higher than for example ratio in the Baltic Sea Proper area.

Consequently, the calculation model predictions seem to reach quite nice consistence with measured values in qualitative and in quantitative considerations.

7 SUMMARY AND CONCLUSIONS

In the study consequences of severe radioactive releases to Nordic marine environment – the Baltic Sea area and the North Atlantic - has been considered. The research activity has covered areas of Nordic marine input data, marine flows and dilution effects, radioactive source term evaluations for nuclear power plants and for submarine vessels, scenario calculations for accidental releases of nuclear power plants and for submarines, model validation against measured data of the Baltic Sea and radiation dose estimates to human and to biota.

As a reference, the released amounts from a 3000 MW_{th} nuclear power plant reactor size were used for the Baltic Sea area accidents. Based on source term analyses, the chosen release fractions in the study were: iodine 20% (of the total core inventory), caesium 10%, tellurium 10%, strontium 0.5%, ruthenium 0.5%. The considered release event to marine environment were assumed to start ten hours after shutdown of the reactor. Total released amounts of the most important nuclides were estimated to be: $4.85 \cdot 10^{17}$ Bq (I-131), $7.29 \cdot 10^{16}$ Bq (Cs-134) and $4.17 \cdot 10^{16}$ Bq (Cs-137).

Due to the highly contaminated sea food after a hypothetical severe release into sea, the arising doses to human would be high especially in local sea area near the release point. Based on the results, annual individual doses could be ten to some hundreds of millisieverts from local sea area. The most important nuclides were Cs-134, Cs-137 and I-131 causing 96% of the total ingestion dose.

In the Baltic Sea area, the dose rates and doses will decrease significantly due to dilution of large marine basin. During the first two years after release, the fish dose pathway dominates in total dose, but thereafter the external exposure from shoreline sediments will be dominating. The estimated total individual dose from a hypothetical severe release at the Baltic Sea is after one year 0.01 mSv and after five years 0.1 mSv. The collective dose estimates in the Baltic Sea area are 98 manSv after one year from release, and 880 manSv after five years which corresponds to about expected 20 detrimental effects to human in future.

In case of hypothetical submarine accidents at the North Atlantic, the marine fluxes and flow circumstances in general around the accident point, are important factors as considering the radiation consequences to biota and to human. This is significant feature for example at Icelandic waters. According to simulation results, maximum concentration near the source region at the Icelandic coast sinks below 1% only after 300 days.

In case of submarine accident at Faroe Islands waters, the entire Faroese shelf is affected by cloud after 100 days from begin of the release. After 300 days the cloud stretches out over large parts of the Norwegian Sea including the Norwegian coast.

In case of submarine accident at the Norway coast, already after 150 days, the cloud, which follows the Norwegian coast towards the north with the Norwegian Current, is dispersed down to a maximum concentration of 0.01%. The vertical profiles point to a substantial downward mixing.

Consequences of an accident of a modern submarine for Kattegat region was calculated on the basis of conservative scenario. The calculations indicate that generally the concentrations of radionuclides in seafood would be under the international guideline levels. However, near the release point of an accident, the guideline levels could be exceeded for some marine organisms. The calculated collective dose rates to man as well as to a critical group, are significantly lower than doses from natural sources. For the Kattegat region the doses can be equal or higher than from natural exposure. The Kattegat marine region seems to be also sensitive to the consequences of a radioactive release.

In the consideration of model validation related to the Baltic Sea area, measured data were qualitatively and quantitatively compared with modelling results of nuclear power plants release scenarios. The calculation model predictions seem to reach quite nice consistence with measured values in qualitative and in quantitative considerations.

Title	Consequences of severe radioactive releases to Nordic Marine environment
Author(s)	Iosjpe[1], M., Isaksson[2], M., Joensen[3], H.P., Lahtinen[4], J., Logemann[5], K., Pálsson[6], S. E., Roos[7], P., Suolanen[8], V., Vartti[4], V.-P.
Affiliation(s)	1 Norwegian Radiation Protection Authority, Norway 2 University of Gothenburg, Sweden 3 Fróðskaparsetur Føroya, Faroe Islands 4 Radiation and Nuclear Safety Authority, Finland 5 University of Iceland, Iceland 6 Geislavarnir Rikisins, Iceland 7 Technical University of Denmark, Denmark 8 Technical Research Centre of Finland, Finland
ISBN	978-87-7893-372-0
Date	January 2014
Project	NKS-B / COSEMA
No. of pages	96
No. of tables	11
No. of illustrations	66
No. of references	114

Abstract

Consequences of hypothetical severe radioactive releases to Nordic marine environment – the Baltic Sea and the North Atlantic - has been considered.

As a reference, releases from a 3000 MW_{th} nuclear power plant reactor size was used for the Baltic Sea area accidents. Individual dose to human could be ten to some hundreds of millisieverts in local sea area. In the Baltic Sea area, individual dose was 0.01 mSv after one year and 0.1 mSv after five years from the release event. The collective dose estimate was 880 manSv.

In case of hypothetical submarine accidents at the North Atlantic, the marine fluxes are important factors. According to simulation results, e.g. maximum concentration near the source region at the Icelandic coast sinks below 1% only after 300 days.

Consequences of an accident of a modern submarine for e.g. to Kattegat region was calculated. The arising doses can be equal or higher than from natural sources. The models predictions seem to reach nice consistence with measured values in qualitative and quantitative considerations.

Key words severe radioactive releases, accidents, marine environment, nuclear power plants, submarines, doses, validation